HOLTEC INTERNATIONAL

Holtec Center, 555 Lincoln Drive West, Marlton, NJ 08053
Telephone (856) 797-0900
Fax (856) 797-0909

Mr. John Goshen
c/o Document Control Desk
U. S. Nuclear Regulatory Commission
Washington, DC 20555-0001

July 29, 2011

Subject: Response to NRC First Request for Additional Information on License Amendment Request No. 9 to Holtec International HI-STORM 100 Certificate of Compliance No. 1014

References:
[1] NRC Letter (Goshen) to Holtec (Morin), dated June 20, 2011
[2] Holtec Letter 5014705, dated September 10, 2010
[3] Holtec Letter 5014708, dated October 1, 2010
[4] USNRC Docket No. 72-1014, TAC No. L24476

Dear Mr. Goshen:

By letter dated June 20, 2011 [1] NRC provided a first request for additional information (RAI) on License Amendment Request (LAR) #9 to Certificate of Compliance (CoC) 1014, as supplemented [2,3]. This letter transmits the responses to the RAI.

Attachments to this letter are as follows:

Attachment #	Content	Proprietary Status	Number of Pages
1	Responses to RAI	Non-Proprietary	13
2	Proposed CoC/TS Appendix B-100U	Non-Proprietary	66
3	FSAR pages supporting the response	Non-Proprietary	85
4	Appendix G to HI-2104599R1	Proprietary	37
5	Appendix F to HI-2104599R1	Proprietary	5
6	Holtec Position Paper DS-338	Proprietary	26
7	Holtec Drawing 4501R6	Proprietary	7
8	Affidavit (10 CFR 2.390)	Non-Proprietary	5

In addition, an enclosed DVD labeled "Thermal Models for LAR 1014-9 RAI Response" contains the proprietary thermal models requested in the RAI.

Attachment 8 is an affidavit requesting the information in Attachments 4 through 7 and the thermal models on the enclosed DVD be withheld from the public in accordance with 10 CFR 2.390 due to their proprietary nature.

Document ID: 5014725

NMSS01
NMSS

HOLTEC
INTERNATIONAL

Holtec Center, 555 Lincoln Drive West, Marlton, NJ 08053
Telephone (856) 797-0900
Fax (856) 797-0909

If you have any questions regarding this transmittal, please do not hesitate to contact me at 856-797-0900 x687.

Sincerely,

Tammy S. Morin
Licensing Manager
Holtec Technical Services, Holtec International

cc: Mr. Michael Waters, USNRC (w/o attachments or enclosure)
Mr. Douglas Weaver, USNRC (w/o attachments or enclosure)
Holtec Group 1

Holtec Response to First Request for Additional Information on License Amendment Request 1014-9

3.0 STRUCTURAL EVALUATION

3-1 To justify a lower bound generic site shear wave velocity of 500 fps, perform a soil structure interaction (SSI) analysis that accounts for the uncertainty in the site shear wave velocity as provided in the guidance for SSI analysis in NUREG-0800 "Standard Review Plan for the Review of Safety Analysis Reports for Nuclear Power Plants," Section 3.7.2.

In order to establish a lower bound site soil shear wave velocity of 500 fps, uncertainty with respect to soil shear wave velocity must have been considered in the generic SSI analysis. Because the quality of the site soil data is also uncertain, a lower bound value, consistent with NUREG-0800 guidance, of 250 fps should be used in the revised SSI analysis in order to generically specify a lower bound site value of 500 fps.

This information is required to evaluate compliance with 10 CFR Part 72.212(b)(2)(i)(B).

Holtec Response: Rather than revise the SSI analysis to consider a lower bound shear wave velocity of 250 fps, Table 2.I.2 of the FSAR has been revised to clearly define 500 fps as the lower bound, strain compatible effective shear wave velocity including the potential variability (i.e., uncertainty) in the site soil properties. This means that a site must demonstrate that, when the lower bound values for shear wave velocity (based on the site soil investigation data) are used as input, the free-field site response analysis yields a strain compatible effective shear wave velocity greater than or equal to 500 fps for Space A (see FSAR Figure 2.I.5). The lower bound shear wave velocities used as input to the free-field site response analysis shall be determined using the following formula (which is derived from Section 3.7.2 of NUREG-0800):

$$V_{LB} = \frac{V_{BE}}{\sqrt{1 + COV}}$$

where V_{BE} is the best estimate shear wave velocity for a given soil layer based on the soil investigation data, and *COV* is the coefficient of variation for the site soil properties. For well-investigated sites, the *COV* should be no less than 0.5. For sites that are not well investigated, the *COV* shall be set equal to 1.0.

The requirements for determining the strain compatible effective shear wave velocities at a particular site are added to CoC Appendix B-100U Table 3-4.

3-2 Provide an analysis for long-term differential settlement using an appropriate finite element model.

Using the methodology discussed in the Final Safety Analysis Report (FSAR) Section 2.I.2.i to capture the effect of long-term settlement under the action of applied loads, the elastic modulus of the soil in Space C, which is located directly beneath the Support Foundation Pad (SFP) in the finite element model shown in Figure 3.I.14, is reduced. Only the soil directly beneath the SFP is included in the model. All of the soil beyond the edges of the SFP is not included in the model. Such a model cannot capture the flexural effects that occur in the SFP due to long-term settlement (softening) of the soil beneath the SFP, because the soil adjacent to the edges of the SFP has been omitted. This omitted soil would have provided greater vertical stiffness to the edges of the SFP creating a dishing effect in the SFP and much higher flexural moments.

This information is required to evaluate compliance with 10 CFR Part 72.212(b)(2)(i)(B).

Holtec Response: In order to capture the long-term differential settlement effects on the pads more accurately, the existing structural analysis model has been extended in both lateral directions, thereby including the soil in Space B and Space D (see FSAR Figure 2.I.5). The lateral extent of the structural analysis model is sufficiently large (111 ft from the edge of the SFP and TSP) to capture the flexural moments due to long-term differential settlement. The figure below shows the extended finite element (FE) model.

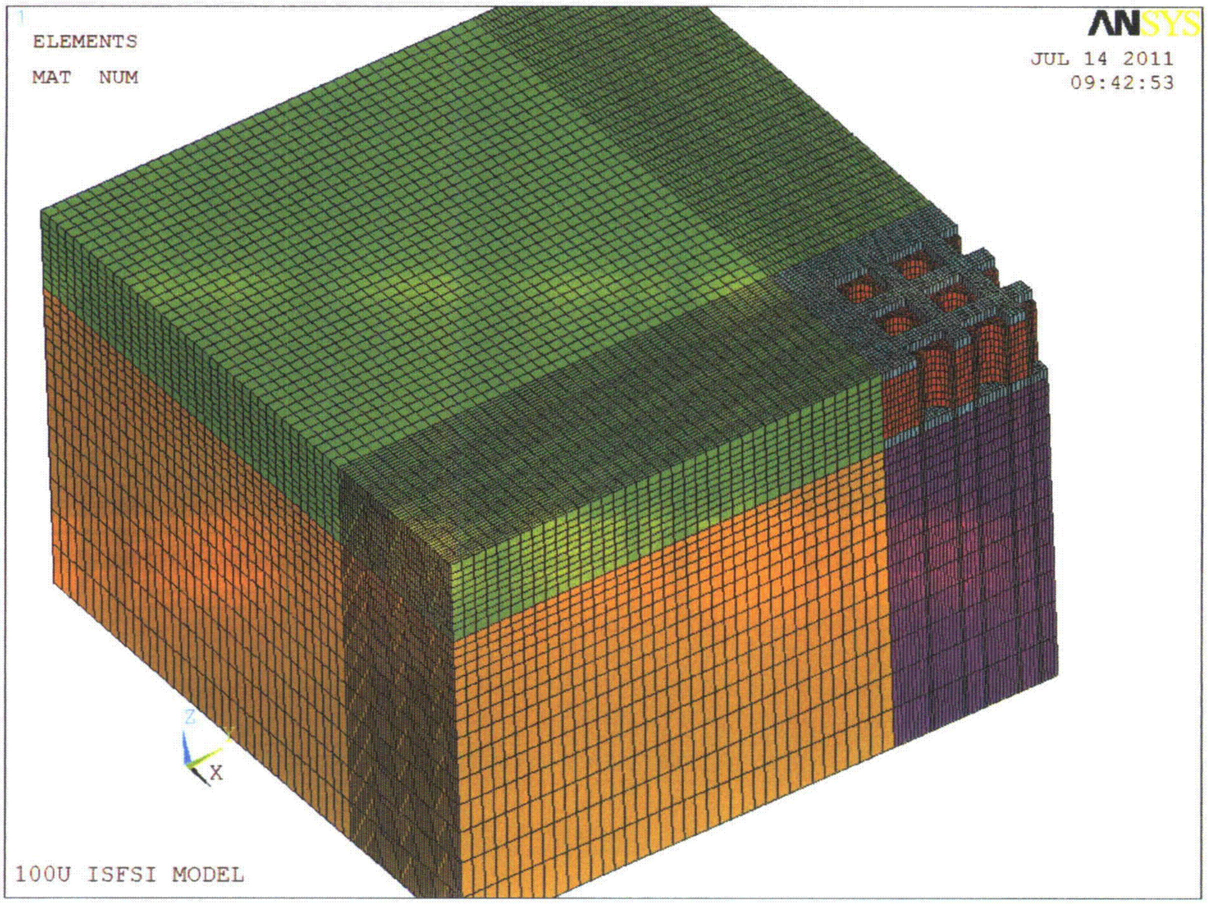

For the HI-STORM 100U ISFSI with the optional retaining walls installed, an additional simulation model is considered to evaluate the flexural moments on the SFP while excavation activities associated with the construction of a new underground ISFSI are being performed. In this model (see figure below), the lateral soil surrounding the retaining walls is removed on all sides to obtain a bounding solution. Further details pertaining to the above two analyses and the corresponding results are captured in Appendix G of Holtec Report HI-2104599 Rev. 1 (which is provided as Attachment 4 to this submittal).

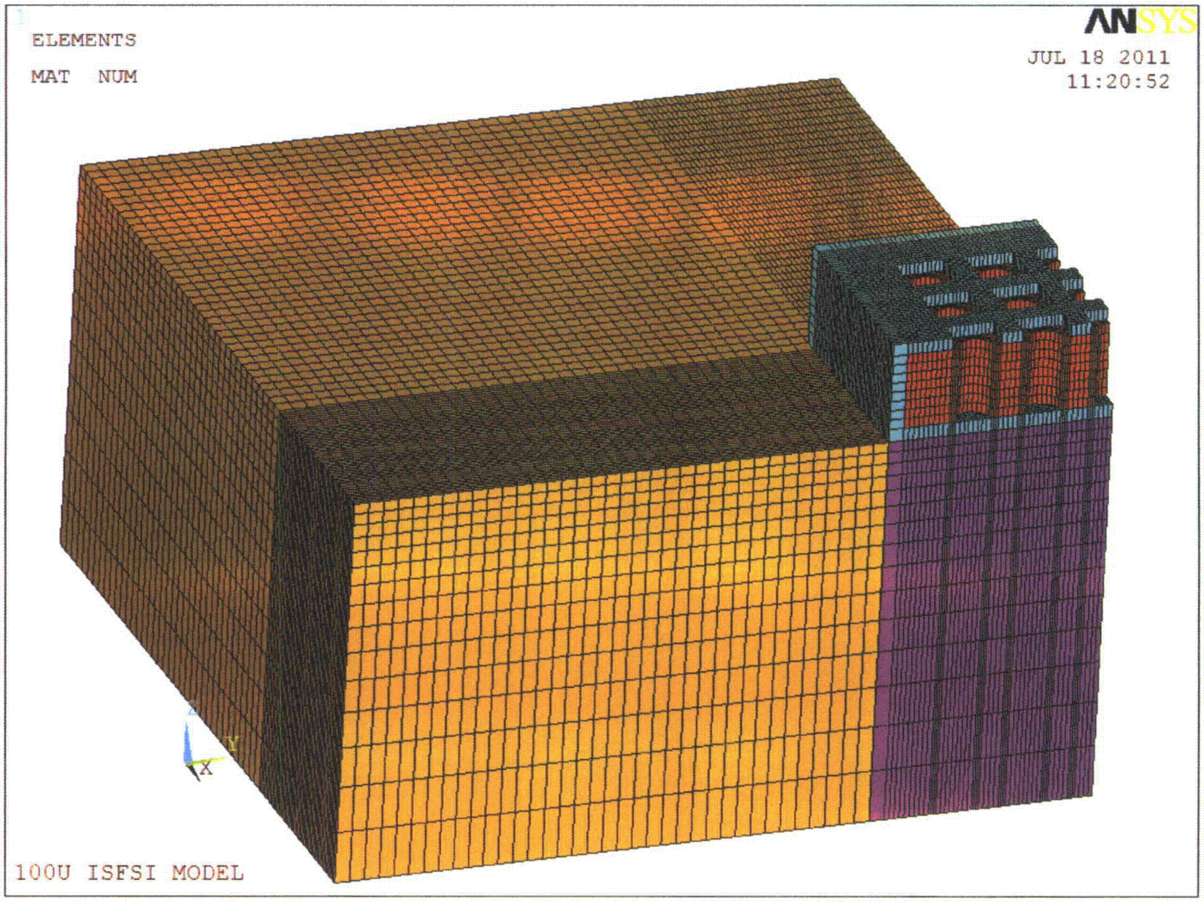

It is also noted that, as part of this RAI submittal, the SSI analysis results presented in FSAR Table 3.I.7 have been updated to remove the unintended conservatism previously described in the note below Table 3.I.6 in Rev. 9A of the HI-STORM FSAR. Correspondingly, the loads applied to the structural analysis models (see FSAR Table 3.I.8) have been updated to reflect the latest SSI analysis results in FSAR Table 3.I.7.

The latest results from the structural analysis of the ISFSI structures, including the simulation models described in this RAI response, are summarized in FSAR Table 3.I.10. All safety factors remain above 1.0 indicating that the strength requirements of ACI 318-05 continue to be met.

For completeness, a revised FSAR Section 3.I (Rev. 9B) is provided in Attachment 3 to this submittal. The section continues to show revision bars from Rev. 9A, however note that changes made as a result of this RAI response are limited to subsection 3.I.4.7.3, Tables 3.I.6 through 3.I.13, with the exception of 3.I.9 and 3.I.11, and Figure 3.I.14-B. Minor editorial changes we done to figure titles to align them with the current text.

3-3 Provide an analysis which demonstrates that ignoring soil column(s) adjacent to the Top Surface Pad (TSP) and SFP effects is conservative, with respect to TSP and SFP design basis loadings.

The structural analysis for ISFSI structures provided in HI-2104599 Rev.0 only models the soil column directly below the TSP and SFP while ignoring the effects of the lateral soil columns. The assumption that a free surface at the lateral boundary of the ISFSI is conservative has not been adequately demonstrated. Also see RAI 3-2.

This information is required to evaluate compliance with 10 CFR Part 72.212(b)(2)(i)(B).

Holtec Response: See response to 3-2.

3-4 Demonstrate that defining the retaining wall, when used, as the Excavation Exclusion Zone (EEZ) boundary will not cause adverse effects on the structural integrity of the TSP or SFP under design basis loadings including earthquake.

Section 2.1.2 HI STORM 100U VVM Components, ISFSI Structures, and Corrosion Mitigation Measures, item (vi) Retaining Wall states: "If a retaining wall is installed at or beyond the RPS then the wall becomes the EEZ boundary."

The staff identified a potential excavation depth of 30 feet beyond the bottom surface of the SFP in Section 3.2.3 of the SER for Amendment 7 of the HI-STORM 100 Cask System, which could be as close as the Radiation Protected Space for the ISFSI if a retaining wall is used. The safety concern identified was specific to the loss of shielding of the lateral soil should an earthquake event occur simultaneously with excavation activities.

A potential open pit adjacent to the Radiation Protection Space (RPS) with a retaining wall installed also presents a safety concern with respect to the structural integrity of the SFP and TSP for normal, off-normal, or accident conditions. Staff does not have reasonable assurance that the subgrade integrity below the SFP has been sufficiently analyzed for excavation activities to demonstrate no adverse effects on the SFP and subsequently the TSP.

This information is required to evaluate compliance with 10 CFR Part 72.212(b)(2)(i)(B).

Holtec Response: Section 2.I.2.vi of the HI-STORM 100 FSAR has been revised to clarify the limitations on excavation activities with and without a retaining wall installed. Most notably, when a retaining wall is installed on one or more sides of the 100U ISFSI, excavation activities associated with the construction of a new underground ISFSI can be performed directly adjacent to the retaining wall(s) at depths <u>above</u> the bottom surface of the existing SFP. Soil excavations below the elevation corresponding to the bottom surface of the existing SFP are not permitted within a distance from the RPS equal to ten times the planned excavation depth, regardless of whether a retaining wall is installed or not, unless a site-specific seismic analysis is performed demonstrating the stability of the RPS boundary and the structural integrity of the ISFSI structure.

3-5 Demonstrate that the alignment key(s) at the top and bottom of the retaining wall have sufficient strength to resist all design basis loads.

An analysis was provided to demonstrate general structural adequacy of the retaining wall with respect to design basis loads, however, no analysis was apparent for the strength capacity of the keys. Since the keys are necessary for the retaining wall to perform its safety function with respect to shielding, a structural evaluation must be provided.

This information is required to satisfy the requirements of 10 CFR Part 72.212(b)(2)(i)(B).

Holtec Response: A structural evaluation of the shear connections at the top and bottom of the retaining wall has been performed and documented in Appendix F of Holtec Report HI-2104599 Rev. 1 (which is provided as Attachment 5 to this submittal). The results are also summarized in Table 3.I.13 of the HI-STORM 100 FSAR. Furthermore, as a result of this RAI, changes have been made to the shear keys at the top and bottom of the retaining wall to increase their strength and to improve constructability. In particular, the bottom shear key has been eliminated and replaced by #8 dowels at 12" spacing on both faces of the retaining wall, and the size of the top shear key has been increased. The dowels at the bottom of the retaining wall have been sized to resist the shear force that develops at the intersection between the retaining wall and the SFP during the Design Basis Earthquake. The dowels, however, are not capable of developing the same moment capacity as the retaining wall. Therefore, the retaining wall is conservatively analyzed as being simply supported along its top and bottom edges. Sheet 7 of Holtec Drawing 4501 has been revised to show the new details.

3-6 Provide a copy of Reference 2.I.6, Holtec Position Paper, DS-338, "A Methodology to Compute the Equivalent Elastic Properties of the Subgrade Continuum to Incorporate the Effect of Long-Term Settlement."

This information is required to evaluate compliance with 10 CFR Part 72.212(b)(2)(i)(B).

Holtec Response: A copy of Reference 2.I.6 is provided as Attachment 6 to this submittal.

3-7 In FSAR Table 2.I.11 and CoC Table 3-3 revise the definition of D (dead load) to read, "Dead Load including long-term differential settlement effects." This makes the definition consistent with American Concrete Institute (ACI)-318 (2005). Also, on page 2.I.8 change "long-term settlement" to differential settlement.

This information is needed to provide clarity and consistency in the FSAR.

Holtec Response: The requested changes have been made to Supplement 2.I (Table 2.I.11 and page 2.I.8) and CoC Table 3-3.

3-8 Revise Drawing 4501 Sht.3 Rev 5 to illustrate consistent location of Top of Grade.

The main drawing shows a different Top of Grade location than the detail drawing of the expansion joint.

This information is needed to provide clarity and consistency in the FSAR.

Holtec Response: Drawing 4501 Sht. 3 has been revised to delete the Top of Grade location from the expansion joint detail. The Top of Grade location is shown correctly in Section B-B on Sht. 3. The revised drawing is provided as Attachment 7 to this submittal.

4.0 THERMAL EVALUATION

General Note for Thermal RAIs: The License Amendment Request (LAR) 1014-9 proposed to change the HI-TRAC thermal models from 2D thermal hydraulic models to 3D thermal hydraulic models. As a result, re-analysis of the short-term operations and accident conditions specific to the HI-TRAC were performed. The re-analysis resulted in changes to the heat load limits for vacuum drying, the requirement to have supplemental cooling, the representative calculation for time-to-boil, the generic fire analysis of the HI-TRAC, and the calculation of loss of water in the water jacket. We observe that five of the six subject RAIs (noted with an asterisk) are outside of the scope of this LAR and are focused on FSAR text matter that supports previous NRC SERs and Certificates of Compliance on this docket. Nevertheless, we have endeavored to provide a full and complete response to these questions to formally document where the information can be found in the licensing basis documents.

4-1 Explain why the 75% blocked air inlets criteria was not used when analyzing the effect of the increased flow resistance on fuel temperature.

In the HI-STORM FSAR, Section 4.6.1.3, "Partial Blockage of Air Inlets under the Off-Normal and Accident Events," the applicant analyzes and explains the effect of a 50% partial blockage of air inlets for the off-normal conditions. The analysis included the computed temperatures and the corresponding multipurpose canister internal pressure. The reported pressure for this analysis (FSAR Table 4.6.2) is 100.4 psig, with a margin of 9.6 psig below the limit of 110 psig for the off-normal conditions. The applicant is required to explain why a 75% partial blockage of air inlet was not analyzed and provide the impact on the pressure margin for the off-normal conditions.

This information is required to evaluate compliance with 10 CFR 72.24(d), 10 CFR 72.122(h)(1), 10 CFR 72.128(a)(4), and 10 CFR 72.236(f).

Holtec Response*:

Holtec Response to First Request for Additional Information on License Amendment Request 1014-9

The HI-STORM 100 FSAR Revision 9, Table 2.0.2 contains the summary of the HI-STORM overpack design criteria. On page 2.0-28 it lists the off-normal condition of partial blockage of air inlets as 50% of air inlets blocked. This condition is further discussed in Section 2.2.2.5 of the FSAR and evaluated in Section 4.6.1.3.

It should also be noted that a 24-hour surveillance of the inlet vents is required per LCO 3.1.2 (if not using temperature monitoring) to ensure that inlet vents are free of any blockage/debris and the user is required to remove any blockage observed. This ensures that the HI-STORM and MPC temperatures and pressures always remain within the prescribed limits.

4-2 Describe the corrective action needed for continued safe storage when the concrete temperature exceeds the short term temperature limit during the fire.

The applicant stated in FSAR Section 4.6.2.1 that the overpack external shell temperatures exceed the short term temperature limit during the fire and referenced NUREG 1536. "The NRC accepts that concrete temperatures may exceed the temperature criteria of ACI 349 for accidents if the temperatures result from a fire." However, NUREG 1536 also states that a corrective action may be required for continued safe storage. Therefore, the applicant should describe the corrective action in FSAR or Technical Specifications (TS) for continued safe storage when the overpack temperatures exceed the short-term temperature limit during the fire.

This information is required to evaluate compliance with 10 CFR 72.24(d), 10 CFR 72.122(c), 10 CFR 72.122(h)(1), 10 CFR 72.128(a)(4), and 10 CFR 72.236(f).

Holtec Response*:

The paragraph in the NUREG-1536 from which the sentence above is quoted discusses the fact that concrete may be damaged if during or subsequent to the fire, the system is doused with water causing localized loss of shielding. This would then require some corrective action for continued use. In addition short temperature excursions due to the fire may also require corrective actions for continued storage.

> "Some structures, systems, and components may experience the most severe conditions if exposure to high temperatures is followed by dousing (as by rain or fire water). A small amount of exterior concrete spalling may result from a fire, the application of fire suppression water, rain on heated surfaces or other high-temperature condition. The damage from these events is readily detectable, and appropriate recovery or corrective measures may be presumed. Therefore, the loss of such a small amount of shielding material is not expected to cause a storage system to exceed the regulatory requirements in 10 CFR 72.106 and, therefore, need not be estimated or evaluated in the SAR. The NRC accepts that concrete temperatures may exceed the temperature criteria of ACI 349 for accidents if the temperatures result from a fire. In that case, corrective action may be required for continued safe storage."

It should be noted that none of the concrete in the HI-STORM 100 System is exposed to the ambient directly, i.e. all of the concrete is installed within the steel shells of the overpack and the lid; therefore spalling or any loss of concrete during this event would not be a concern.

The FSAR Sections 3.4.4.2.2 and 4.6.2 indicate that the excursion above the ACI-349-85 short term temperature limit of 350°F occurs in a very limited area of the overpack and for a short duration. The affected concrete material is located at the HI-STORM overpack outer shell up to a depth of one inch of concrete for less than 4 minutes. It is further summarized in Table 3.7.1 that there is no structural impact due to the fire event and there is no shielding impact resulting from this increased temperature. Therefore no specific corrective actions for continued safe storage are specified in the FSAR.

4-3 Revise the reference of NUREG 1536 (4.0, V, 5.b) to NUREG 1536 (Rev 1, 4.5.4.5).

On page 4.6-4 of the supplied HI-STORM FSAR, Rev.9A, the applicant referenced an prior version of NUREG 1536 (4.0, V, 5.b). The applicant should revise the FSAR to reference NUREG 1536 (Rev 1) to maintain current information updated in the FSAR.

This information is necessary to provide clarity and consistency in the FSAR.

Holtec Response*:

It is unclear to Holtec why the NRC Staff is requesting a change to the reference on page 4.6-4, from NUREG-1536 Rev. 0 to Rev. 1 when no specific change to this section (HI-STORM overpack fire) has been proposed in this LAR. The statements taken from NUREG-1536 Rev. 0 continue to be valid and no change is requested to the fire analysis of the loaded HI-STORM overpack which would necessitate meeting the current Staff review guidance (NUREG-1536 Rev.1).

4-4 (1) Explain why the 32-hour time period is selected for 100% blocked inlet analysis specified on Table 4.6.5, and (2) add the periodic surveillance program in TS for guidance to perform cask operations.

The applicant evaluated the effect of an event of 100% blockage of air inlets in HI-STORM 100 FSAR 4.6.2.4 (Rev. 9A) for the accident events. The 32-hour blocked inlet ducts maximum temperatures are shown in Table 4.6.5 of the FSAR. However, it is not clear to the staff why the 32-hour time period was selected to evaluate the temperatures of the components. The applicant should explain the selection of this time limit (24 hours) used in the accident analysis.

This information is required to evaluate compliance with 10 CFR 72.24(d), 10 CFR 72.122(h)(1), 10 CFR 72.128(a)(4), and 10 CFR 72.236(f).

Holtec Response*:

The permissible 32-hour time limit for the 100% blocked duct event accident condition is derived from the results of the transient analysis performed for this event (see FSAR Table 4.6.5 for temperature results). At approximately 32 hours, the concrete temperature approaches the ACI-349-85 limit of 350°F. However, the fuel cladding still has considerable margin to its temperature limit of 1058°F (ISG-11 Rev. 3). A periodic surveillance per LCO 3.1.2 of 24 hours exists in the Technical Specifications. This physical surveillance is required unless the cask has temperature monitoring equipment (Technical Specifications, Appendix A). The bases for this LCO are provided in Chapter 12 and explains this LCO addresses events that can be reasonably anticipated to occur from time to time (Design Event Class I and II of ANSI/ANS 57.9). It is realistic to assume blockage from this type of event can be cleared within this time frame. As noted in the Bases, once the system is declared inoperable the user has up 32 hours to clear the vents. In addition, if the HI-STORM System is deployed in area susceptible to Design Event Class III and IV which are low frequency, unexpected events (such as flood), users are required to address them on a site-specific basis per TS Appendix B Section 3.4.9.

A plot of the temperature rise of the fuel cladding during this transient event is provided below for information.

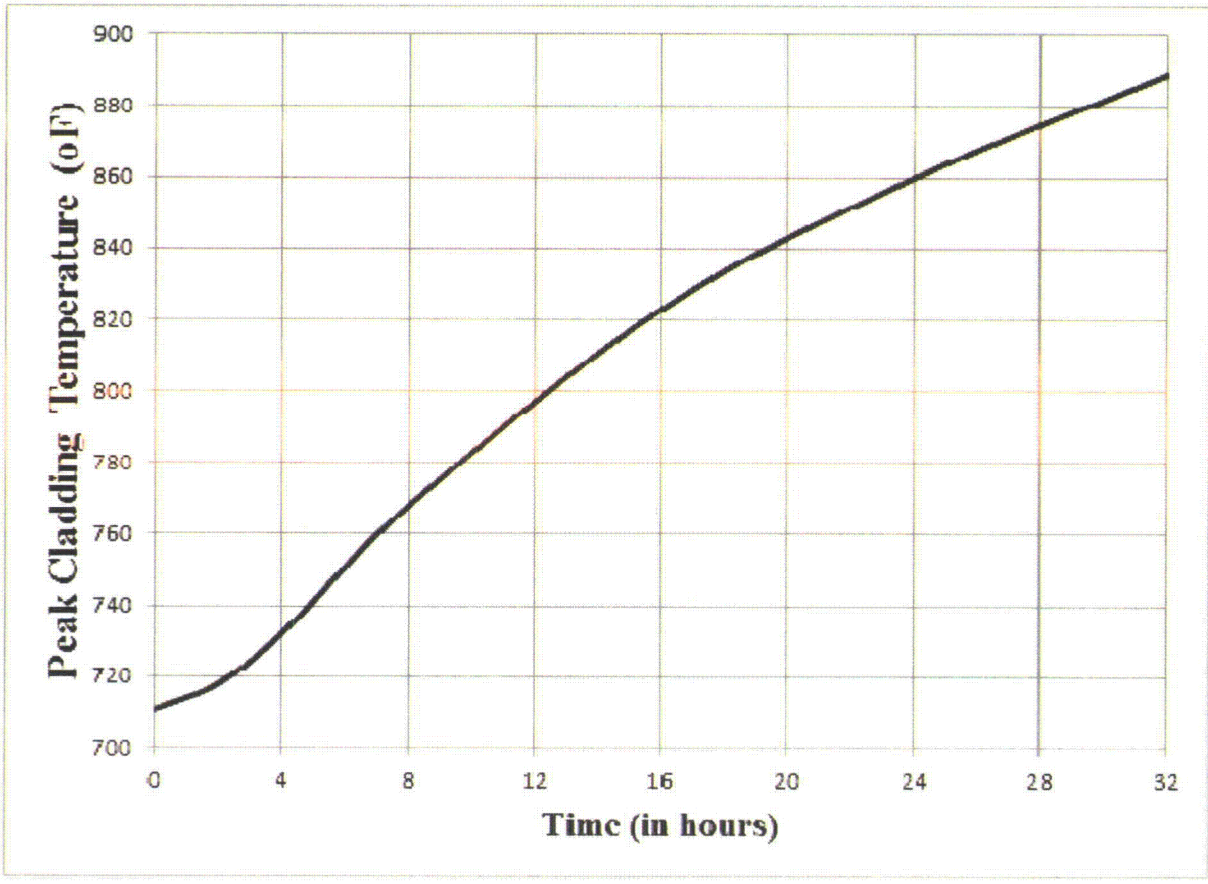

4-5 Provide the applicable FLUENT computer model used to evaluate the increased decay heat thresholds for both unlimited and time restricted vacuum drying meet the safety requirements.

The applicant updated the thermal model/methodology for the HI-TRAC transfer cask from a 2-Dimensional (D) thermal-hydraulic model to an inherently more accurate 3-D model, and utilized the 3-D model to simplify the requirements for short term operations of HI-STORM 100 System and predicted the results with the proposed changes:

a. there is no need for a supplemental cooling system to maintain peak cladding temperatures below the ISG-11 Rev. 3 limits.
The staff agrees with removal of the supplemental cooling system (SCS) and clarifies that the SCS is not applicable for transfer and storage of HI-STORM 100 System, in compliance with 10 CFR 72.236(f).

b. the decay heat thresholds are increased for both unlimited and time restricted vacuum drying.
The staff needs the models to verify/assure that the proposed changes of the decay heat thresholds for (a) vacuum drying time limit (TS Appendix A, 3.1.1) and (b) fuel burnup (TS Appendix A, Table 3-1), still meet the safety requirements of Part 72.

This information is required to evaluate compliance with 10 CFR 72.24(d), 10 CFR 72.122(h)(1), 10 CFR 72.128(a)(4), and 10 CFR 72.236(f).

Holtec Response:

The files containing the thermal analysis for vacuum drying are provided with this response. The thermal analysis of vacuum drying conditions supporting this LAR (Reference Holtec Letter 5014718, dated February 28, 2011) have been re-performed to address a potential error in the radiation heat transfer model of FLUENT version 6.3.26. Since the discovery of this error in version 6.3.26 of the CFD code FLUENT, the code manufacturer ANSYS has validated the problem and issued a Class 3 error to its users.

Because the original LAR reported temperatures and pressures for short-term operating conditions involving the HI-TRAC using version 6.3.26 of FLUENT that had a potential error, Holtec has re-run the calculations for all reported conditions involving the HI-TRAC and has provided the updated files with this response as well as updated Tables 4.5.4, 4.5.5, 4.6.2, and 4.6.3 below. These tables will be incorporated in the FSAR revision after approval of this LAR.

Table 4.5.4 HI-TRAC ONSITE TRANSFER - TEMPERATURE AND PRESSURE MARGINS			
	Maximum Temperatures (oF)		
Component	Computed	Permissible Limit (Note 1)	Margin
Fuel Cladding	714	752	38
MPC Basket	711	950	239
Basket Peripheral Panels	597	950	353
MPC Shell	469	775	306
HI-TRAC Inner Shell	336	800	464
Radial Lead	280	600	320
HI-TRAC Water Jacket Shell	253	800	547
Water Jacket Bulk Water	250	307	57
Axial Neutron Shield (Note 2)	297	350	53
Pressure (psig)			
MPC (Note 3)	101.9	110	8.1

Note 1: Temperatures and Pressure limits under HI-TRAC short-term operation are specified in Tables 2.2.1 and 2.2.3.
Note 2: Maximum section average temperature.
Note 3: The MPC pressure is computed under the maximum backfill pressure specified in Table 4.4.12.

Table 4.5.5 MAXIMUM FUEL TEMPERATURES UNDER VACUUM DRYING OPERATIONS				
Threshold Heat Load (Note 1)	Time Limit	Temperature (°F)	Temperature Limit (Note 2)	Margin (°F)
Q1	None	1046	1058	12
Q2	40 hrs	1035	1058	23

Notes:
1) Threshold heat loads defined in Table 4.5.1.
2) Temperature limit of moderate burnup fuel shown. Vacuum drying of high burn-up fuel is not permitted (See Subsection 4.5.3).

Table 4.6.2 OFF-NORMAL AND ACCIDENT CONDITION MAXIMUM MPC PRESSURES	
Condition	**Pressure (psig)**
Off-Normal Conditions	
Off-Normal Ambient	101.4
Partial Blockage of Inlet Ducts	100.4
Accident Conditions	
Extreme Ambient Temperature	104.4
100% Blockage of Air Inlets	118.1
Burial Under Debris	134.8
HI-TRAC Jacket Water Loss	107.9
HI-TRAC Fire Accident	105.2

Table 4.6.3 HI-TRAC JACKET WATER LOSS ACCIDENT MAXIMUM TEMPERATURES	
Component	**Temperature (°F)**
Fuel Cladding	786
MPC Basket	783
MPC Shell	513
HI-TRAC Inner Shell	408
HI-TRAC Water Jacket Shell	293

4-6 Explain the basis of the water mass of 6,500 lbs that is used for the MPC cavity.

The applicant computed and added the time-to-boil limits for various decay heat loads and initial spent fuel pool temperatures in Table 4.5.3 of HI-STORM FSAR under a conservative set of assumptions (such as the neglected heat loss by natural convection and radiation, the use of the smaller 100-ton design, and the understated water mass in the MPC cavity). The applicant should explain the details or provide the data to prove that the water mass of 6,500 lb (FSAR Table 4.5.2) is understated when compared to the "potential" water mass existed in the MPC cavity.

This information is required by to evaluate compliance with 10 CFR 72.24(d).

Holtec Response*:

The changes made to Section 4.5 were quite extensive and the whole section was presented as a new revision (Rev. 9A); however no changes were made to the HI-TRAC transfer cask weights and thermal inertia data in Table 4.5.2. We apologize if this created any confusion.

The MPC cavity free volume is used to determine the water mass in the MPC prior to blowdown and drying operations for time to boil calculations. Table 4.4.8 provides the free volume of the MPC cavity for the various MPC models. The most limiting is the MPC-68 with 228.2 ft^3 and considering the density of water (62.4 lb/ft^3) results in over 14,000 lbs of water in the MPC. As is stated in Section 4.5.2, the mass of water is understated. Table 4.5.2 indicates that the mass of water used in the calculation is 6500 lbs; therefore this conservatively underestimates the thermal inertia of the system and the time it will take for the water in the system to boil.

CERTIFICATE OF COMPLIANCE NO. 1014

APPENDIX B-100U

APPROVED CONTENTS AND DESIGN FEATURES

FOR THE HI-STORM 100 CASK SYSTEM (MODEL NO. 100U ADDITION)

TABLE OF CONTENTS

1.0 Definitions

Refer to Appendix A for Definitions.

2.0 APPROVED CONTENTS

2.1 Fuel Specifications and Loading Conditions

2.1.1 Fuel To Be Stored In The HI-STORM SFSC System Model 100U

a. INTACT FUEL ASSEMBLIES, and NON-FUEL HARDWARE meeting the limits specified in Table 2.1-1 and other referenced tables may be stored.

b. For MPCs partially loaded with stainless steel clad fuel assemblies, all remaining fuel assemblies in the MPC shall meet the decay heat generation limit for the stainless steel clad fuel assemblies.

c. For MPCs partially loaded with array/class 6x6A, 6x6B, 6x6C, 7x7A, or 8x8A fuel assemblies, all remaining ZR clad INTACT FUEL ASSEMBLIES in the MPC shall meet the decay heat generation limits for the 6x6A, 6x6B, 6x6C, 7x7A and 8x8A fuel assemblies.

d. All BWR fuel assemblies may be stored with or without ZR channels with the exception of array/class 10x10D and 10x10E fuel assemblies, which may be stored with or without ZR or stainless steel channels.

2.1.2 Uniform Fuel Loading

Any authorized fuel assembly may be stored in any fuel storage location, subject to other restrictions related to NON-FUEL HARDWARE specified in the CoC.

(continued)

2.0 Approved Contents

2.1 Fuel Specifications and Loading Conditions (cont'd)

2.1.3 Regionalized Fuel Loading

Users may choose to store fuel using regionalized loading in lieu of uniform loading to allow higher heat emitting fuel assemblies to be stored than would otherwise be able to be stored using uniform loading. Regionalized loading is limited to those fuel assemblies with ZR cladding. Figures 2.1-1 through 2.1-4 define the regions for the MPC-24, MPC-24E, MPC-32, MPC-68 models, respectively[1]. Fuel assembly burnup, decay heat, and cooling time limits for regionalized loading are specified in Section 2.4.2. Fuel assemblies used in regionalized loading shall meet all other applicable limits specified in Tables 2.1-1 through 2.1-3.

2.2 Violations

If any Fuel Specifications or Loading Conditions of 2.1 are violated, the following actions shall be completed:

2.2.1 The affected fuel assemblies shall be placed in a safe condition.

2.2.2 Within 24 hours, notify the NRC Operations Center.

2.2.3 Within 30 days, submit a special report which describes the cause of the violation, and actions taken to restore compliance and prevent recurrence.

2.3 Not Used

[1] These figures are only intended to distinguish the fuel loading regions. Other details of the basket design are illustrative and may not reflect the actual basket design details. The design drawings should be consulted for basket design details.

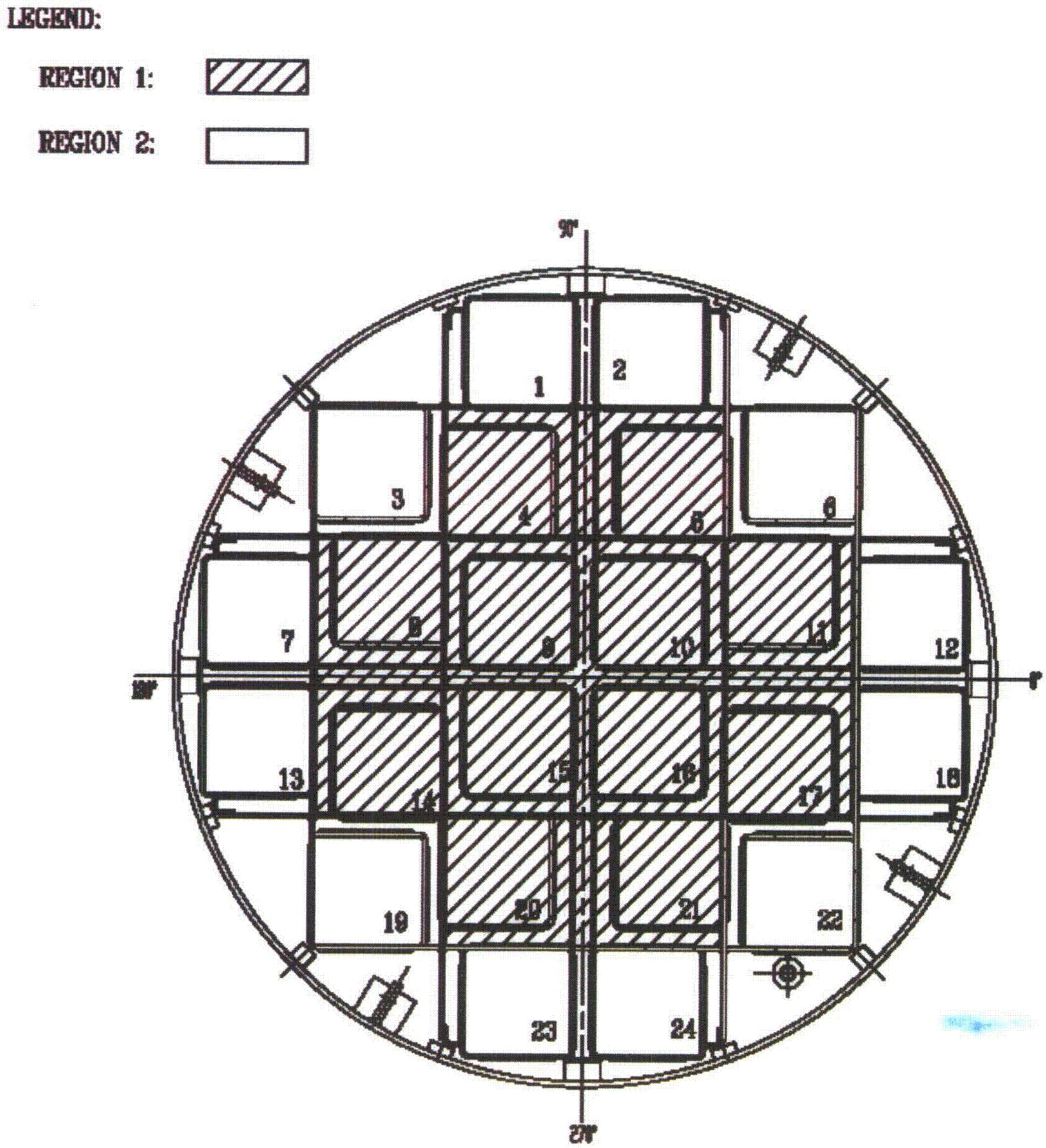

Figure 2.1-1
Fuel Loading Regions - MPC-24

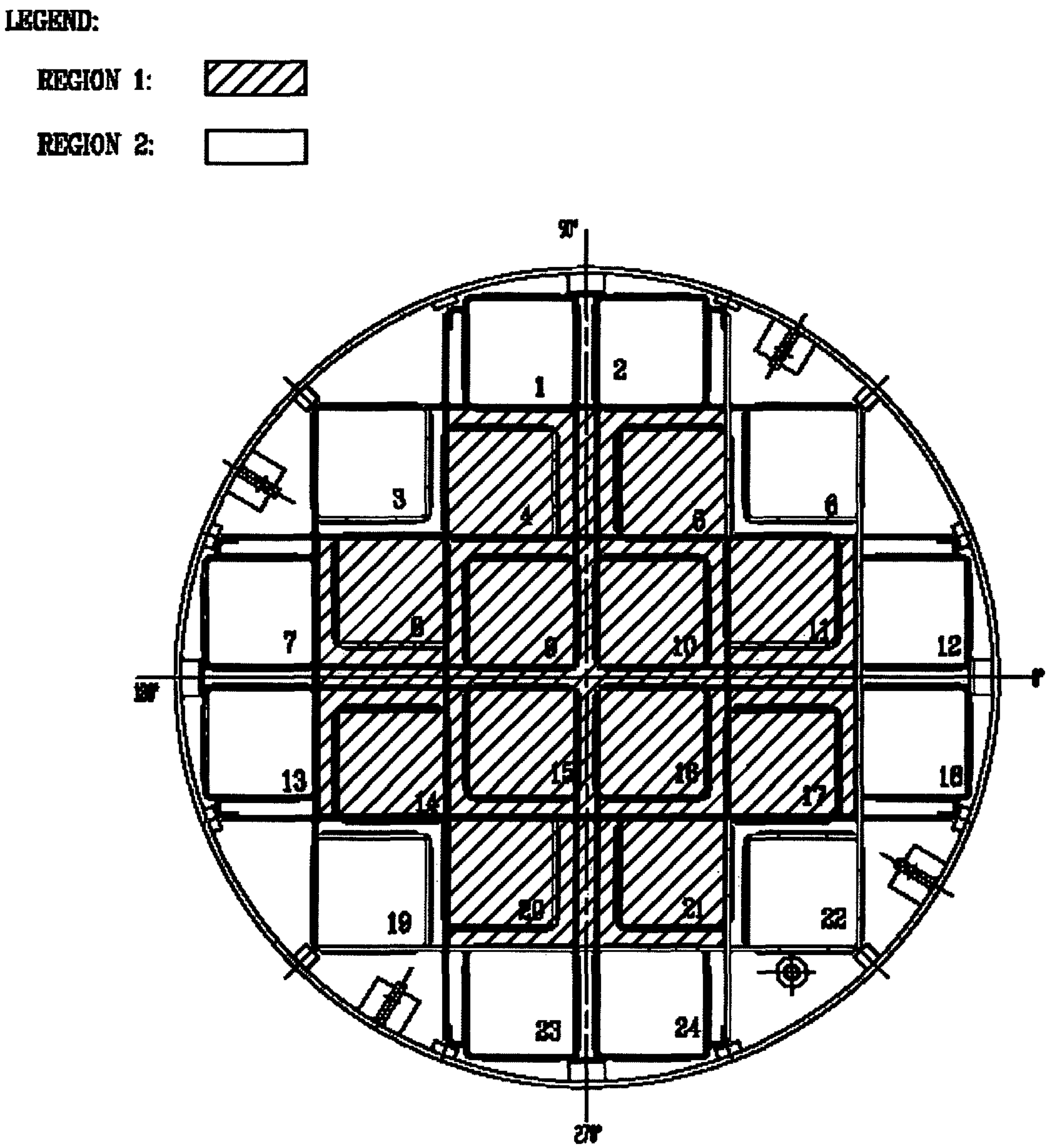

Figure 2.1-2
Fuel Loading Regions - MPC-24E

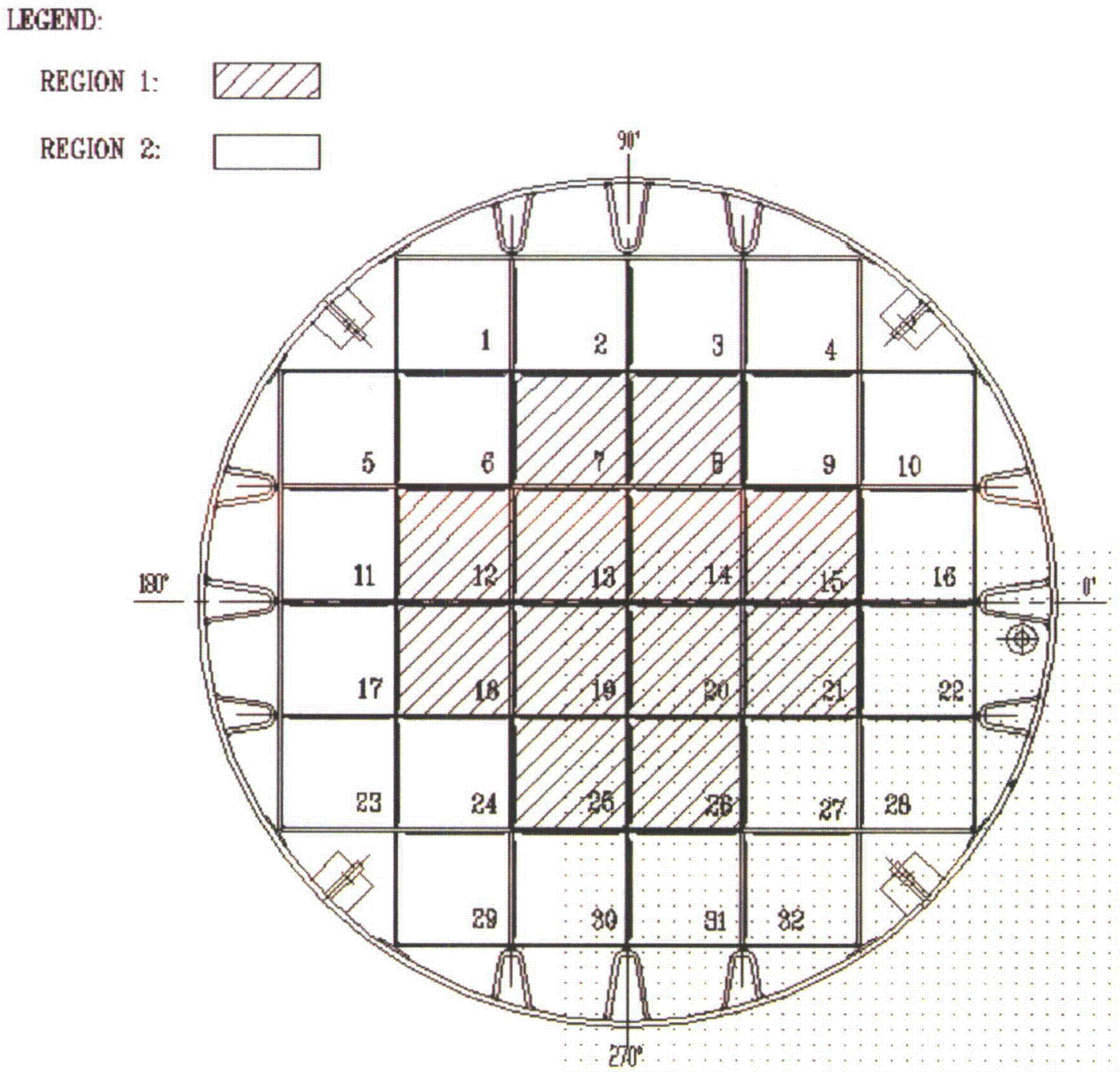

Figure 2.1-3
Fuel Loading Regions - MPC-32

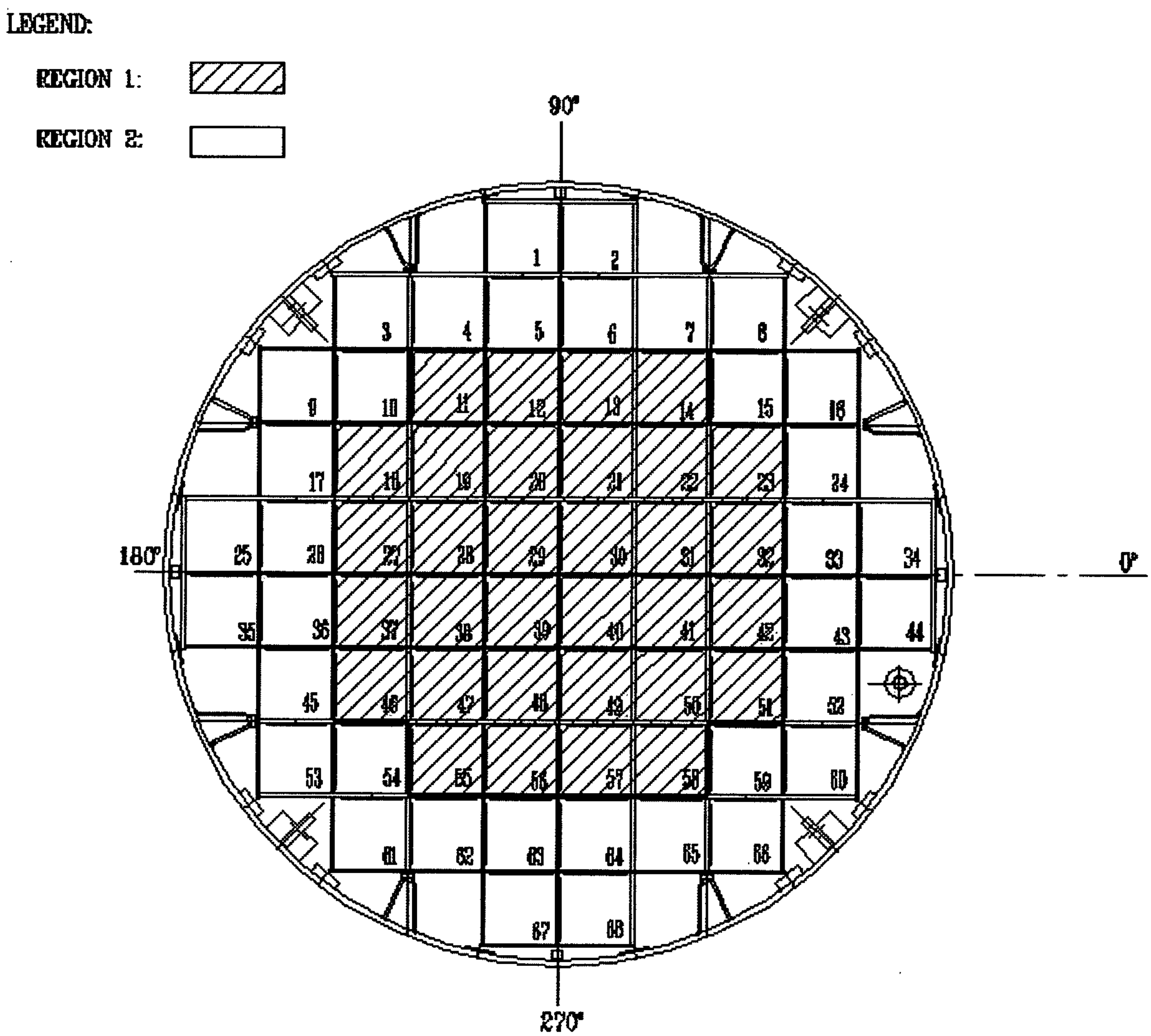

Figure 2.1-4
Fuel Loading Regions - MPC-68

Table 2.1-1 (page 1 of 8)
Fuel Assembly Limits

I. MPC MODEL: MPC-24

A. Allowable Contents

1. Uranium oxide, PWR INTACT FUEL ASSEMBLIES listed in Table 2.1-2, with or without NON-FUEL HARDWARE and meeting the following specifications (Note 1):

a. Cladding Type:	ZR or Stainless Steel (SS) as specified in Table 2.1-2 for the applicable fuel assembly array/class.
b. Initial Enrichment:	As specified in Table 2.1-2 for the applicable fuel assembly array/class.
c. Post-irradiation Cooling Time and Average Burnup Per Assembly:	
i. Array/Classes 14x14D,14x14E, and 15x15G	Cooling time ≥ 8 years and an average burnup ≤ 40,000 MWD/MTU.
ii. All Other Array/Classes	Cooling time and average burnup as specified in Section 2.4.
ii. NON-FUEL HARDWARE	As specified in Table 2.1-4.

Table 2.1-1 (page 2 of 8)
Fuel Assembly Limits

I. MPC MODEL: MPC-24 (continued)

A. Allowable Contents (continued)

d. Decay Heat Per Fuel Storage Location:	
i. Array/Classes 14x14D, 14x14E, and 15x15G	≤ 710 Watts
ii. All Other Array/Classes	As specified in Section 2.4.
e. Fuel Assembly Length:	≤ 176.8 inches (nominal design)
f. Fuel Assembly Width:	≤ 8.54 inches (nominal design)
g. Fuel Assembly Weight:	≤ 1720 lbs (including NON-FUEL HARDWARE) for assemblies that do not require fuel spacers, otherwise ≤ 1680 lbs (including NON-FUEL HARDWARE)

B. Quantity per MPC: Up to 24 fuel assemblies.

C. One NSA is authorized for loading into the MPC-24.

Note 1: Fuel assemblies containing BPRAs, TPDs, WABAs, water displacement guide tube plugs, orifice rod assemblies, or vibration suppressor inserts, with or without ITTRs, may be stored in any fuel storage location. Fuel assemblies containing APSRs or NSAs may only be loaded in fuel storage locations 9, 10, 15, and/or 16. Fuel assemblies containing CRAs, RCCAs, CEAs may only be stored in fuel storage locations 4, 5, 8 - 11, 14 - 17, 20 and/or 21 (see Figure 2.1-1). These requirements are in addition to any other requirements specified for uniform or regionalized fuel loading.

Table 2.1-1 (page 3 of 8)
Fuel Assembly Limits

II. MPC MODEL: MPC-68

A. Allowable Contents

1. Uranium oxide or MOX BWR INTACT FUEL ASSEMBLIES listed in Table 2.1-3, with or without channels and meeting the following specifications:

a. Cladding Type:	ZR or Stainless Steel (SS) as specified in Table 2.1-3 for the applicable fuel assembly array/class
b. Maximum PLANAR-AVERAGE INITIAL ENRICHMENT:	As specified in Table 2.1-3 for the applicable fuel assembly array/class.
c. Initial Maximum Rod Enrichment	As specified in Table 2.1-3 for the applicable fuel assembly array/class.
d. Post-irradiation Cooling Time and Average Burnup Per Assembly	
i. Array/Classes 6x6A, 6x6B, 6x6C, 7x7A, and 8x8A	Cooling time ≥ 18 years and an average burnup ≤ 30,000 MWD/MTU (or MWD/MTIHM).
ii. Array/Class 8x8F	Cooling time ≥ 10 years and an average burnup ≤ 27,500 MWD/MTU.
iii. Array/Classes 10x10D and 10x10E	Cooling time ≥ 10 years and an average burnup ≤ 22,500 MWD/MTU.
iv. All Other Array/Classes	As specified in Section 2.4.

Table 2.1-1 (page 4 of 8)
Fuel Assembly Limits

II. MPC MODEL: MPC-68 (continued)

A. Allowable Contents (continued)

e. Decay Heat Per Assembly

i. Array/Classes 6x6A, 6X6B, 6x6C, 7x7A, and 8x8A	≤ 115 Watts
ii. Array/Class 8x8F	≤ 183.5 Watts
iii. Array/Classes 10x10D and 10x10E	≤ 95 Watts
iv. All Other Array/Classes	As specified in Section 2.4.

f. Fuel Assembly Length

i. Array/Class 6x6A, 6x6B, 6x6C, 7x7A, or 8x8A	≤ 135.0 inches (nominal design)
ii. All Other Array/Classes	≤ 176.5 inches (nominal design)

g. Fuel Assembly Width

i. Array/Class 6x6A, 6x6B, 6x6C, 7x7A, or 8x8A	≤ 4.70 inches (nominal design)
ii. All Other Array/Classes	≤ 5.85 inches (nominal design)

h. Fuel Assembly Weight

i. Array/Class 6x6A, 6x6B, 6x6C, 7x7A, or 8x8A	≤ 400 lbs, including channels
ii. All Other Array/Classes	≤ 730 lbs, including channels

B. Quantity per MPC: Up to 68 fuel assemblies.

C. Dresden Unit 1 fuel assemblies with one Antimony-Beryllium neutron source are authorized for loading. The Antimony-Beryllium source material shall be in a water rod location.

D. Array/Class 10x10D and 10x10E fuel assemblies in stainless steel channels must be stored in fuel storage locations 19 - 22, 28 - 31, 38 -41, and/or 47 - 50 (see Figure 2.1-4).

Table 2.1-1 (page 5 of 8)
Fuel Assembly Limits

III. MPC MODEL: MPC-24E

A. Allowable Contents

1. Uranium oxide, PWR INTACT FUEL ASSEMBLIES listed in Table 2.1-2, with or without NON-FUEL HARDWARE and meeting the following specifications (Note 1):

a. Cladding Type:	ZR or Stainless Steel (SS) as specified in Table 2.1-2 for the applicable fuel assembly array/class
b. Initial Enrichment:	As specified in Table 2.1-2 for the applicable fuel assembly array/class.
c. Post-irradiation Cooling Time and Average Burnup Per Assembly:	
i. Array/Classes 14x14D, 14x14E, and 15x15G	Cooling time ≥ 8 years and an average burnup ≤ 40,000 MWD/MTU.
ii. All Other Array/Classes	As specified in Section 2.4.
iii. NON-FUEL HARDWARE	As specified in Table 2.1-4.

Table 2.1-1 (page 6 of 8)
Fuel Assembly Limits

III. MPC MODEL: MPC-24E (continued)

A. Allowable Contents (continued)

d. Decay Heat Per Fuel Storage Location:	
i. Array/Classes 14x14D, 14x14E, and 15x15G	≤ 710 Watts.
ii. All other Array/Classes	As specified in Section 2.4.
e. Fuel Assembly Length:	≤ 176.8 inches (nominal design)
f. Fuel Assembly Width:	≤ 8.54 inches (nominal design)
g. Fuel Assembly Weight:	≤ 1,720 lbs (including NON-FUEL HARDWARE) for assemblies that do not require fuel spacers, otherwise, ≤ 1,680 lbs (including NON-FUEL HARDWARE)

B. Quantity per MPC: Up to 24 fuel assemblies.

C. One NSA is permitted for loading.

Note 1: Fuel assemblies containing BPRAs, TPDs, WABAs, water displacement guide tube plugs, orifice rod assemblies, or vibration suppressor inserts, with or without ITTRs, may be stored in any fuel storage location. Fuel assemblies containing APSRs or NSAs may only be loaded in fuel storage locations 9, 10, 15, and/or 16 (see Figure 2.1-2). Fuel assemblies containing CRAs, RCCAs, or CEAs may only be stored in fuel storage locations 4, 5, 8 - 11, 14 - 17, 20 and/or 21 (see Figure 2.1-2). These requirements are in addition to any other requirements specified for uniform or regionalized fuel loading.

Table 2.1-1 (page 7 of 8)
Fuel Assembly Limits

IV. MPC MODEL: MPC-32

A. Allowable Contents

1. Uranium oxide, PWR INTACT FUEL ASSEMBLIES listed in Table 2.1-2, with or without NON-FUEL HARDWARE and meeting the following specifications (Note 1):

a. Cladding Type:	ZR or Stainless Steel (SS) as specified in Table 2.1-2 for the applicable fuel assembly array/class
b. Initial Enrichment:	As specified in Table 2.1-2 for the applicable fuel assembly array/class.
c. Post-irradiation Cooling Time and Average Burnup Per Assembly:	
i. Array/Classes 14x14D, 14x14E, and 15x15G	Cooling time ≥ 9 years and an average burnup ≤ 30,000 MWD/MTU or cooling time ≥ 20 years and an average burnup ≤ 40,000 MWD/MTU.
ii. All Other Array/Classes	As specified in Section 2.4.
iii. NON-FUEL HARDWARE	As specified in Table 2.1-4.

Table 2.1-1 (page 8 of 8)
Fuel Assembly Limits

IV. MPC MODEL: MPC-32 (continued)

A. Allowable Contents (continued)

d. Decay Heat Per Fuel Storage Location:	
i. Array/Classes 14x14D, 14x14E, and 15x15G	≤ 500 Watts.
ii. All Other Array/Classes	As specified in Section 2.4.
e. Fuel Assembly Length	≤ 176.8 inches (nominal design)
f. Fuel Assembly Width	≤ 8.54 inches (nominal design)
g. Fuel Assembly Weight	≤ 1,720 lbs (including NON-FUEL HARDWARE) for assemblies that do not require fuel spacers, otherwise, ≤ 1,680 lbs (including NON-FUEL HARDWARE)

B. Quantity per MPC: Up to 32 fuel assemblies.

C. One NSA is permitted for loading.

Note 1: Fuel assemblies containing BPRAs, TPDs, WABAs, water displacement guide tube plugs, orifice rod assemblies, or vibration suppressor inserts, with or without ITTRs, may be stored in any fuel storage location. Fuel assemblies containing NSAs may only be loaded in fuel storage locations 13, 14, 19 and/or 20 (see Figure 2.1-3). Fuel assemblies containing CRAs, RCCAs, CEAs or APSRs may only be loaded in fuel storage locations 7, 8, 12-15, 18-21, 25 and/or 26 (see Figure 2.1-3). These requirements are in addition to any other requirements specified for uniform or regionalized fuel loading.

Table 2.1-2 (page 1 of 4)
PWR FUEL ASSEMBLY CHARACTERISTICS (Note 1)

Fuel Assembly Array/Class	14x14A	14x14B	14x14C	14x14D	14x14E
Clad Material	ZR	ZR	ZR	SS	SS
Design Initial U (kg/assy.) (Note 3)	≤ 365	≤ 412	≤ 438	≤ 400	≤ 206
Initial Enrichment (MPC-24 and 24E without soluble boron credit) (wt % ^{235}U)	≤ 4.6 (24) ≤ 5.0 (24E)	≤ 4.6 (24) ≤ 5.0 (24E)	≤ 4.6 (24) ≤ 5.0 (24E)	≤ 4.0 (24) ≤ 5.0 (24E)	≤ 5.0 (24) ≤ 5.0 (24E)
Initial Enrichment (MPC-24, 24E, or 32, with soluble boron credit - see Note 5) (wt % ^{235}U)	≤ 5.0	≤ 5.0	≤ 5.0	≤ 5.0	≤ 5.0
No. of Fuel Rod Locations	179	179	176	180	173
Fuel Rod Clad O.D. (in.)	≥ 0.400	≥ 0.417	≥ 0.440	≥ 0.422	≥ 0.3415
Fuel Rod Clad I.D. (in.)	≤ 0.3514	≤ 0.3734	≤ 0.3880	≤ 0.3890	≤ 0.3175
Fuel Pellet Dia. (in.)(Note 7)	≤ 0.3444	≤ 0.3659	≤ 0.3805	≤ 0.3835	≤ 0.3130
Fuel Rod Pitch (in.)	≤ 0.556	≤ 0.556	≤ 0.580	≤ 0.556	Note 6
Active Fuel Length (in.)	≤ 150	≤ 150	≤ 150	≤ 144	≤ 102
No. of Guide and/or Instrument Tubes	17	17	5 (Note 4)	16	0
Guide/Instrument Tube Thickness (in.)	≥ 0.017	≥ 0.017	≥ 0.038	≥ 0.0145	N/A

Table 2.1-2 (page 2 of 4)
PWR FUEL ASSEMBLY CHARACTERISTICS (Note 1)

Fuel Assembly Array/Class	**15x15A**	**15x15B**	**15x15C**	**15x15D**	**15x15E**	**15x15F**
Clad Material	ZR	ZR	ZR	ZR	ZR	ZR
Design Initial U (kg/assy.) (Note 3)	≤ 473	≤ 473	≤ 473	≤ 495	≤ 495	≤ 495
Initial Enrichment (MPC-24 and 24E without soluble boron credit) (wt % ^{235}U)	≤ 4.1 (24) ≤ 4.5 (24E)	≤ 4.1 (24) ≤ 4.5 (24E)	≤ 4.1 (24) ≤ 4.5 (24E)	≤ 4.1 (24) ≤ 4.5 (24E)	≤ 4.1 (24) ≤ 4.5 (24E)	≤ 4.1 (24) ≤ 4.5 (24E)
Initial Enrichment (MPC-24, 24E, or 32 with soluble boron credit - see Note 5)(wt % ^{235}U)	≤ 5.0	≤ 5.0	≤ 5.0	≤ 5.0	≤ 5.0	≤ 5.0
No. of Fuel Rod Locations	204	204	204	208	208	208
Fuel Rod Clad O.D. (in.)	≥ 0.418	≥ 0.420	≥ 0.417	≥ 0.430	≥ 0.428	≥ 0.428
Fuel Rod Clad I.D. (in.)	≤ 0.3660	≤ 0.3736	≤ 0.3640	≤ 0.3800	≤ 0.3790	≤ 0.3820
Fuel Pellet Dia. (in.) (Note 7)	≤ 0.3580	≤ 0.3671	≤ 0.3570	≤ 0.3735	≤ 0.3707	≤ 0.3742
Fuel Rod Pitch (in.)	≤ 0.550	≤ 0.563	≤ 0.563	≤ 0.568	≤ 0.568	≤ 0.568
Active Fuel Length (in.)	≤ 150	≤ 150	≤ 150	≤ 150	≤ 150	≤ 150
No. of Guide and/or Instrument Tubes	21	21	21	17	17	17
Guide/Instrument Tube Thickness (in.)	≥ 0.0165	≥ 0.015	≥ 0.0165	≥ 0.0150	≥ 0.0140	≥ 0.0140

Table 2.1-2 (page 3 of 4)
PWR FUEL ASSEMBLY CHARACTERISTICS (Note 1)

Fuel Assembly Array/ Class	**15x15G**	**15x15H**	**16x16A**	**17x17A**	**17x17B**	**17x17C**
Clad Material	SS	ZR	ZR	ZR	ZR	ZR
Design Initial U (kg/assy.)(Note 3)	≤ 420	≤ 495	≤ 448	≤ 433	≤ 474	≤ 480
Initial Enrichment (MPC-24and 24E without soluble boron credit) (wt % ^{235}U)	≤ 4.0 (24) ≤ 4.5 (24E)	≤ 3.8 (24) ≤ 4.2 (24E)	≤ 4.6 (24) ≤ 5.0 (24E)	≤ 4.0 (24) ≤ 4.4 (24E)	≤ 4.0 (24) ≤ 4.4 (24E)	≤ 4.0 (24) ≤ 4.4 (24E)
Initial Enrichment (MPC-24, 24E, or 32 with soluble boron credit - see Note 5) (wt % ^{235}U)	≤ 5.0	≤ 5.0	≤ 5.0	≤ 5.0	≤ 5.0	≤ 5.0
No. of Fuel Rod Locations	204	208	236	264	264	264
Fuel Rod Clad O.D. (in.)	≥ 0.422	≥ 0.414	≥ 0.382	≥ 0.360	≥ 0.372	≥ 0.377
Fuel Rod Clad I.D. (in.)	≤ 0.3890	≤ 0.3700	≤ 0.3350	≤ 0.3150	≤ 0.3310	≤ 0.3330
Fuel Pellet Dia. (in.) (Note 7)	≤ 0.3825	≤ 0.3622	≤ 0.3255	≤ 0.3088	≤ 0.3232	≤ 0.3252
Fuel Rod Pitch (in.)	≤ 0.563	≤ 0.568	≤ 0.506	≤ 0.496	≤ 0.496	≤ 0.502
Active Fuel Length (in.)	≤ 144	≤ 150	≤ 150	≤ 150	≤ 150	≤ 150
No. of Guide and/or Instrument Tubes	21	17	5 (Note 4)	25	25	25
Guide/Instrument Tube Thickness (in.)	≥ 0.0145	≥ 0.0140	≥ 0.0350	≥ 0.016	≥ 0.014	≥ 0.020

Table 2.1-2 (page 4 of 4)
PWR FUEL ASSEMBLY CHARACTERISTICS

Notes:

1. All dimensions are design nominal values. Maximum and minimum dimensions are specified to bound variations in design nominal values among fuel assemblies within a given array/class.
2. Deleted.
3. Design initial uranium weight is the nominal uranium weight specified for each assembly by the fuel manufacturer or reactor user. For each PWR fuel assembly, the total uranium weight limit specified in this table may be increased up to 2.0 percent for comparison with users' fuel records to account for manufacturer's tolerances.
4. Each guide tube replaces four fuel rods.
5. Soluble boron concentration per LCO 3.3.1of Appendix A-100U.
6. This fuel assembly array/class includes only the Indian Point Unit 1 fuel assembly. This fuel assembly has two pitches in different sectors of the assembly. These pitches are 0.441 inches and 0.453 inches.
7. Annular fuel pellets are allowed in the top and bottom 12" of the active fuel length.

Table 2.1-3 (page 1 of 5)
BWR FUEL ASSEMBLY CHARACTERISTICS (Note 1)

Fuel Assembly Array/Class	**6x6A**	**6x6B**	**6x6C**	**7x7A**	**7x7B**	**8x8A**
Clad Material	ZR	ZR	ZR	ZR	ZR	ZR
Design Initial U (kg/assy.) (Note 3)	≤ 110	≤ 110	≤ 110	≤ 100	≤ 198	≤ 120
Maximum PLANAR-AVERAGE INITIAL ENRICHMENT (wt.% ^{235}U)	≤ 2.7	≤ 2.7 for the UO_2 rods. See Note 4 for MOX rods	≤ 2.7	≤ 2.7	≤ 4.2	≤ 2.7
Initial Maximum Rod Enrichment (wt.% ^{235}U)	≤ 4.0	≤ 4.0	≤ 4.0	≤ 5.5	≤ 5.0	≤ 4.0
No. of Fuel Rod Locations	35 or 36	35 or 36 (up to 9 MOX rods)	36	49	49	63 or 64
Fuel Rod Clad O.D. (in.)	≥ 0.5550	≥ 0.5625	≥ 0.5630	≥ 0.4860	≥ 0.5630	≥ 0.4120
Fuel Rod Clad I.D. (in.)	≤ 0.5105	≤ 0.4945	≤ 0.4990	≤ 0.4204	≤ 0.4990	≤ 0.3620
Fuel Pellet Dia. (in.)	≤ 0.4980	≤ 0.4820	≤ 0.4880	≤ 0.4110	≤ 0.4910	≤ 0.3580
Fuel Rod Pitch (in.)	≤ 0.710	≤ 0.710	≤ 0.740	≤ 0.631	≤ 0.738	≤ 0.523
Active Fuel Length (in.)	≤ 120	≤ 120	≤ 77.5	≤ 80	≤ 150	≤ 120
No. of Water Rods (Note 11)	1 or 0	1 or 0	0	0	0	1 or 0
Water Rod Thickness (in.)	> 0	> 0	N/A	N/A	N/A	≥ 0
Channel Thickness (in.)	≤ 0.060	≤ 0.060	≤ 0.060	≤ 0.060	≤ 0.120	≤ 0.100

Table 2.1-3 (2 of 5)
BWR FUEL ASSEMBLY CHARACTERISTICS (Note 1)

Fuel Assembly Array/Class	**8x8B**	**8x8C**	**8x8D**	**8x8E**	**8x8F**	**9x9A**
Clad Material	ZR	ZR	ZR	ZR	ZR	ZR
Design Initial U (kg/assy.) (Note 3)	≤ 192	≤ 190	≤ 190	< 190	≤ 191	≤ 180
Maximum PLANAR-AVERAGE INITIAL ENRICHMENT (wt.% ^{235}U)	≤ 4.2	≤ 4.2	≤ 4.2	≤ 4.2	≤ 4.0	≤ 4.2
Initial Maximum Rod Enrichment (wt.% ^{235}U)	≤ 5.0	≤ 5.0	≤ 5.0	≤ 5.0	≤ 5.0	≤ 5.0
No. of Fuel Rod Locations	63 or 64	62	60 or 61	59	64	74/66 (Note 5)
Fuel Rod Clad O.D. (in.)	≥ 0.4840	≥ 0.4830	≥ 0.4830	≥ 0.4930	≥ 0.4576	≥ 0.4400
Fuel Rod Clad I.D. (in.)	≤ 0.4295	≤ 0.4250	≤ 0.4230	≤ 0.4250	≤ 0.3996	≤ 0.3840
Fuel Pellet Dia. (in.)	≤ 0.4195	≤ 0.4160	≤ 0.4140	≤ 0.4160	≤ 0.3913	≤ 0.3760
Fuel Rod Pitch (in.)	≤ 0.642	≤ 0.641	≤ 0.640	≤ 0.640	≤ 0.609	≤ 0.566
Design Active Fuel Length (in.)	≤ 150	≤ 150	≤ 150	≤ 150	≤ 150	≤ 150
No. of Water Rods (Note 11)	1 or 0	2	1 - 4 (Note 7)	5	N/A (Note 12)	2
Water Rod Thickness (in.)	≥ 0.034	> 0.00	> 0.00	≥ 0.034	≥ 0.0315	> 0.00
Channel Thickness (in.)	≤ 0.120	≤ 0.120	≤ 0.120	≤ 0.100	≤ 0.055	≤ 0.120

Table 2.1-3 (page 3 of 5)
BWR FUEL ASSEMBLY CHARACTERISTICS (Note 1)

Fuel Assembly Array/Class	**9x9B**	**9x9C**	**9x9D**	**9x9E (Note 13)**	**9x9F (Note 13)**	**9x9G**
Clad Material	ZR	ZR	ZR	ZR	ZR	ZR
Design Initial U (kg/assy.)(Note 3)	≤ 180	≤ 182	≤ 182	≤ 183	≤ 183	≤ 164
Maximum PLANAR-AVERAGE INITIAL ENRICHMENT (wt.% ^{235}U)	≤ 4.2	≤ 4.2	≤ 4.2	≤ 4.0	≤ 4.0	≤ 4.2
Initial Maximum Rod Enrichment (wt.% ^{235}U)	≤ 5.0	≤ 5.0	≤ 5.0	≤ 5.0	≤ 5.0	≤ 5.0
No. of Fuel Rod Locations	72	80	79	76	76	72
Fuel Rod Clad O.D. (in.)	≥ 0.4330	≥ 0.4230	≥ 0.4240	≥ 0.4170	≥ 0.4430	≥ 0.4240
Fuel Rod Clad I.D. (in.)	≤ 0.3810	≤ 0.3640	≤ 0.3640	≤ 0.3640	≤ 0.3860	≤ 0.3640
Fuel Pellet Dia. (in.)	≤ 0.3740	≤ 0.3565	≤ 0.3565	≤ 0.3530	≤ 0.3745	≤ 0.3565
Fuel Rod Pitch (in.)	≤ 0.572	≤ 0.572	≤ 0.572	≤ 0.572	≤ 0.572	≤ 0.572
Design Active Fuel Length (in.)	≤ 150	≤ 150	≤ 150	≤ 150	≤ 150	≤ 150
No. of Water Rods (Note 11)	1 (Note 6)	1	2	5	5	1 (Note 6)
Water Rod Thickness (in.)	> 0.00	≥ 0.020	≥ 0.0300	≥ 0.0120	≥ 0.0120	≥ 0.0320
Channel Thickness (in.)	≤ 0.120	≤ 0.100	≤ 0.100	≤ 0.120	≤ 0.120	≤ 0.120

Table 2.1-3 (page 4 of 5)
BWR FUEL ASSEMBLY CHARACTERISTICS (Note 1)

Fuel Assembly Array/Class	**10x10A**	**10x10B**	**10x10C**	**10x10D**	**10x10E**
Clad Material	ZR	ZR	ZR	SS	SS
Design Initial U (kg/assy.) (Note 3)	≤ 188	≤ 188	≤ 179	≤ 125	≤ 125
Maximum PLANAR-AVERAGE INITIAL ENRICHMENT (wt.% ^{235}U)	≤ 4.2	≤ 4.2	≤ 4.2	≤ 4.0	≤ 4.0
Initial Maximum Rod Enrichment (wt.% ^{235}U)	≤ 5.0	≤ 5.0	≤ 5.0	≤ 5.0	≤ 5.0
No. of Fuel Rod Locations	92/78 (Note 8)	91/83 (Note 9)	96	100	96
Fuel Rod Clad O.D. (in.)	≥ 0.4040	≥ 0.3957	≥ 0.3780	≥ 0.3960	≥ 0.3940
Fuel Rod Clad I.D. (in.)	≤ 0.3520	≤ 0.3480	≤ 0.3294	≤ 0.3560	≤ 0.3500
Fuel Pellet Dia. (in.)	≤ 0.3455	≤ 0.3420	≤ 0.3224	≤ 0.3500	≤ 0.3430
Fuel Rod Pitch (in.)	≤ 0.510	≤ 0.510	≤ 0.488	≤ 0.565	≤ 0.557
Design Active Fuel Length (in.)	≤ 150	≤ 150	≤ 150	≤ 83	≤ 83
No. of Water Rods (Note 11)	2	1 (Note 6)	5 (Note 10)	0	4
Water Rod Thickness (in.)	≥ 0.0300	> 0.00	≥ 0.031	N/A	≥ 0.022
Channel Thickness (in.)	≤ 0.120	≤ 0.120	≤ 0.055	≤ 0.080	≤ 0.080

Table 2.1-3 (page 5 of 5)
BWR FUEL ASSEMBLY CHARACTERISTICS

Notes:

1. All dimensions are design nominal values. Maximum and minimum dimensions are specified to bound variations in design nominal values among fuel assemblies within a given array/class.

2. Not Used.

3. Design initial uranium weight is the nominal uranium weight specified for each assembly by the fuel manufacturer or reactor user. For each BWR fuel assembly, the total uranium weight limit specified in this table may be increased up to 1.5 percent for comparison with users' fuel records to account for manufacturer tolerances.

4. $\leq$ 0.635 wt. % ^{235}U and $\leq$ 1.578 wt. % total fissile plutonium (^{239}Pu and ^{241}Pu), (wt. % of total fuel weight, i.e., UO_2 plus PuO_2).

5. This assembly class contains 74 total rods; 66 full length rods and 8 partial length rods.

6. Square, replacing nine fuel rods.

7. Variable.

8. This assembly contains 92 total fuel rods; 78 full length rods and 14 partial length rods.

9. This assembly class contains 91 total fuel rods; 83 full length rods and 8 partial length rods.

10. One diamond-shaped water rod replacing the four center fuel rods and four rectangular water rods dividing the assembly into four quadrants.

11. These rods may also be sealed at both ends and contain Zr material in lieu of water.

12. This assembly is known as "QUAD+." It has four rectangular water cross segments dividing the assembly into four quadrants.

13. For the SPC 9x9-5 fuel assembly, each fuel rod must meet either the 9x9E or the 9x9F set of limits for clad O.D., clad I.D., and pellet diameter.

Table 2.1-4
NON-FUEL HARDWARE COOLING AND AVERAGE BURNUP (Notes 1, 2, 3, and 8)

Post-irradiation Cooling Time (years)	**INSERTS** (Note 4) **BURNUP (MWD/MTU)**	**NSA or GUIDE TUBE HARDWARE** (Note 5) **BURNUP (MWD/MTU)**	**CONTROL COMPONENT** (Note 6) **BURNUP (MWD/MTU)**	**APSR BURNUP (MWD/MTU)**
≥ 3	≤ 24,635	NA (Note 7)	NA	NA
≥ 4	≤ 30,000	≤ 20,000	NA	NA
≥ 5	≤ 36,748	≤ 25,000	≤ 630,000	≤ 45,000
≥ 6	≤ 44,102	≤ 30,000	-	≤ 54,500
≥ 7	≤ 52,900	≤ 40,000	-	≤ 68,000
≥ 8	≤ 60,000	≤ 45,000	-	≤ 83,000
≥ 9	-	≤ 50,000	-	≤ 111,000
≥ 10	-	≤ 60,000	-	≤ 180,000
≥ 11	-	≤ 75,000	-	≤ 630,000
≥ 12	-	≤ 90,000	-	-
≥ 13	-	≤ 180,000	-	-
≥ 14	-	≤ 630,000	-	-

Notes:
1. Burnups for NON-FUEL HARDWARE are to be determined based on the burnup and uranium mass of the fuel assemblies in which the component was inserted during reactor operation.
2. Linear interpolation between points is permitted, except that NSA or Guide Tube Hardware and APSR burnups > 180,000 MWD/MTU and ≤ 630,000 MWD/MTU must be cooled ≥ 14 years and ≥ 11 years, respectively.
3. Applicable to uniform loading and regionalized loading.
4. Includes Burnable Poison Rod Assemblies (BPRAs), Wet Annular Burnable Absorbers (WABAs), and vibration suppressor inserts.
5. Includes Thimble Plug Devices (TPDs), water displacement guide tube plugs, and orifice rod assemblies.
6. Includes Control Rod Assemblies (CRAs), Control Element Assemblies (CEAs), and Rod Cluster Control Assemblies (RCCAs).
7. NA means not authorized for loading at this cooling time.
8. Non-fuel hardware burnup and cooling times are not applicable to ITTRs since they are installed post irradiation.

2.4 Decay Heat, Burnup, and Cooling Time Limits for ZR-Clad Fuel

This section provides the limits on ZR-clad fuel assembly decay heat, burnup, and cooling time for storage in the HI-STORM 100 System Model 100U. The method to calculate the limits and verify compliance, including examples, is provided in Chapter 12 of the HI-STORM 100 FSAR.

2.4.1 Uniform Fuel Loading Decay Heat Limits for ZR-clad fuel

Table 2.4-1 provides the maximum allowable decay heat per fuel storage location for ZR-clad fuel in uniform fuel loading for each MPC model.

Table 2.4-1

Maximum Allowable Decay Heat per Fuel Storage Location

(Uniform Loading, ZR-Clad)

MPC Model	**Decay Heat per Fuel Storage Location** (kW)
	Intact Fuel Assemblies
MPC-24	≤ 1.266
MPC-24E	≤ 1.266
MPC-32	≤ 0.949
MPC-68	≤ 0.447

2.4.2 Regionalized Fuel Loading Decay Heat Limits for ZR-Clad Fuel (INTACT FUEL only)

The maximum allowable decay heat per fuel storage location for fuel in regionalized loading is determined using the following equations:

$Q(X) = 2 \times \alpha□ \times Q_0 / (1 + X^y)$

$y = 0.23 / X^{0.1}$

$q_2 = Q(X) / (n_1 \times X + n_2)$

$q_1 = q_2 \times X$

Where:

Q_0 = Maximum uniform storage MPC decay heat (34 kW)

α= Penalty Factor (0.894)

X = Inner region to outer region assembly decay heat ratio
($0.5 \leq X \leq 3$)

n_1 = Number of storage locations in inner region from Table 2.4-2.

n_2 = Number of storage locations in outer region from Table 2.4-2.

Table 2.4-2

Fuel Storage Regions per MPC

MPC Model	Number of Storage Locations in Inner Region (Region 1)	Number of Storage Locations in Outer Region (Region 2)
MPC-24 and MPC-24E	12	12
MPC-32	12	20
MPC-68	32	36

2.4.3 Burnup Limits as a Function of Cooling Time for ZR-Clad Fuel

The maximum allowable fuel assembly average burnup varies with the following parameters:

- Minimum fuel assembly cooling time
- Maximum fuel assembly decay heat
- Minimum fuel assembly average enrichment

The maximum allowable ZR-clad fuel assembly average burnup for a given MINIMUM ENRICHMENT is calculated as described below for minimum cooling times between 3 and 20 years using the maximum permissible decay heat determined in Section 2.4.1 or 2.4.2. Different fuel assembly average burnup limits may be calculated for different minimum enrichments (by individual fuel assembly) for use in choosing the fuel assemblies to be loaded into a given MPC.

2.4.3.1 Choose a fuel assembly minimum enrichment, E_{235}.

2.4.3.2 Calculate the maximum allowable fuel assembly average burnup for a minimum cooling time between 3 and 20 years using the equation below.

$$Bu = (A \times q) + (B \times q^2) + (C \times q^3) + [D \times (E_{235})^2] + (E \times q \times E_{235}) + (F \times q^2 \times E_{235}) + G$$

Where:

Bu = Maximum allowable average burnup per fuel assembly (MWD/MTU)

q = Maximum allowable decay heat per fuel storage location determined in Section 2.4.1 or 2.4.2 (kW)

E_{235} = Minimum fuel assembly average enrichment (wt. % ^{235}U) (e.g., for 4.05 wt.%, use 4.05)

A through G = Coefficients from Tables 2.4-3 and 2.4-4 for the applicable fuel assembly array/class and minimum cooling time

2.4.3.3 Calculated burnup limits shall be rounded down to the nearest integer.

2.4.3.4 Calculated burnup limits greater than 68,200 MWD/MTU for PWR fuel and 65,000 MWD/MTU for BWR must be reduced to be equal to these values.

2.4.3.5 Linear interpolation of calculated burnups between cooling times for a given fuel assembly maximum decay heat and minimum enrichment is permitted. For example, the allowable burnup for a cooling time of 4.5 years may be interpolated between those burnups calculated for 4 year and 5 years.

2.4.3.6 Each ZR-clad fuel assembly to be stored must have a MINIMUM ENRICHMENT greater than or equal to the value used in Step 2.4.3.2.

2.4.4 When complying with the maximum fuel storage location decay heat limits, users must account for the decay heat from both the fuel assembly and any NON-FUEL HARDWARE, as applicable for the particular fuel storage location, to ensure the decay heat emitted by all contents in a storage location does not exceed the limit.

Table 2.4-3 (Page 1 of 8)

PWR Fuel Assembly Cooling Time-Dependent Coefficients
(ZR-Clad Fuel)

Cooling Time (years)	Array/Class 14x14A						
	A	B	C	D	E	F	G
≥ 3	19311.5	275.367	-59.0252	-139.41	2851.12	-451.845	-615.413
≥ 4	33865.9	-5473.03	851.121	-132.739	3408.58	-656.479	-609.523
≥ 5	46686.2	-13226.9	2588.39	-150.149	3871.87	-806.533	-90.2065
≥ 6	56328.9	-20443.2	4547.38	-176.815	4299.19	-927.358	603.192
≥ 7	64136	-27137.5	6628.18	-200.933	4669.22	-1018.94	797.162
≥ 8	71744.1	-34290.3	9036.9	-214.249	4886.95	-1037.59	508.703
≥ 9	77262	-39724.2	11061	-228.2	5141.35	-1102.05	338.294
≥ 10	82939.8	-45575.6	13320.2	-233.691	5266.25	-1095.94	-73.3159
≥ 11	86541	-49289.6	14921.7	-242.092	5444.54	-1141.6	-83.0603
≥ 12	91383	-54456.7	17107	-242.881	5528.7	-1149.2	-547.579
≥ 13	95877.6	-59404.7	19268	-240.36	5524.35	-1094.72	-933.64
≥ 14	97648.3	-61091.6	20261.7	-244.234	5654.56	-1151.47	-749.836
≥ 15	102533	-66651.5	22799.7	-240.858	5647.05	-1120.32	-1293.34
≥ 16	106216	-70753.8	24830.1	-237.04	5647.63	-1099.12	-1583.89
≥ 17	109863	-75005	27038	-234.299	5652.45	-1080.98	-1862.07
≥ 18	111460	-76482.3	28076.5	-234.426	5703.52	-1104.39	-1695.77
≥ 19	114916	-80339.6	30126.5	-229.73	5663.21	-1065.48	-1941.83
≥ 20	119592	-86161.5	33258.2	-227.256	5700.49	-1100.21	-2474.01

Table 2.4-3 (Page 2 of 8)

PWR Fuel Assembly Cooling Time-Dependent Coefficients
(ZR-Clad Fuel)

Cooling Time (years)	Array/Class 14x14B						
	A	B	C	D	E	F	G
≥ 3	18036.1	63.7639	-24.7251	-130.732	2449.87	-347.748	-858.192
≥ 4	30303.4	-4304.2	598.79	-118.757	2853.18	-486.453	-459.902
≥ 5	40779.6	-9922.93	1722.83	-138.174	3255.69	-608.267	245.251
≥ 6	48806.7	-15248.9	3021.47	-158.69	3570.24	-689.876	833.917
≥ 7	55070.5	-19934.6	4325.62	-179.964	3870.33	-765.849	1203.89
≥ 8	60619.6	-24346	5649.29	-189.701	4042.23	-795.324	1158.12
≥ 9	64605.7	-27677.1	6778.12	-205.459	4292.35	-877.966	1169.88
≥ 10	69083.8	-31509.4	8072.42	-206.157	4358.01	-875.041	856.449
≥ 11	72663.2	-34663.9	9228.96	-209.199	4442.68	-889.512	671.567
≥ 12	74808.9	-36367	9948.88	-214.344	4571.29	-942.418	765.261
≥ 13	78340.3	-39541.1	11173.8	-212.8	4615.06	-957.833	410.807
≥ 14	81274.8	-42172.3	12259.9	-209.758	4626.13	-958.016	190.59
≥ 15	83961.4	-44624.5	13329.1	-207.697	4632.16	-952.876	20.8575
≥ 16	84968.5	-44982.1	13615.8	-207.171	4683.41	-992.162	247.54
≥ 17	87721.6	-47543.1	14781.4	-203.373	4674.3	-988.577	37.9689
≥ 18	90562.9	-50100.4	15940.4	-198.649	4651.64	-982.459	-247.421
≥ 19	93011.6	-52316.6	17049.9	-194.964	4644.76	-994.63	-413.021
≥ 20	95567.8	-54566.6	18124	-190.22	4593.92	-963.412	-551.983

Table 2.4-3 (Page 3 of 8)

PWR Fuel Assembly Cooling Time-Dependent Coefficients
(ZR-Clad Fuel)

Cooling Time (years)	Array/Class 14x14C						
	A	B	C	D	E	F	G
≥ 3	18263.7	174.161	-57.6694	-138.112	2539.74	-369.764	-1372.33
≥ 4	30514.5	-4291.52	562.37	-124.944	2869.17	-481.139	-889.883
≥ 5	41338	-10325.7	1752.96	-141.247	3146.48	-535.709	-248.078
≥ 6	48969.7	-15421.3	2966.33	-163.574	3429.74	-587.225	429.331
≥ 7	55384.6	-20228.9	4261.47	-180.846	3654.55	-617.255	599.251
≥ 8	60240.2	-24093.2	5418.86	-199.974	3893.72	-663.995	693.934
≥ 9	64729	-27745.7	6545.45	-205.385	3986.06	-650.124	512.528
≥ 10	68413.7	-30942.2	7651.29	-216.408	4174.71	-702.931	380.431
≥ 11	71870.6	-33906.7	8692.81	-218.813	4248.28	-704.458	160.645
≥ 12	74918.4	-36522	9660.01	-218.248	4283.68	-696.498	-29.0682
≥ 13	77348.3	-38613.7	10501.8	-220.644	4348.23	-702.266	-118.646
≥ 14	79817.1	-40661.8	11331.2	-218.711	4382.32	-710.578	-236.123
≥ 15	82354.2	-42858.3	12257.3	-215.835	4405.89	-718.805	-431.051
≥ 16	84787.2	-44994.5	13185.9	-213.386	4410.99	-711.437	-572.104
≥ 17	87084.6	-46866.1	14004.8	-206.788	4360.3	-679.542	-724.721
≥ 18	88083.1	-47387.1	14393.4	-208.681	4420.85	-709.311	-534.454
≥ 19	90783.6	-49760.6	15462.7	-203.649	4403.3	-705.741	-773.066
≥ 20	93212	-51753.3	16401.5	-197.232	4361.65	-692.925	-964.628

Table 2.4-3 (Page 4 of 8)

PWR Fuel Assembly Cooling Time-Dependent Coefficients
(ZR-Clad Fuel)

Cooling Time (years)	Array/Class 15x15A/B/C						
	A	B	C	D	E	F	G
≥ 3	15037.3	108.689	-18.8378	-127.422	2050.02	-242.828	-580.66
≥ 4	25506.6	-2994.03	356.834	-116.45	2430.25	-350.901	-356.378
≥ 5	34788.8	-7173.07	1065.9	-124.785	2712.23	-424.681	267.705
≥ 6	41948.6	-11225.3	1912.12	-145.727	3003.29	-489.538	852.112
≥ 7	47524.9	-14770.9	2755.16	-165.889	3253.9	-542.7	1146.96
≥ 8	52596.9	-18348.8	3699.72	-177.17	3415.69	-567.012	1021.41
≥ 9	56055.4	-20837.1	4430.93	-192.168	3625.93	-623.325	1058.61
≥ 10	59611.3	-23402.1	5179.52	-195.105	3699.18	-626.448	868.517
≥ 11	62765.3	-25766.5	5924.71	-195.57	3749.91	-627.139	667.124
≥ 12	65664.4	-28004.8	6670.75	-195.08	3788.33	-628.904	410.783
≥ 13	67281.7	-29116.7	7120.59	-202.817	3929.38	-688.738	492.309
≥ 14	69961.4	-31158.6	7834.02	-197.988	3917.29	-677.565	266.561
≥ 15	72146	-32795.7	8453.67	-195.083	3931.47	-681.037	99.0606
≥ 16	74142.6	-34244.8	9023.57	-190.645	3905.54	-663.682	10.8885
≥ 17	76411.4	-36026.3	9729.98	-188.874	3911.21	-663.449	-151.805
≥ 18	77091	-36088	9884.09	-188.554	3965.08	-708.55	59.3839
≥ 19	79194.5	-37566.4	10477.5	-181.656	3906.93	-682.4	-117.952
≥ 20	81600.4	-39464.5	11281.9	-175.182	3869.49	-677.179	-367.705

Table 2.4-3 (Page 5 of 8)

PWR Fuel Assembly Cooling Time-Dependent Coefficients
(ZR-Clad Fuel)

Cooling Time (years)	Array/Class 15x15D/E/F/H						
	A	B	C	D	E	F	G
≥ 3	14376.7	102.205	-20.6279	-126.017	1903.36	-210.883	-493.065
≥ 4	24351.4	-2686.57	297.975	-110.819	2233.78	-301.615	-152.713
≥ 5	33518.4	-6711.35	958.544	-122.85	2522.7	-371.286	392.608
≥ 6	40377	-10472.4	1718.53	-144.535	2793.29	-426.436	951.528
≥ 7	46105.8	-13996.2	2515.32	-157.827	2962.46	-445.314	1100.56
≥ 8	50219.7	-16677.7	3198.3	-175.057	3176.74	-492.727	1223.62
≥ 9	54281.2	-19555.6	3983.47	-181.703	3279.03	-499.997	1034.55
≥ 10	56761.6	-21287.3	4525.98	-195.045	3470.41	-559.074	1103.3
≥ 11	59820	-23445.2	5165.43	-194.997	3518.23	-561.422	862.68
≥ 12	62287.2	-25164.6	5709.9	-194.771	3552.69	-561.466	680.488
≥ 13	64799	-27023.7	6335.16	-192.121	3570.41	-561.326	469.583
≥ 14	66938.7	-28593.1	6892.63	-194.226	3632.92	-583.997	319.867
≥ 15	68116.5	-29148.6	7140.09	-192.545	3670.39	-607.278	395.344
≥ 16	70154.9	-30570.1	7662.91	-187.366	3649.14	-597.205	232.318
≥ 17	72042.5	-31867.6	8169.01	-183.453	3646.92	-603.907	96.0388
≥ 18	73719.8	-32926.1	8596.12	-177.896	3614.57	-592.868	46.6774
≥ 19	75183.1	-33727.4	8949.64	-172.386	3581.13	-586.347	3.57256
≥ 20	77306.1	-35449	9690.02	-173.784	3636.87	-626.321	-205.513

Table 2.4-3 (Page 6 of 8)

PWR Fuel Assembly Cooling Time-Dependent Coefficients
(ZR-Clad Fuel)

Cooling Time (years)	Array/Class 16X16A						
	A	B	C	D	E	F	G
≥ 3	16226.8	143.714	-32.4809	-136.707	2255.33	-291.683	-699.947
≥ 4	27844.2	-3590.69	444.838	-124.301	2644.09	-411.598	-381.106
≥ 5	38191.5	-8678.48	1361.58	-132.855	2910.45	-473.183	224.473
≥ 6	46382.2	-13819.6	2511.32	-158.262	3216.92	-532.337	706.656
≥ 7	52692.3	-18289	3657.18	-179.765	3488.3	-583.133	908.839
≥ 8	57758.7	-22133.7	4736.88	-199.014	3717.42	-618.83	944.903
≥ 9	62363.3	-25798.7	5841.18	-207.025	3844.38	-625.741	734.928
≥ 10	66659.1	-29416.3	6993.31	-216.458	3981.97	-642.641	389.366
≥ 11	69262.7	-31452.7	7724.66	-220.836	4107.55	-681.043	407.121
≥ 12	72631.5	-34291.9	8704.8	-219.929	4131.5	-662.513	100.093
≥ 13	75375.3	-36589.3	9555.88	-217.994	4143.15	-644.014	-62.3294
≥ 14	78178.7	-39097.1	10532	-221.923	4226.28	-667.012	-317.743
≥ 15	79706.3	-40104	10993.3	-218.751	4242.12	-670.665	-205.579
≥ 16	82392.6	-42418.9	11940.7	-216.278	4274.09	-689.236	-479.752
≥ 17	84521.8	-44150.5	12683.3	-212.056	4245.99	-665.418	-558.901
≥ 18	86777.1	-45984.8	13479	-204.867	4180.8	-621.805	-716.366
≥ 19	89179.7	-48109.8	14434.5	-206.484	4230.03	-648.557	-902.1
≥ 20	90141.7	-48401.4	14702.6	-203.284	4245.54	-670.655	-734.604

Table 2.4-3 (Page 7 of 8)

PWR Fuel Assembly Cooling Time-Dependent Coefficients
(ZR-Clad Fuel)

Cooling Time (years)	Array/Class 17x17A						
	A	B	C	D	E	F	G
≥ 3	15985.1	3.53963	-9.04955	-128.835	2149.5	-260.415	-262.997
≥ 4	27532.9	-3494.41	428.199	-119.504	2603.01	-390.91	-140.319
≥ 5	38481.2	-8870.98	1411.03	-139.279	3008.46	-492.881	388.377
≥ 6	47410.9	-14479.6	2679.08	-162.13	3335.48	-557.777	702.164
≥ 7	54596.8	-19703.2	4043.46	-181.339	3586.06	-587.634	804.05
≥ 8	60146.1	-24003.4	5271.54	-201.262	3830.32	-621.706	848.454
≥ 9	65006.3	-27951	6479.04	-210.753	3977.69	-627.805	615.84
≥ 10	69216	-31614.7	7712.58	-222.423	4173.4	-672.33	387.879
≥ 11	73001.3	-34871.1	8824.44	-225.128	4238.28	-657.259	101.654
≥ 12	76326.1	-37795.9	9887.35	-226.731	4298.11	-647.55	-122.236
≥ 13	78859.9	-40058.9	10797.1	-231.798	4402.14	-669.982	-203.383
≥ 14	82201.3	-43032.5	11934.1	-228.162	4417.99	-661.61	-561.969
≥ 15	84950	-45544.6	12972.4	-225.369	4417.84	-637.422	-771.254
≥ 16	87511.8	-47720	13857.7	-219.255	4365.24	-585.655	-907.775
≥ 17	90496.4	-50728.9	15186	-223.019	4446.51	-613.378	-1200.94
≥ 18	91392.5	-51002.4	15461.4	-220.272	4475.28	-636.398	-1003.81
≥ 19	94343.9	-53670.8	16631.6	-214.045	4441.31	-616.201	-1310.01
≥ 20	96562.9	-55591.2	17553.4	-209.917	4397.67	-573.199	-1380.64

Table 2.4-3 (Page 8 of 8)

PWR Fuel Assembly Cooling Time-Dependent Coefficients
(ZR-Clad Fuel)

Cooling Time (years)	Array/Class 17x17B/C						
	A	B	C	D	E	F	G
≥ 3	14738	47.5402	-13.8187	-127.895	1946.58	-219.289	-389.029
≥ 4	25285.2	-3011.92	350.116	-115.75	2316.89	-319.23	-220.413
≥ 5	34589.6	-7130.34	1037.26	-128.673	2627.27	-394.58	459.642
≥ 6	42056.2	-11353.7	1908.68	-150.234	2897.38	-444.316	923.971
≥ 7	47977.6	-15204.8	2827.4	-173.349	3178.25	-504.16	1138.82
≥ 8	52924	-18547.6	3671.08	-183.025	3298.64	-501.278	1064.68
≥ 9	56465.5	-21139.4	4435.67	-200.386	3538	-569.712	1078.78
≥ 10	60190.9	-23872.7	5224.31	-203.233	3602.88	-562.312	805.336
≥ 11	63482.1	-26431.1	6035.79	-205.096	3668.84	-566.889	536.011
≥ 12	66095	-28311.8	6637.72	-204.367	3692.68	-555.305	372.223
≥ 13	67757.4	-29474.4	7094.08	-211.649	3826.42	-606.886	437.412
≥ 14	70403.7	-31517.4	7807.15	-207.668	3828.69	-601.081	183.09
≥ 15	72506.5	-33036.1	8372.59	-203.428	3823.38	-594.995	47.5175
≥ 16	74625.2	-34620.5	8974.32	-199.003	3798.57	-573.098	-95.0221
≥ 17	76549	-35952.6	9498.14	-193.459	3766.52	-556.928	-190.662
≥ 18	77871.9	-36785.5	9916.91	-195.592	3837.65	-599.45	-152.261
≥ 19	79834.8	-38191.6	10501.9	-190.83	3812.46	-589.635	-286.847
≥ 20	81975.5	-39777.2	11174.5	-185.767	3795.78	-595.664	-475.978

Table 2.4-4 (Page 1 of 10)

BWR Fuel Assembly Cooling Time-Dependent Coefficients
(ZR-Clad Fuel)

Cooling Time (years)	Array/Class 7x7B						
	A	B	C	D	E	F	G
≥ 3	26409.1	28347.5	-16858	-147.076	5636.32	-1606.75	1177.88
≥ 4	61967.8	-6618.31	-4131.96	-113.949	6122.77	-2042.85	-96.7439
≥ 5	91601.1	-49298.3	17826.5	-132.045	6823.14	-2418.49	-185.189
≥ 6	111369	-80890.1	35713.8	-150.262	7288.51	-2471.1	86.6363
≥ 7	126904	-108669	53338.1	-167.764	7650.57	-2340.78	150.403
≥ 8	139181	-132294	69852.5	-187.317	8098.66	-2336.13	97.5285
≥ 9	150334	-154490	86148.1	-193.899	8232.84	-2040.37	-123.029
≥ 10	159897	-173614	100819	-194.156	8254.99	-1708.32	-373.605
≥ 11	166931	-186860	111502	-193.776	8251.55	-1393.91	-543.677
≥ 12	173691	-201687	125166	-202.578	8626.84	-1642.3	-650.814
≥ 13	180312	-215406	137518	-201.041	8642.19	-1469.45	-810.024
≥ 14	185927	-227005	148721	-197.938	8607.6	-1225.95	-892.876
≥ 15	191151	-236120	156781	-191.625	8451.86	-846.27	-1019.4
≥ 16	195761	-244598	165372	-187.043	8359.19	-572.561	-1068.19
≥ 17	200791	-256573	179816	-197.26	8914.28	-1393.37	-1218.63
≥ 18	206068	-266136	188841	-187.191	8569.56	-730.898	-1363.79
≥ 19	210187	-273609	197794	-182.151	8488.23	-584.727	-1335.59
≥ 20	213731	-278120	203074	-175.864	8395.63	-457.304	-1364.38

Table 2.4-4 (Page 2 of 10)

BWR Fuel Assembly Cooling Time-Dependent Coefficients
(ZR-Clad Fuel)

Cooling Time (years)	Array/Class 8x8B						
	A	B	C	D	E	F	G
≥ 3	28219.6	28963.7	-17616.2	-147.68	5887.41	-1730.96	1048.21
≥ 4	66061.8	-10742.4	-1961.82	-123.066	6565.54	-2356.05	-298.005
≥ 5	95790.7	-53401.7	19836.7	-134.584	7145.41	-2637.09	-298.858
≥ 6	117477	-90055.9	41383.9	-154.758	7613.43	-2612.69	-64.9921
≥ 7	134090	-120643	60983	-168.675	7809	-2183.3	-40.8885
≥ 8	148186	-149181	81418.7	-185.726	8190.07	-2040.31	-260.773
≥ 9	159082	-172081	99175.2	-197.185	8450.86	-1792.04	-381.705
≥ 10	168816	-191389	113810	-195.613	8359.87	-1244.22	-613.594
≥ 11	177221	-210599	131099	-208.3	8810	-1466.49	-819.773
≥ 12	183929	-224384	143405	-207.497	8841.33	-1227.71	-929.708
≥ 13	191093	-240384	158327	-204.95	8760.17	-811.708	-1154.76
≥ 14	196787	-252211	169664	-204.574	8810.95	-610.928	-1208.97
≥ 15	203345	-267656	186057	-208.962	9078.41	-828.954	-1383.76
≥ 16	207973	-276838	196071	-204.592	9024.17	-640.808	-1436.43
≥ 17	213891	-290411	211145	-202.169	9024.19	-482.1	-1595.28
≥ 18	217483	-294066	214600	-194.243	8859.35	-244.684	-1529.61
≥ 19	220504	-297897	219704	-190.161	8794.97	-10.9863	-1433.86
≥ 20	227821	-318395	245322	-194.682	9060.96	-350.308	-1741.16

Table 2.4-4 (Page 3 of 10)

BWR Fuel Assembly Cooling Time-Dependent Coefficients
(ZR-Clad Fuel)

Cooling Time (years)	Array/Class 8x8C/D/E						
	A	B	C	D	E	F	G
≥ 3	28592.7	28691.5	-17773.6	-149.418	5969.45	-1746.07	1063.62
≥ 4	66720.8	-12115.7	-1154	-128.444	6787.16	-2529.99	-302.155
≥ 5	96929.1	-55827.5	21140.3	-136.228	7259.19	-2685.06	-334.328
≥ 6	118190	-92000.2	42602.5	-162.204	7907.46	-2853.42	-47.5465
≥ 7	135120	-123437	62827.1	-172.397	8059.72	-2385.81	-75.0053
≥ 8	149162	-152986	84543.1	-195.458	8559.11	-2306.54	-183.595
≥ 9	161041	-177511	103020	-200.087	8632.84	-1864.4	-433.081
≥ 10	171754	-201468	122929	-209.799	8952.06	-1802.86	-755.742
≥ 11	179364	-217723	137000	-215.803	9142.37	-1664.82	-847.268
≥ 12	186090	-232150	150255	-216.033	9218.36	-1441.92	-975.817
≥ 13	193571	-249160	165997	-213.204	9146.99	-1011.13	-1119.47
≥ 14	200034	-263671	180359	-210.559	9107.54	-694.626	-1312.55
≥ 15	205581	-275904	193585	-216.242	9446.57	-1040.65	-1428.13
≥ 16	212015	-290101	207594	-210.036	9212.93	-428.321	-1590.7
≥ 17	216775	-299399	218278	-204.611	9187.86	-398.353	-1657.6
≥ 18	220653	-306719	227133	-202.498	9186.34	-181.672	-1611.86
≥ 19	224859	-314004	235956	-193.902	8990.14	145.151	-1604.71
≥ 20	228541	-320787	245449	-200.727	9310.87	-230.252	-1570.18

Table 2.4-4 (Page 4 of 10)

BWR Fuel Assembly Cooling Time-Dependent Coefficients
(ZR-Clad Fuel)

Cooling Time (years)	Array/Class 9x9A						
	A	B	C	D	E	F	G
≥ 3	30538.7	28463.2	-18105.5	-150.039	6226.92	-1876.69	1034.06
≥ 4	71040.1	-16692.2	1164.15	-128.241	7105.27	-2728.58	-414.09
≥ 5	100888	-60277.7	24150.1	-142.541	7896.11	-3272.86	-232.197
≥ 6	124846	-102954	50350.8	-161.849	8350.16	-3163.44	-91.1396
≥ 7	143516	-140615	76456.5	-185.538	8833.04	-2949.38	-104.802
≥ 8	158218	-171718	99788.2	-196.315	9048.88	-2529.26	-259.929
≥ 9	172226	-204312	126620	-214.214	9511.56	-2459.19	-624.954
≥ 10	182700	-227938	146736	-215.793	9555.41	-1959.92	-830.943
≥ 11	190734	-246174	163557	-218.071	9649.43	-1647.5	-935.021
≥ 12	199997	-269577	186406	-223.975	9884.92	-1534.34	-1235.27
≥ 13	207414	-287446	204723	-228.808	10131.7	-1614.49	-1358.61
≥ 14	215263	-306131	223440	-220.919	9928.27	-988.276	-1638.05
≥ 15	221920	-321612	239503	-217.949	9839.02	-554.709	-1784.04
≥ 16	226532	-331778	252234	-216.189	9893.43	-442.149	-1754.72
≥ 17	232959	-348593	272609	-219.907	10126.3	-663.84	-1915.3
≥ 18	240810	-369085	296809	-219.729	10294.6	-859.302	-2218.87
≥ 19	244637	-375057	304456	-210.997	10077.8	-425.446	-2127.83
≥ 20	248112	-379262	309391	-204.191	9863.67	100.27	-2059.39

Table 2.4-4 (Page 5 of 10)

BWR Fuel Assembly Cooling Time-Dependent Coefficients
(ZR-Clad Fuel)

Cooling Time (years)	Array/Class 9x9B						
	A	B	C	D	E	F	G
≥ 3	30613.2	28985.3	-18371	-151.117	6321.55	-1881.28	988.92
≥ 4	71346.6	-15922.9	631.132	-128.876	7232.47	-2810.64	-471.737
≥ 5	102131	-60654.1	23762.7	-140.748	7881.6	-3156.38	-417.979
≥ 6	127187	-105842	51525.2	-162.228	8307.4	-2913.08	-342.13
≥ 7	146853	-145834	79146.5	-185.192	8718.74	-2529.57	-484.885
≥ 8	162013	-178244	103205	-197.825	8896.39	-1921.58	-584.013
≥ 9	176764	-212856	131577	-215.41	9328.18	-1737.12	-1041.11
≥ 10	186900	-235819	151238	-218.98	9388.08	-1179.87	-1202.83
≥ 11	196178	-257688	171031	-220.323	9408.47	-638.53	-1385.16
≥ 12	205366	-280266	192775	-223.715	9592.12	-472.261	-1661.6
≥ 13	215012	-306103	218866	-231.821	9853.37	-361.449	-1985.56
≥ 14	222368	-324558	238655	-228.062	9834.57	3.47358	-2178.84
≥ 15	226705	-332738	247316	-224.659	9696.59	632.172	-2090.75
≥ 16	233846	-349835	265676	-221.533	9649.93	913.747	-2243.34
≥ 17	243979	-379622	300077	-222.351	9792.17	1011.04	-2753.36
≥ 18	247774	-386203	308873	-220.306	9791.37	1164.58	-2612.25
≥ 19	254041	-401906	327901	-213.96	9645.47	1664.94	-2786.2
≥ 20	256003	-402034	330566	-215.242	9850.42	1359.46	-2550.06

Table 2.4-4 (Page 6 of 10)

BWR Fuel Assembly Cooling Time-Dependent Coefficients
(ZR-Clad Fuel)

Cooling Time (years)	Array/Class 9x9C/D						
	A	B	C	D	E	F	G
≥ 3	30051.6	29548.7	-18614.2	-148.276	6148.44	-1810.34	1006
≥ 4	70472.7	-14696.6	-233.567	-127.728	7008.69	-2634.22	-444.373
≥ 5	101298	-59638.9	23065.2	-138.523	7627.57	-2958.03	-377.965
≥ 6	125546	-102740	49217.4	-160.811	8096.34	-2798.88	-259.767
≥ 7	143887	-139261	74100.4	-184.302	8550.86	-2517.19	-275.151
≥ 8	159633	-172741	98641.4	-194.351	8636.89	-1838.81	-486.731
≥ 9	173517	-204709	124803	-212.604	9151.98	-1853.27	-887.137
≥ 10	182895	-225481	142362	-218.251	9262.59	-1408.25	-978.356
≥ 11	192530	-247839	162173	-217.381	9213.58	-818.676	-1222.12
≥ 12	201127	-268201	181030	-215.552	9147.44	-232.221	-1481.55
≥ 13	209538	-289761	203291	-225.092	9588.12	-574.227	-1749.35
≥ 14	216798	-306958	220468	-222.578	9518.22	-69.9307	-1919.71
≥ 15	223515	-323254	237933	-217.398	9366.52	475.506	-2012.93
≥ 16	228796	-334529	250541	-215.004	9369.33	662.325	-2122.75
≥ 17	237256	-356311	273419	-206.483	9029.55	1551.3	-2367.96
≥ 18	242778	-369493	290354	-215.557	9600.71	659.297	-2589.32
≥ 19	246704	-377971	302630	-210.768	9509.41	1025.34	-2476.06
≥ 20	249944	-382059	308281	-205.495	9362.63	1389.71	-2350.49

Table 2.4-4 (Page 7 of 10)

BWR Fuel Assembly Cooling Time-Dependent Coefficients
(ZR-Clad Fuel)

Cooling Time (years)	Array/Class 9x9E/F						
	A	B	C	D	E	F	G
≥ 3	30284.3	26949.5	-16926.4	-147.914	6017.02	-1854.81	1026.15
≥ 4	69727.4	-17117.2	1982.33	-127.983	6874.68	-2673.01	-359.962
≥ 5	98438.9	-58492	23382.2	-138.712	7513.55	-3038.23	-112.641
≥ 6	119765	-95024.1	45261	-159.669	8074.25	-3129.49	221.182
≥ 7	136740	-128219	67940.1	-182.439	8595.68	-3098.17	315.544
≥ 8	150745	-156607	88691.5	-193.941	8908.73	-2947.64	142.072
≥ 9	162915	-182667	109134	-198.37	8999.11	-2531	-93.4908
≥ 10	174000	-208668	131543	-210.777	9365.52	-2511.74	-445.876
≥ 11	181524	-224252	145280	-212.407	9489.67	-2387.49	-544.123
≥ 12	188946	-240952	160787	-210.65	9478.1	-2029.94	-652.339
≥ 13	193762	-250900	171363	-215.798	9742.31	-2179.24	-608.636
≥ 14	203288	-275191	196115	-218.113	9992.5	-2437.71	-1065.92
≥ 15	208108	-284395	205221	-213.956	9857.25	-1970.65	-1082.94
≥ 16	215093	-301828	224757	-209.736	9789.58	-1718.37	-1303.35
≥ 17	220056	-310906	234180	-201.494	9541.73	-1230.42	-1284.15
≥ 18	224545	-320969	247724	-206.807	9892.97	-1790.61	-1381.9
≥ 19	226901	-322168	250395	-204.073	9902.14	-1748.78	-1253.22
≥ 20	235561	-345414	276856	-198.306	9720.78	-1284.14	-1569.18

Table 2.4-4 (Page 8 of 10)

BWR Fuel Assembly Cooling Time-Dependent Coefficients
(ZR-Clad Fuel)

Cooling Time (years)	Array/Class 9x9G						
	A	B	C	D	E	F	G
≥ 3	35158.5	26918.5	-17976.7	-149.915	6787.19	-2154.29	836.894
≥ 4	77137.2	-19760.1	2371.28	-130.934	8015.43	-3512.38	-455.424
≥ 5	113405	-77931.2	35511.2	-150.637	8932.55	-4099.48	-629.806
≥ 6	139938	-128700	68698.3	-173.799	9451.22	-3847.83	-455.905
≥ 7	164267	-183309	109526	-193.952	9737.91	-3046.84	-737.992
≥ 8	182646	-227630	146275	-210.936	10092.3	-2489.3	-1066.96
≥ 9	199309	-270496	184230	-218.617	10124.3	-1453.81	-1381.41
≥ 10	213186	-308612	221699	-235.828	10703.2	-1483.31	-1821.73
≥ 11	225587	-342892	256242	-236.112	10658.5	-612.076	-2134.65
≥ 12	235725	-370471	285195	-234.378	10604.9	118.591	-2417.89
≥ 13	247043	-404028	323049	-245.79	11158.2	-281.813	-2869.82
≥ 14	253649	-421134	342682	-243.142	11082.3	400.019	-2903.88
≥ 15	262750	-448593	376340	-245.435	11241.2	581.355	-3125.07
≥ 16	270816	-470846	402249	-236.294	10845.4	1791.46	-3293.07
≥ 17	279840	-500272	441964	-241.324	11222.6	1455.84	-3528.25
≥ 18	284533	-511287	458538	-240.905	11367.2	1459.68	-3520.94
≥ 19	295787	-545885	501824	-235.685	11188.2	2082.21	-3954.2
≥ 20	300209	-556936	519174	-229.539	10956	2942.09	-3872.87

Table 2.4-4 (Page 9 of 10)

BWR Fuel Assembly Cooling Time-Dependent Coefficients
(ZR-Clad Fuel)

Cooling Time (years)	Array/Class 10x10A/B						
	A	B	C	D	E	F	G
≥ 3	29285.4	27562.2	-16985	-148.415	5960.56	-1810.79	1001.45
≥ 4	67844.9	-14383	395.619	-127.723	6754.56	-2547.96	-369.267
≥ 5	96660.5	-55383.8	21180.4	-137.17	7296.6	-2793.58	-192.85
≥ 6	118098	-91995	42958	-162.985	7931.44	-2940.84	60.9197
≥ 7	135115	-123721	63588.9	-171.747	8060.23	-2485.59	73.6219
≥ 8	148721	-151690	84143.9	-190.26	8515.81	-2444.25	-63.4649
≥ 9	160770	-177397	104069	-197.534	8673.6	-2101.25	-331.046
≥ 10	170331	-198419	121817	-213.692	9178.33	-2351.54	-472.844
≥ 11	179130	-217799	138652	-209.75	9095.43	-1842.88	-705.254
≥ 12	186070	-232389	151792	-208.946	9104.52	-1565.11	-822.73
≥ 13	192407	-246005	164928	-209.696	9234.7	-1541.54	-979.245
≥ 14	200493	-265596	183851	-207.639	9159.83	-1095.72	-1240.61
≥ 15	205594	-276161	195760	-213.491	9564.23	-1672.22	-1333.64
≥ 16	209386	-282942	204110	-209.322	9515.83	-1506.86	-1286.82
≥ 17	214972	-295149	217095	-202.445	9292.34	-893.6	-1364.97
≥ 18	219312	-302748	225826	-198.667	9272.27	-878.536	-1379.58
≥ 19	223481	-310663	235908	-194.825	9252.9	-785.066	-1379.62
≥ 20	227628	-319115	247597	-199.194	9509.02	-1135.23	-1386.19

Table 2.4-4 (Page 10 of 10)

BWR Fuel Assembly Cooling Time-Dependent Coefficients
(ZR-Clad Fuel)

Cooling Time (years)	Array/Class 10x10C						
	A	B	C	D	E	F	G
≥ 3	31425.3	27358.9	-17413.3	-152.096	6367.53	-1967.91	925.763
≥ 4	71804	-16964.1	1000.4	-129.299	7227.18	-2806.44	-416.92
≥ 5	102685	-62383.3	24971.2	-142.316	7961	-3290.98	-354.784
≥ 6	126962	-105802	51444.6	-164.283	8421.44	-3104.21	-186.615
≥ 7	146284	-145608	79275.5	-188.967	8927.23	-2859.08	-251.163
≥ 8	162748	-181259	105859	-199.122	9052.91	-2206.31	-554.124
≥ 9	176612	-214183	133261	-217.56	9492.17	-1999.28	-860.669
≥ 10	187756	-239944	155315	-219.56	9532.45	-1470.9	-1113.42
≥ 11	196580	-260941	174536	-222.457	9591.64	-944.473	-1225.79
≥ 12	208017	-291492	204805	-233.488	10058.3	-1217.01	-1749.84
≥ 13	214920	-307772	221158	-234.747	10137.1	-897.23	-1868.04
≥ 14	222562	-326471	240234	-228.569	9929.34	-183.47	-2016.12
≥ 15	228844	-342382	258347	-226.944	9936.76	117.061	-2106.05
≥ 16	233907	-353008	270390	-223.179	9910.72	360.39	-2105.23
≥ 17	244153	-383017	304819	-227.266	10103.2	380.393	-2633.23
≥ 18	249240	-395456	321452	-226.989	10284.1	169.947	-2623.67
≥ 19	254343	-406555	335240	-220.569	10070.5	764.689	-2640.2
≥ 20	260202	-421069	354249	-216.255	10069.9	854.497	-2732.77

3.0 DESIGN FEATURES

3.1 Site

3.1.1 Site Location

The HI-STORM 100 Cask System is authorized for general use by 10 CFR Part 50 license holders at various site locations under the provisions of 10 CFR 72, Subpart K.

3.2 Design Features Important for Criticality Control

3.2.1 MPC-24

1. Flux trap size: ≥ 1.09 in.
2. ^{10}B loading in the neutron absorbers: ≥ 0.0267 g/cm^2 (Boral) and ≥ 0.0223 g/cm^2 (METAMIC)

3.2.2 MPC-68

1. Fuel cell pitch: ≥ 6.43 in.
2. ^{10}B loading in the neutron absorbers: ≥ 0.0372 g/cm2 (Boral) and ≥ 0.0310 g/cm2 (METAMIC)

3.2.3 MPC-24E

1. Flux trap size:

   i. Cells 3, 6, 19, and 22: ≥ 0.776 inch

   ii. All Other Cells: ≥ 1.076 inches
2. ^{10}B loading in the neutron absorbers: ≥ 0.0372 g/cm^2 (Boral) and ≥ 0.0310 g/cm^2 (METAMIC)

3.2.4 MPC-32

1. Fuel cell pitch: ≥ 9.158 inches
2. ^{10}B loading in the neutron absorbers: ≥ 0.0372 g/cm^2 (Boral) and ≥ 0.0310 g/cm^2 (METAMIC)

3.2.5 Not Used

DESIGN FEATURES

3.2 Design features Important for Criticality Control (cont'd)

3.2.6 Fuel spacers shall be sized to ensure that the active fuel region of intact fuel assemblies remains within the neutron poison region of the MPC basket with water in the MPC.

3.2.7 The B_4C content in METAMIC shall be ≤ 33.0 wt.%.

3.2.8 Neutron Absorber Tests

Section 9.1.5.3 of the HI-STORM 100 FSAR is hereby incorporated by reference into the HI-STORM 100 CoC. The minimum ^{10}B for the neutron absorber shall meet the minimum requirements for each MPC model specified in Sections 3.2.1 through 3.2.4 above.

3.3 Codes and Standards

The American Society of Mechanical Engineers Boiler and Pressure Vessel Code (ASME Code), 1995 Edition with Addenda through 1997, is the governing Code for the HI-STORM 100 System MPCs, OVERPACKs, and TRANSFER CASKs, as clarified in Specification 3.3.1 below, except for Code Sections V and IX. The ASME Code paragraphs applicable to the 100U VVM are listed in Table 3-2. The latest effective editions of ASME Code Sections V and IX, including addenda, may be used for activities governed by those sections, provided a written reconciliation of the later edition against the 1995 Edition, including addenda, is performed by the certificate holder. American Concrete Institute (ACI) 349-85 is the governing Code for plain concrete as clarified in Appendix 1.D of the Final Safety Analysis Report for the HI-STORM 100 Cask System.

3.3.1 <u>Alternatives to Codes, Standards, and Criteria</u>

Table 3-1 of Appendix B to CoC-1014 lists approved alternatives to the ASME Code for the design of the MPCs and TRANSFER CASKs of the HI-STORM 100U System.

3.3.2 <u>Construction/Fabrication Alternatives to Codes, Standards, and Criteria</u>

Proposed alternatives to the ASME Code, Section III, 1995 Edition with Addenda through 1997 including modifications to the alternatives allowed by Specification 3.3.1 may be used on a case-specific basis when authorized by the Director of the Office of Nuclear Material Safety and Safeguards or designee. The request for such alternative should demonstrate that:

1. The proposed alternatives would provide an acceptable level of quality and safety, or

(continued)

DESIGN FEATURES

3.3.2 Construction/Fabrication Alternatives to Codes, Standards, and Criteria (cont'd)

2. Compliance with the specified requirements of the ASME Code, Section III, 1995 Edition with Addenda through 1997, would result in hardship or unusual difficulty without a compensating increase in the level of quality and safety.

Requests for alternatives shall be submitted in accordance with 10 CFR 72.4.

(continued)

DESIGN FEATURES

Table 3-1: Not Used

Table 3-2
Applicable Code Paragraphs for Underground VVMs

	Item	Code Paragraph†	Explanation and Applicability
1.	Definition of primary and secondary members	NF-1215	
2.	Jurisdictional boundary	NF-1133	The "intervening elements" are termed interfacing SSCs in this FSAR.
3.	Certification of Material	NF-2130(b) and (c)	Materials shall be certified to the applicable Section II of the ASME Code or equivalent ASTM Specification.
4.	Heat treatment of material	NF-2170 and NF-2180	
5.	Storage of welding material	NF-2400	
6.	Structural Analysis of Interfacing SSCs	ACI 318-05	The VVM Interface Pad and Support Foundation are reinforced concrete structures. Loadings come from the external environment and from the VVM. Sections of the Code that may reasonably be applied to subterranean application are applicable.
7.	Welding procedure	Section IX	
8.	Welding material	Section II	
9.	Loading conditions	NF-3111	
10.	Allowable stress values	NF-3112.3	
11.	Rolling and sliding supports	NF-3424	
12.	Differential thermal expansion	NF-3127	
13.	Stress analysis	NF-3143 NF-3380 NF-3522 NF-3523	Provisions for stress analysis for Class 3 plate and shell supports and for linear supports are applicable for CEC shells and CLOSURE LID.
14.	Cutting of plate stock	NF-4211 NF-4211.1	
15.	Forming	NF-4212	
16.	Forming tolerance	NF-4221	Applies to the CEC Divider Shell and CEC Container Shell
17.	Fitting and Aligning Tack Welds	NF-4231 NF-4231.1	
18.	Alignment	NF-4232	
19.	Storage of Welding Materials	NF-4411	
20.	Cleanliness of Weld Surfaces	NF-4412	Applies to structural and non-structural welds

Table 3-2 (continued)
Applicable Code Paragraphs for Underground VVMs

	Item	Code Paragraph†	Explanation and Applicability
21.	Backing Strips, Peening	NF-4421 NF-4422	Applies to structural and non-structural welds
22.	Pre-heating and Interpass Temperature	NF-4611 NF-4612 NF-4613	Applies to structural and non-structural welds
23.	Non-Destructive Examination	NF-5360	Invokes Section V
24.	NDE Personnel Certification	NF-5522 NF-5523 NF-5530	-

† All references to the ASME Code refer to applicable sections of the 1995 edition with addenda through 1997, except for Code Sections V and IX, where the latest effective editions of ASME Code Sections V and IX, including addenda, may be used, provided a written reconciliation of the later edition against the 1995 Edition, including addenda, is performed by the certificate holder.

DESIGN FEATURES (continued)

3.4 Site-Specific Parameters and Analyses

Site-specific parameters and analyses that will require verification by the system user are, as a minimum, as follows:

1. The temperature of 80° F is the maximum average yearly temperature.
2. The allowed temperature extremes, averaged over a 3-day period, shall be greater than -40° F and less than 125° F.
3. The analyzed flood condition of 15 fps water velocity and a height of 125 feet of water (full submergence of the loaded cask) are not exceeded.
4. The potential for fire and explosion shall be addressed, based on site-specific considerations. The user shall demonstrate that the site-specific potential for fire is bounded by the fire conditions analyzed by the Certificate Holder, or an analysis of the site-specific fire considerations shall be performed.
5. The resultant zero period acceleration at the top of the grade and at the elevation of the Support Foundation Pad (SFP) at the host site (computed by the Newmark's rule as the sum of A+0.4*B+0.4*C, where A, B, C denote the free field ZPA's in the three orthogonal directions in decreasing magnitude, i.e., A ≥ B ≥ C) shall be less than or equal to 1.3 and 1.228, respectively.
6. a. The criteria used to qualify the protection of the reactor building base mat foundation at the nuclear plant shall also be used to insure that sub-grade supporting the SFP shall not violate the plant's acceptance criteria for the potential of liquefaction.

   b. The depth averaged densities and strain compatible shear wave velocities in the different regions of the subgrade shall meet the minimum requirements of Table 3-4.
7. The moment and shear capacities of the ISFSI Structures shall meet the structural requirements under the load combinations in Table 3-3.
8. Radiation Protection Space (RPS) as defined in Subsection 5.7.9 of Appendix A-100U, is intended to ensure that the subgrade material in and around the lateral space occupied by the VVMs remains essentially intact under all service conditions including during an excavation activity adjacent to the RPS.
9. The Support Foundation Pad (mat) for a VVM array established in any one construction campaign shall be of monolithic construction, to the extent practicable, to maximize the physical stability of the underground installation.

(continued)

TABLE 3-3 LOAD COMBINATIONS FOR THE TOP SURFACE PAD, VVM INTERFACE PAD, SUPPORT FOUNDATION PAD, AND THE RETAINING WALL PER ACI-318 (2005)	
Load Combination	
LC-1	1.4D
LC-2	1.2D + 1.6L
LC-3	1.2D + E + L

where:
D: Dead Load including long-term differential settlement effects.
L: Live Load
E: DBE for the Site

Table 3-4 Values of Principal Design Parameters for the Underground ISFSI	
Thickness of the Support Foundation Pad, inch (nominal)	≥33
Thickness of the VVM Interface Pad, inch (nominal)	≥34
Thickness of the Top Surface Pad, inch (nominal) Thickness of Retaining Wall, inch (nominal)	≥30 ≥24
Rebar Size* (min.) and Layout* (max)	#11 @ 9" each face, each direction
Rebar Concrete Cover (top and bottom)*, inch	per 7.7.1 of ACI 318 (2005)
Compressive Strength of Concrete at ≤28 days*, psi	≥4500
Lower Bound Shear Wave Velocity in the Subgrade lateral to the VVM (Figure 3.4-1 Space A), fps**	≥500
Lower Bound Shear Wave Velocity in the Subgrade below the Support Foundation Pad (Figure 3.4-1 Space C & D), fps**	≥485
Lower Bound Shear Wave Velocity in the Subgrade laterally surrounding the ISFSI (Figure 3.4-1 Space B), fps**	≥450

* Applies to Support Foundation Pad, VVM Interface Pad, Top Surface Pad and Retaining Wall

** Strain compatible effective shear wave velocities shall be computed using the guidance provided in Section 16 of the International Building Code, 2009 Edition. Users must account for potential variability in the subgrade shear wave velocity in accordance with Section 3.7.2 of NUREG-0800.

(continued)

DESIGN FEATURES (continued)

3.4 Site-Specific Parameters and Analyses (continued)

10. Prior to an excavation activity contiguous to an RPS, a seismic qualification of the ISFSI in the structurally most vulnerable configuration (i.e., maximum amount of earth removed) shall be performed to verify that the stability of the SFP, the TSP and the shielding material within the RPS, with or without the Retaining Wall, is maintained. If a Retaining Wall is not installed on the side of the ISFSI where excavation is to take place, then an Excavation Exclusion Zone shall be established inside which excavation is prohibited by performing an appropriate SSI analysis.

11. In cases where engineered features (i.e., berms and shield walls) are used to ensure that the requirements of 10 CFR 72.104(a) are met, such features are to be considered important to safety and must be evaluated to determine the applicable quality assurance category.

12. LOADING OPERATIONS, TRANSPORT OPERATIONS, and UNLOADING OPERATIONS shall only be conducted with working area ambient temperatures $\geq 0^{\circ}$ F.

13. For those users whose site-specific design basis includes an event or events (e.g., flood) that result in the blockage of any VVM inlet or outlet air ducts for an extended period of time (i.e, longer than the total Completion Time of LCO 3.1.2), an analysis or evaluation may be performed to demonstrate adequate heat removal is available for the duration of the event. Adequate heat removal is defined as fuel cladding temperatures remaining below the short term temperature limit. If the analysis or evaluation is not performed, or if fuel cladding temperature limits are unable to be demonstrated by analysis or evaluation to remain below the short term temperature limit for the duration of the event, provisions shall be established to provide alternate means of cooling to accomplish this objective.

14. Users shall establish procedural and/or mechanical barriers to ensure that during LOADING OPERATIONS and UNLOADING OPERATIONS, either the fuel cladding is covered by water, or the MPC is filled with an inert gas.

DESIGN FEATURES (continued)

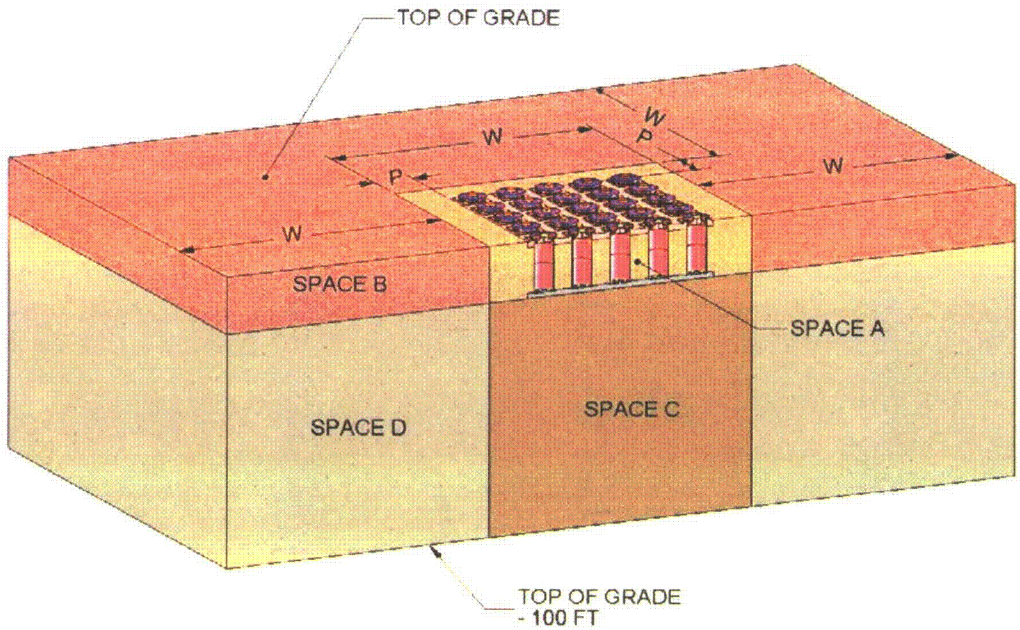

Figure 3.4-1 - SUB-GRADE AND UNDER-GRADE SPACE NOMENCLATURE

3.5 Not Used

(continued)

DESIGN FEATURES (continued)

3.6 Forced Helium Dehydration System

3.6.1 System Description

Use of a forced helium dehydration (FHD) system, (a closed-loop system) is an alternative to vacuum drying the MPC for moderate burnup fuel ($\leq$ 45,000 MWD/MTU) with lower MPC heat load and mandatory for drying MPCs containing one or more high burnup fuel assemblies or higher MPC heat load as indicated in Appendix A-100U Table 3-1. The FHD system shall be designed for normal operation (i.e., excluding startup and shutdown ramps) in accordance with the criteria in Section 3.6.2.

3.6.2 Design Criteria

3.6.2.1 The temperature of the helium gas in the MPC shall be at least 15°F higher than the saturation temperature at coincident pressure.

3.6.2.2 The pressure in the MPC cavity space shall be ≤ 60.3 psig (75 psia).

3.6.2.3 The hourly recirculation rate of helium shall be ≥ 10 times the nominal helium mass backfilled into the MPC for fuel storage operations.

3.6.2.4 The partial pressure of the water vapor in the MPC cavity will not exceed 3 torr. The limit is met if the gas temperature at the demoisturizer outlet is verified by measurement to remain ≤ 21°F for a period of 30 minutes or if the dew point of the gas exiting the MPC is verified by measurement to remain ≤ 22.9°F for ≥ 30 minutes.

3.6.2.5 The condensing module shall be designed to de-vaporize the recirculating helium gas to a dew point ≤ 120°F.

3.6.2.6 The demoisturizing module shall be configured to be introduced into its helium conditioning function after the condensing module has been operated for the required length of time to assure that the bulk moisture vaporization in the MPC (defined as Phase 1 in FSAR Appendix 2.B) has been completed.

3.6.2.7 The helium circulator shall be sized to effect the minimum flow rate of circulation required by these design criteria.

3.6.2.8 The pre-heater module shall be engineered to ensure that the temperature of the helium gas in the MPC meets these design criteria.

(continued)

DESIGN FEATURES (continued)

3.6 Forced Helium Dehydration System (continued)

3.6.3 Fuel Cladding Temperature

A steady-state thermal analysis of the MPC under the forced helium flow scenario shall be performed using the methodology described in HI-STORM 100 FSAR Section 4.4, with due recognition of the forced convection process during FHD system operation. This analysis shall demonstrate that the peak temperature of the fuel cladding, under the most adverse condition of FHD system operation, is below the peak cladding temperature limit for normal conditions of storage for the applicable fuel type (PWR or BWR) and cooling time at the start of dry storage.

3.6.4 Pressure Monitoring During FHD Malfunction

During an FHD malfunction event, described in HI-STORM 100 FSAR Chapter 11 as a loss of helium circulation, the system pressure must be monitored to ensure that the conditions listed therein are met.

DESIGN FEATURES (continued)

3.7 Deleted

DESIGN FEATURES (continued)

3.8 Combustible Gas Monitoring During MPC Lid Welding and Cutting

During MPC lid-to-shell welding and cutting operations, combustible gas monitoring of the space under the MPC lid is required, to ensure that there is no combustible mixture present.

DESIGN FEATURES (continued)

3.9 Corrosion Mitigation Measures

The HI-STORM 100U VVM CEC Container Shell and Bottom Plate shall be protected from corrosion damage due to the corrosivity of the surrounding environment using the following means:

Implementation and Requirements of Corrosion Mitigation Measures

Surrounding Environment's Corrosivity (see note iv)	**Corrosion Mitigation Measures**		
	Coating (see note i)	Concrete Encasement (see note ii)	Cathodic Protection (see note iii)
Mild	Required	Choice of either concrete encasement or cathodic protection; or both	
Aggressive	Required	Optional	Required

Notes:

i. An exterior surface preservative (coating) applied on the CEC in accordance with the acceptance criteria set forth in the FSAR.

ii. Concrete encasement of the CEC external surfaces to establish a high pH buffer around the CEC metal mass in accordance with the requirements set forth in the FSAR.

iii. An impressed current cathodic protection system (ICCPS) in accordance with the design criteria set forth in the FSAR.

iv. Surrounding environment corrosivity is categorized as either mild or aggressive in accordance with the requirements set forth in the FSAR.

DESIGN FEATURES (continued)

3.10 Periodic Corrosion Inspections for Underground Systems

HI-STORM 100U VVM ISFSIs not employing an impressed current cathodic protection system shall be subject to visual and UT inspection of at least one representative VVM to check for significant corrosion of the CEC Container Shell and Bottom Plate at an interval not to exceed 20 years. The VVM chosen for inspection is not required to be in use or to have previously contained a loaded MPC. The VVM considered to be most vulnerable to corrosion degradation shall be selected for inspection. If significant corrosion is identified, either an evaluation to demonstrate sufficient continued structural integrity (sufficient for at least the remainder of the licensing period) shall be performed or the affected VVM shall be promptly scheduled for repair or decommissioning. Through wall corrosion shall not be permitted without promptly scheduling for repair or decommissioning. Promptness of repair or decommissioning shall be commensurate with the extent of degradation of the VVM but shall not exceed 3 years from the date of inspection.

If the representative VVM is determined to require repair or decommissioning, the next most vulnerable VVM shall be selected for inspection. This inspection process shall conclude when a VVM is found that does not require repair or decommissioning. Since the last VVM inspected is considered more prone to corrosion than the remaining un-inspected VVMs, the last VVM inspected becomes the representative VVM for the remaining VVMs.

Inspections

Visual Inspection: Visual inspection of the inner surfaces of the CEC Container Shell and Bottom Plate for indications of significant or through wall corrosion (i.e., holes).

UT Inspection: The UT inspection is performed on the inside surfaces of the CEC. A minimum of 16 data points shall be obtained, 4 near the top, 4 near the mid-height and 4 near the bottom of the CEC Container Shell all approximately 0, 90, 180, and 270 degrees apart; and 4 on the CEC Bottom Plate near the CEC Container Shell approximately 0, 90, 180, and 270 degrees apart. Locations where visual inspection has identified potentially significant corrosion shall also receive UT inspection. Locations suspected of significant corrosion may receive further UT inspection to determine the extent of corrosion.

Inspection Criteria

General wall thinning exceeding 1/8" in depth and local pitting exceeding 1/4" in depth are conditions of significant corrosion.

Assume a CEC length (determined from "top of grade" to bottom of CEC bottom plate): 219.5 in.
CEC outside diameter: 86 in.
CEC condition: exterior is coated
Coating efficiency: 91.5% (i.e. 8.5% of the coated CEC surface is considered bare metal)
Cathodic Protection: Rectifier and distributed Natural Graphite Anodes with carbonaceous backfill
Soil resistivity: 4,000 ohm/cm^2
Current density: 1 mA/ft^2 exposed metal
Outside area of each CEC: 59,300 in^2 (412 ft^2)
Total area for an array of twelve CECs: 4,944 ft^2
Bare CEC metal exposed: 4,944 ft^2 x 0.085 or 420 ft^2
Current required: 420 ft^2 x 1 mA/ft^2 or 420 mA

The following is additional data applicable to Figure 2.I.1.

Approximate Anode quantity: 11
Approximate Anode size: 5 in dia. x 120 in. long
Approximate Backfill quantity: 6,000 lbs of carbonaceous backfill

The total number of anodes required is determined primarily by the total current requirements of the CEC metal to be protected and the optimum current density of the anode material selected.

Graphite is a semi-consumable anode. Graphite typically has experienced corrosion rates of 1.5 to 2.16 lbs /amp year [2.I.3] or as determined by experiment, 0.08 grams per square meter of anode per amp-hour of current (at 30 C, 40 mA/cm^2 anode current density) [2.I.4]. A computed anode life of less than 40 years is acceptable as long as appropriate measures are taken to facilitate the replacement of anodes during the design phase and appropriate maintenance planning measures are implemented. Use of carbonaceous backfill should be considered since it can substantially lengthen the anode life. Inert (non-consumable) platinized anodes may also be considered.

v. Concrete Encasement (Corrosion Mitigation Measure)

If concrete encasement is used, it shall be implemented in accordance with the requirements in Supplement 3.I, Subsection 3.I.4.1 and appropriate references.

The following points shall also be taken into consideration:

- The effect of the concrete encasement on the ICCPS, if an ICCPS is also implemented.
- The concrete encasement should not interfere with the settlement of the TSP (which provides the transporter support surface) without appropriate evaluation.

vi. Retaining Wall

Because the subgrade within and around an operating 100U ISFSI serves a principal shielding function, it is essential that any excavation activity adjacent to the ISFSI (e.g., to build an extension of the ISFSI), must not disturb the soil in the Radiation Protection Space (RPS) shown in the licensing drawings (Section 1.I.5).

The extent of the RPS is set down to ensure, with sufficient margin of safety, that the ISFSI will continue to meet all relevant safety criteria under all applicable conditions of storage including normal, off-normal, extreme environmental phenomena and accident conditions. For example, the RPS must provide sufficient buffer so that design basis projectiles (large, medium, and penetrant missiles) will not access an MPC stored in a VVM cavity. In this case, as explained in Supplement 3.I, the incident missile is assumed to act when a deep cavity has been excavated contiguous to the RPS and the direction of action of the missile is oriented to achieve maximum penetration of the sub-grade towards the CEC shell.

A retaining wall at the edge of or beyond the RPS is recommended if an excavation activity is planned adjacent to the RPS boundary while the ISFSI is in active service. The retaining wall, as shown in the licensing drawing, shall be keyed to the TSP and connected using dowels to the SFP so that it is laterally restrained from movement but does not transmit any bending moment to the SFP or the TSP. The minimum structural design requirements on the retaining wall are provided in Table 2.I.2 and the licensing drawing in 1.I.5.The applicable load combinations for the structural analysis of the retaining wall pursuant to ACI-318(2005) are provided in Table 2.I.11.

When a retaining wall is installed on one or more sides of the 100U ISFSI, excavation activities associated with the construction of a new underground ISFSI can be performed directly adjacent to the retaining wall(s) at depths above the bottom surface of the existing SFP. Soil excavations below the bottom surface of the existing SFP shall be treated as though no retaining walls are installed and, therefore, are subject to the limitations of the following paragraph.

For the case where a retaining wall is not installed, no excavation activities associated with the construction of a new underground ISFSI shall take place within a distance from the RPS equal to ten times the planned excavation depth. Alternatively, the Excavation Exclusion Zone (EEZ), defined as the minimum distance from the centerline of a VVM located on the periphery of the ISFSI to where the effect of DBE is sufficiently attenuated such that a full depth excavation will not cause collapse of the lateral sub-grade at the RPS boundary during an earthquake, can be determined by a site specific seismic analysis. If a retaining wall is installed at or beyond the RPS then the wall becomes the EEZ boundary, but only for excavation depths above the bottom surface of the existing SFP.

2.I.3 Service Conditions and Applicable Loads

The categories of loads on the HI-STORM 100U VVM are identified below. They parallel those for the aboveground systems.

- Normal Condition: dead weight, handling of the Closure Lid, soil overburden pressure from subgrade, live load due to cask transporter movement, snow loads, and buoyancy effect of

TABLE 2.I.2
DESIGN DATA FOR HI-STORM 100U ISFSI

	Item	Value(Minimum or nominal, as applicable)	Comment
1.	Support Foundation Pad, VVM Interface Pad and Top Support Pad, and Retaining Wall	▪ Minimum Concrete density = 145 lb/ft^3 ▪ Minimum concrete compressive strength @ ≤ 28 days = 4,500 psi ▪ Grade 60 Rebar - Minimum yield strength of rebar = 60,000 psi; rebar is #11@9" (each face, each direction) ▪ Minimum concrete cover on rebar per section 7.7.1 of ACI-318(05)	See Licensing Drawings in Section 1.I.5 for detailed concrete pad/wall thickness.
2.	Depth averaged density of subgrade in Space A (see Figure 2.I.5), lb/ft^3	120	A lower average density value may be used in shielding analysis in Supplement 5.I for conservatism.
3.	Depth averaged density of subgrade in Space B (see Figure 2.I.5), lb/ft^3	110	A lower average density value may be used in shielding analysis in Supplement 5.I for conservatism.
4.	Depth depth averaged density of subgrade in Space C (see Figure 2.I.5), lb/ft^3	120	Not required for shielding.
5.	Depth depth averaged density of subgrade in Space D (see Figure 2.I.5), lb/ft^3	120	This space will typically contain native soil. Not required for shielding.
6.	Lower bound, strain compatible effective shear wave velocity in Space A, V ft/sec (see Notes 1 and 2)	500	This space will typically contain engineered fill.
7.	Lower bound, strain compatible effective shear wave velocity in Space B, V ft/sec (see Notes 1 and 2)	450	This space will typically contain native soil.
8.	Lower bound, strain compatible effective shear wave velocity in Space C, V ft/sec (see Notes 1 and 2)	485	This space may be remediated with vertical reinforcement such as pilings to enhance V.

TABLE 2.I.2 (continued)
DESIGN DATA FOR HI-STORM 100U ISFSI

	Item	Value	Comment
9.	Lower bound, strain compatible effective shear wave velocity in Space D, V ft/sec (see Notes 1 and 2)	485	This space will typically contain native soil.
10.	Design Basis Earthquake	Ground surface spectra per Figure 2.I.4-A with horizontal ZPA, a_H and vertical ZPA, a_V as: $a_H = 1.0g$ $a_V = 0.75g$ and foundation surface spectra per Figure 2.I.4-B.	Horizontal and vertical spectra shown in Figures 2.I.4-A and 2.I.4-B are based on 5% damping. Following the Newmark 100-40-40 response combination technique [2.I.13] endorsed by the Regulatory Guide 1.92 [2.I.14], the *resultant ZPA* for a 3-D earthquake site is defined as: $a_R = a_1 + 0.4a_2 + 0.4a_3$, where a_1, a_2 and a_3 are the site's ZPAs in three orthogonal directions and $a_1 \geq a_2 \geq a_3$. Hence, the DBE *resultant ZPAs* at ground surface and foundation surface elevations are 1.3 g's (=1.0×1.0g's + 0.4×0.75 g's) and 1.228 g's (=1.0×0.94g's + 0.4×0.72 g's), respectively.
11.	Maximum permissible long-term settlement of the SFP	0.2 inches	
12.	Maximum permissible long-term settlement of the TSP with respect to the SFP	0.4 inches	

TABLE 2.I.2 (continued)
DESIGN DATA FOR HI-STORM 100U ISFSI

<u>Note 1:</u>
Strain compatible shear wave velocities in each space at an ISFSI site (see Figure 2.I.5) shall be computed using the guidance provided in Section 16 of the International Building Code, 2009 Edition [2.I.9]. The equivalent wave velocity is defined so that the wave transit time for an equivalent homogeneous material of the same total depth is the same as the actual layered substrate.

$$V = \frac{d}{\sum \frac{d_i}{v_i}}$$

d_i = thickness of i^{th} layer within the region (ft.);
v_i = strain compatible shear wave velocity of i^{th} layer within the region (ft./sec.);
d = total thickness of substrate region (e.g. 20', 80')
V = Equivalent Strain Compatible Shear Wave Velocity for substrate thickness "d".

<u>Note 2:</u>
The lower bound, strain compatible effective shear wave velocities at a particular site must account for the potential variability (i.e., uncertainty) in the site soil properties in accordance with Section 3.7.2 of NUREG-0800. This means that a site must demonstrate that, when the lower bound values for shear wave velocity (based on the site soil investigation data) are used as input, the free-field site response analysis yields a strain compatible effective shear wave velocity greater than the minimum value provided in this table for each space. The lower bound shear wave velocities used as input to the free-field site response analysis shall be determined using the following formula:

$$V_{LB} = \frac{V_{BE}}{\sqrt{1 + COV}}$$

where V_{BE} is the best estimate shear wave velocity for a given soil layer based on the soil investigation data, and *COV* is the coefficient of variation for the site soil properties. For well-investigated sites, the *COV* should be no less than 0.5. For sites that are not well investigated, the *COV* shall be set equal to 1.0.

SUPPLEMENT 3.I

STRUCTURAL EVALUATION FOR THE HI-STORM 100U SYSTEM

3.I.0 OVERVIEW

In this supplement, the structural adequacy of the HI-STORM 100U Vertical Ventilated Module (VVM) is evaluated pursuant to the guidelines of NUREG-1536. The organization of technical information in this supplement mirrors the format and content of Chapter 3 except that it only contains material directly pertinent to the HI-STORM 100U VVM.

The HI-STORM 100U VVM serves as the storage space for the loaded MPC and consists of the CEC (the Container Shell, the Divider Shell and MPC Guides, and a welded Bottom Plate), and a lid consisting of plain concrete encased in structural steel arranged to provide appropriate inlet and outlet air passages (the Closure Lid). These individual components are collectively referred to as VVM Components. Interfacing SSCs that surround and support the VVM, as well as proximate structures, collectively referred to as ISFSI Structures are explained in Supplement 2.I. Section 1.I.2 contains a complete description of the VVM components and ISFSI Structures (accompanied by appropriate figures) and their respective functions within the HI-STORM 100U ISFSI. The essential design details of both the VVM Components and the ISFSI Structures are set down in the licensing drawing in Supplement 1.I. The design basis loadings for the facility are provided in Supplement 2.I. The applicable codes, standards, and practices governing the structural analysis of the HI-STORM 100U module, as well as the design criteria, are also presented in Supplement 2.I. Throughout this supplement, in the context of the VVM components, the term "*safety factor*" is defined as the *ratio of the allowable stress (load) or displacement for the applicable load combination to the maximum computed stress (load) or displacement.*

For the ISFSI Structures made of reinforced concrete, the safety factor is defined as the ratio of the ultimate moment (or shear) capacity to the actual maximum moment (or shear) developed under the factored load combination.

MPC structural integrity has been evaluated in Chapter 3. In this supplement, the integrity of the MPC, due to its rattling motion inside the VVM storage cavity during a seismic event (a new loading condition in the underground storage configuration) is considered.

3.I.1 STRUCTURAL DESIGN

3.I.1.1 Discussion

The HI-STORM 100U system consists of three principal components: the Multi-Purpose Canister (MPC), the HI-STORM 100U storage module, herein denoted as the Vertical Ventilated Module (VVM), and the HI-TRAC transfer cask. This supplement to Chapter 3 presents the structural evaluation of the VVM Components for the applicable load cases summarized in Supplement 2.I (Table 2.I.5). In Section 3.I.4, the safety factors for each load case for the VVM Components are

HOLTEC INTERNATIONAL COPYRIGHTED MATERIAL

quantified. In addition, the safety evaluation of the ISFSI Structures is carried out using the factored load combinations from ACI-318(2005) (see Table 2.I.11). Summary tables of bounding safety factors are provided for governing load combination for the ISFSI Structures. A licensing drawing for the HI-STORM 100U VVM is provided in Section 1.I.5. Table 2.I.1 provides a listing of the applicable regulations and codes and standards for the VVM Components and the ISFSI structures. The design of the VVM components and the ISFSI Structures is fully articulated in the licensing drawing and Table 2.I.2. The applicable Design Basis Earthquake is defined by the free field spectra shown in Figure 2.I.4.

3.I.1.2 Design Criteria

Design (and acceptance) criteria for the HI-STORM 100U VVM Components and the ISFSI structures are summarized in Tables 2.I.1 and 2.I.6.

3.I.1.3 Loads

Individual loads, applicable to the HI-STORM 100U System, are defined in Sections 2.I.4, 2.I.5 and 2.I.6, and the load cases applicable to the VVM Components are summarized in Table 2.I.5. Table 2.I.11 contains load combinations applicable to the ISFSI Structures (reinforced concrete structures) in the HI-STORM 100U ISFSI.

3.I.1.4 Allowables

Allowable stresses for carbon steel and Alloy X used in the structural components of the HI-STORM 100U and the stored MPC are provided in Sections 3.1 and 3.3. The relevant data from those sections are reproduced here, as Tables 3.I.3 (a)-(d) to make the supplement self-contained.

3.I.1.5 Brittle Fracture

Brittle fracture considerations for HI-STORM 100U are bounded by HI-STORM 100 and 100S because of the VVM's underground configuration, and the use of the same material types and thicknesses as in the aboveground overpacks.

3.I.1.6 Fatigue

The HI-STORM 100U system is not subject to significant long-term cyclic loads. Therefore, failure due to fatigue is not a concern for the HI-STORM 100U system.

3.I.1.7 Buckling

The CEC Container Shell is the only component of the VVM subject to axial compression. However, since the shell is backed by a substrate, welded to a Bottom Plate at its base, and surrounded by the ISFSI Pad at the top, instability is not considered credible. The Divider Shell does not experience any axial compressive stress that might induce buckling.

HOLTEC INTERNATIONAL COPYRIGHTED MATERIAL

3.I.2 WEIGHTS AND CENTERS OF GRAVITY

Table 3.I.1 provides bounding weights of the individual HI-STORM 100U components.

The locations of the calculated centers of gravity (C.G.s) are presented in Table 3.I.2 and are computed using the bounding weights. All centers of gravity are located on the VVM centerline.

Bounding weight values for the CEC and the Closure Lid include an overage on the weight generated by the CAD drawing package.

3.I.3 MECHANICAL PROPERTIES OF MATERIALS

Tables 2.I.3 and 2.I.8 list applicable codes, materials of construction, and ITS designations for all functional parts in the HI-STORM 100U system except for the MPC and its internals, which remain unchanged (listed in Table 2.2.6).

3.I.3.1 VVM Steel Properties

Applicable material property and allowable stress tables in Chapter 3 for the VVM are reproduced in Tables 3.I.3 (a)-(c) for convenience.

3.I.3.2 Unreinforced Concrete

The primary function of the unreinforced concrete in the HI-STORM 100U VVM Closure Lid is shielding. Unreinforced concrete is not considered as a primary load-bearing (structural) member. However, its ability to withstand compressive, bearing and penetrant loads under the design basis and various service conditions is analyzed. The allowable bearing strength of plain concrete for normal loading conditions is calculated in accordance with ACI-318 (2005) [2.I.5]. Table 3.I.4 provides a bearing limit consistent with the concrete compressive strength in the same table. The procedure specified in ASTM C-39 is utilized to verify that the assumed compressive strength will be realized in the actual in-situ pours. Unless specifically called out in Table 3.I.4, Appendix 1.D provides requirements on unreinforced concrete.

3.I.3.3 Reinforced Concrete

Reinforced concrete is used in the construction of the ISFSI Structures, namely, the retaining wall, the TSP, the VIP, and the SFP. All reinforced concrete load bearing structures in the HI-STORM 100U ISFSI will conform to stress criteria of ACI-318(2005).

3.I.4 GENERAL STANDARDS FOR CASKS

In this section, new or additional material applicable to the HI-STORM 100U system is included. Section 3.4 contains all required information associated with the MPCs and with the HI-TRAC transfer cask and is not repeated here. Results reported in this supplement section are generally applicable only to the HI-STORM 100U VVM.

3.I.4.1 Chemical and Galvanic Reactions

In order to provide reasonable assurance that the VVM will meet its intended Design Life of 40 years (the License Life is 20 years) and perform its intended safety function(s), chemical and galvanic reactions and other potentially degrading mechanisms must be accounted for in its design and construction.

The HI-STORM 100U VVM is a buried structure and as such chemical and galvanic reactions and other potentially degrading factors are, in some respects, more challenging than for aboveground models. Although the CEC is not a part of the MPC containment boundary, it should not corrode to the extent where localized in-leakage of water occurs or where gross general corrosion prevents the component from performing its primary safety function. In the following, considerations in the VVM's design and construction consistent with the applicable guidance provided in ISG-15 [3.I.3] are summarized.

All VVM components are galvanically compatible. Except for the CEC exterior surfaces, all steel surfaces of the VVM are lined and coated with the same surface preservative that is used in the aboveground HI-STORM overpacks. (The surface preservative used to protect HI-STORM 100S steel surfaces is a proven zinc rich inorganic/metallic material that protects galvanically and has self healing characteristics for added assurance). All exposed surfaces interior to the VVM, as stated in Supplement 1.I, are accessible for the reapplication of surface preservative, if necessary.

The steel Divider Shell requires insulation to perform its primary thermal function. The insulation selected shall be suitable for high temperature and high humidity operation and shall be foil faced, jacketed or otherwise made water resistant to ensure the required thermal resistance is maintained in accordance with Supplement 4.I. The high zinc content in the coating of the Divider Shell provides protection for both the Divider Shell and the jacketing or foil from any potential galvanic corrosion concerns. With respect to radiation resistance, the insulation blanket does not contain any organic binders. The damage threshold for ceramics is known to be approximately 1×10^{10} Rads. Chloride corrosion is not a concern since chloride leachables are limited and sufficiently low and the Divider Shell is not made from stainless steel [3.I.20]. Stress corrosion cracking of the foil or jacketing, whether made from stainless steel or other material is not an applicable corrosion mechanism due to minimal stresses derived from self-weight. The foil or jacketing and attachment hardware shall either have sufficient corrosion resistance (e.g. stainless steel, aluminum or galvanized steel) or shall be protected with a suitable surface preservative. The insulation is adequately secured to prevent significant blockage of the ventilation passages in case of failure of a single attachment (strap, clamp, bolt or other attachment hardware). The following table provides the acceptance criteria for the selection of insulation material for the Divider Shell and ranks them in order of importance.

Acceptance Criteria for the Selection of the Insulation Material	
Rank	**Criteria**
1	Adequate thermal resistance
2	Adequate high temperature resistance
3	Adequate humidity resistance
4	Adequate radiation resistance
5	Adequate resistance to the ambient environment
6	Sufficiently low chloride leachables
7	Adequate integrity and resistance to degradation and corrosion during long-term storage

Kaowool® ceramic fiber insulation [3.I.20] is selected as one that satisfies the acceptance criteria to the maximum degree. The Kaowool® insulation material provides excellent resistance to chemical attack and is not degraded by oil or water. Alternatively, a Holtec approved equivalent that meets the acceptance criteria set forth in the table above may be used.

The CEC Container Shell, which is exposed to the substrate, requires additional pre-emptive measures to prevent corrosion, if the substrate is of aggressive chemistry. This subsection provides a description of corrosion mitigation measures required to be implemented to protect the HI-STORM 100 VVM. Because the guiding principle in the HI-STORM systems is to target a service life of 100 years so as to guarantee a design life of 40 years, these corrosion prevention measures are in addition to the preemptively incorporated standard corrosion allowance of 1/8-inch applied to the subterranean parts of the CEC in direct contact with the surrounding substrate. Calculation of the required CEC Container Shell and Bottom Plate thicknesses on a site-specific basis may indicate the availability of an additional corrosion reserve.

Soil Corrosivity and Corrosion Mitigation Measures for the Exterior of the CEC

Corrosion mitigation of the exterior of the CEC warrants special consideration for the following reasons: (i) inaccessibility of the exterior coated surface after installation (ii) potential for a highly aggressive (i.e., corrosive) soil environment at certain sites, and (iii) potential for a high radiation field. Since the buried configuration will not allow for the reapplication of surface preservative, corrosion mitigation measures shall be determined after careful evaluation of the soil's corrosivity at the user's ISFSI site.

To evaluate soil corrosivity, a "10 point" soil-test evaluation procedure, in accordance with the guidelines of Appendix A of ANSI/AWWA C105/A21 [3.I.4], will be utilized. The classical soil evaluation criteria in the aforementioned standard focuses on parameters such as: 1) resistivity, 2) pH, 3) redox (oxidation-reduction) potential, 4) sulfides, 5) moisture content, 6) potential for stray current, and 7) experience with existing installations in the area. Using the procedure outlined in ref. [3.I.4], the ISFSI soil environment corrosivity is categorized as either "mild" for a soil test evaluation resulting in 9 points or less or "aggressive" for a soil test evaluation resulting in 10 points or greater. The following table details the corrosion mitigation measures that shall be implemented based on soil environment corrosivity:

Implementation of Corrosion Mitigation Measures			
Soil Environment Corrosivity	**Corrosion Mitigation Measures**		
	Coating (see note i)	Concrete Encasement (see note ii)	Cathodic Protection (see note iii)
Mild	Required	Choice of either concrete encasement or cathodic protection; or both	
Aggressive	Required	Optional	Required

Notes:
i. An acceptable exterior surface preservative (coating) applied on the CEC.
ii. Concrete encasement of the CEC external surfaces to establish a high pH buffer around the metal mass.
iii. A suitably engineered impressed current cathodic protection system (ICCPS)

The corrosion mitigation measures tabulated above are further detailed in the following subsections:

i. Coating

In addition to the corrosion allowance, the CEC shall be coated with a radiation resistant surface preservative designed for below-grade and/or immersion service. Inorganic and/or metallic coatings are sufficiently radiation resistant for this application; therefore, radiation testing is not required [3.I.5]. Organic coatings such as epoxy, however, must have proven radiation resistance [3.I.5] or must be tested without failure to at least 10^7 Rad. Radiation resistance to lower radiation levels is acceptable on a site-specific basis. Radiation testing shall be performed in accordance with ASTM D 4082 [3.I.6] or equivalent. The coating should be conservatively treated as a Service Level II coating as described in Reg. Guide 1.54 [3.I.7]. As such, the coating shall be subjected to appropriate quality assurance in accordance with the applicable guidance provided by ASTM D 3843-00 [3.I.8]. The coating should preferably be shop applied in accordance with manufacturer's instructions and, if appropriate, applicable guidance from ANSI C 210-03 [3.I.9]. The Keeler & Long polyamide-epoxy coating, according to the manufacturer's product data sheet [3.I.10], is pre-tested to radiation levels up to $1x10^9$ Rads without failure. The following table provides the acceptance criteria for the selection of coatings for the exterior surfaces of the CEC and ranks them in order of importance.

Acceptance Criteria for the Selection of Coatings	
Rank	**Criteria**
1	suitable for immersion and/or below grade service
2a	compatible with the ICCPS (if used) • adequate dielectric strength • adequate resistance to cathodic disbondment

Acceptance Criteria for the Selection of Coatings	
Rank	**Criteria**
2b	compatible with concrete encasement (if used) • adequate resistance to high alkalinity
3	adequate radiation resistance
4	adequate adhesion to steel
5	adequate bendability/ductility/cracking resistance/abrasion resistance
6	adequate strength to resist handling abuse and substrate stress

The Keeler & Long polyamide-epoxy coating is selected as one that satisfies the acceptance criteria to the maximum degree. Alternatively, a Holtec approved equivalent that meets the acceptance criteria set forth in the table above may be used.

ii. Concrete Encasement

The CEC concrete encasement shall provide a minimum of 5 inches of cover to provide a pH buffering effect for additional corrosion mitigation. The above concrete cover thickness has been conservatively determined for a 100-year service life in a strongly aggressive environment based on the concrete corrosion/degradation data provided in the literature [3.I.12, Table 5.3] (1.2 mm/yr surface depth failure rate). The required 5 inch minimum thickness is more conservative than that recommended in ACI Codes, such as ACI 318 [3.3.2], which call for up to 3 inches of concrete cover over steel reinforcement in aggressive environments. Considering that the concrete encasement is restricted to mild soil environments (unless used in conjunction with cathodic protection) and has a non-structural role, the 5 inch concrete encasement thickness is considered more than sufficient to provide reasonable assurance that a 40 year service life can be achieved. The lowest part of the CEC sits in a recessed region of the Support Foundation with an annular gap normally filled with substrate. If present, the CEC concrete encasement slurry will fill this annular gap during construction.

The function of the concrete encasement is for corrosion mitigation only; however, cracks larger than hairline cracks may significantly reduce its effectiveness. To control size and population of cracks, concrete reinforcement is included. The following reinforcement methods may be applied:

a. Fiber reinforcement: Fiber reinforcement may be of several materials, including steel, glass and plastic (polypropylene). The selection of the fiber reinforcement material shall be such that adequate resistance to radiation and high alkalinity is maintained. If using steel fibers, adequate damage protection of the CEC coating shall be ensured during concrete placement per written procedures. Steel fiber shall be implemented using written procedures and the applicable guidance from ACI 544.3R [3.I.25] or a similar consensus code or standard. Fiber reinforcement materials other than steel shall be implemented using written procedures, manufacturer recommendations and applicable guidance from ACI, ASCE and/or ASTM. One such document is ASTM C1116-03 [3.I.26].

b. Steel wire reinforcement: Steel wire reinforcement shall be implemented in accordance with written procedures and the guidance from ACI 318 [3.3.2] or more recent version. For corrosion protection, the steel wire reinforcement shall have a concrete cover of approximately 2 to 3 inches from the interfacing substrate.

Regardless of reinforcement method, the material selected shall be corrosion resistant or otherwise appropriately coated (e.g. epoxy coated steel wire) for corrosion resistance.

The concrete encasement shall be installed in accordance with Holtec approved procedures following applicable guidance from the ACI code (e.g. ACI 318 [3.3.2]), as appropriate, for commercial concrete. Installation procedures shall address mix designs (incorporating Portland cement), testing, mixing, placement, and reinforcement, with the aim to enhance concrete durability and minimize voids and micro-cracks.

iii. Impressed Current Cathodic Protection System (ICCPS)

For a particular ISFSI site, the user may choose to either extend an existing ICCPS to protect the installed ISFSI, or to establish an autonomous ICCPS. The initial startup of the ICCPS must occur within one year after installation of the VVM to ensure timely corrosion mitigation. In addition, the ICCPS should be maintained operable at all times after initial startup except for system shutdowns due to power outages, repair or preventive maintenance and testing, or system modifications. Because there are a multitude of ISFSI variables that will bear upon the design of the ICCPS for a particular site, the essential criteria for its performance and operational characteristics are set down in this FSAR, which the detailed design work for each ISFSI site must follow.

Design Criteria for the Impressed Current Cathodic Protection System
a. The cathodic protection system shall be capable of maintaining the CEC at a minimum (cathodic) potential as required by NACE Standard RP0285-2002 [3.I.21]. b. The ICCPS shall include provisions to infer its proper operation and effectiveness on a periodic basis. c. The system shall be designed to mitigate corrosion of the CEC for its design life. d. The cathodic protection system design, installation, operation, testing, and maintenance shall follow the applicable guidelines of: - 49CFR195 Subpart H "Corrosion Control", Oct. 1, 2004 edition [3.I.13] - NACE Standard RP0285-2002 "Corrosion Control of Underground Storage Tank Systems by Cathodic Protection" [3.I.21]

The following standards and/or publications may also be utilized for additional guidance in the design, installation, operation, testing, and maintenance of the ICCPS as needed (in case of conflict, the guidelines of item d above shall prevail):

- API RP1632, "Cathodic Protection of Underground Petroleum Storage Tanks and Piping Systems" [3.I.22]
- NACE RP0169-96, "Control of External Corrosion on Underground or Submerged Piping Systems" [3.I.23]
- 49CFR192 Subpart I "Requirements for Corrosion Control", Oct. 1, 2004 edition [3.I.24]
- Other standards or publications referenced by any of the above three standards and publications.

Records of system operating data necessary to adequately track the operable status of the ICCPS shall be maintained in accordance with the user's quality assurance program.

Finally, the surface preservative used to coat the CEC must meet the requirements described in (i) above but must also be compatible with cathodic protection and resistant to the alkaline conditions created by cathodic protection and/or concrete encasement. Organic coatings, such as the Keeler & Long coating selected for (i) above, are inherently compatible with both cathodic protection [3.I.11] and concrete [3.I.10].

3.I.4.2 Positive Closure

There are no quick-connect/disconnect ports in the confinement boundary of the HI-STORM 100U system. Because the only access to the MPC is through the VVM Closure Lid, which weighs well over 10 tons, inadvertent opening of the VVM cavity is not feasible.

3.I.4.3 Lifting Devices

As required by Reg. Guide 3.61, lifting operations applicable to the VVM lid are analyzed. Because of the nature of the HI-STORM 100U system, lid placement or removal may occur with a loaded MPC inside the VVM cavity; these are the sole operations requiring analysis in accordance with Reg. Guide 3.61 and are examined in this supplement.

As discussed in Subsection 3.4.3, the lifting component itself (the four lift lugs) must meet the primary stress limits prescribed by ANSI N14.6-1993; the welds in the load path, near the lifting holes, are required to meet the condition that stresses remain below yield under three times the lifted load (per Reg. Guide 3.61). Further, for additional conservatism, away from the lifting location, the ASME Code limit for the Level A service condition applies.

The lifting analysis results summarized below include a 15% inertia amplifier.

<u>HI-STORM 100U VVM Closure Lid Lifting Analysis (Load Case 05 in Table 2.I.5)</u>

The four lifting lugs are analyzed to ANSI N14.6 stress limits using simple strength of materials calculations. Each of four lugs is considered as a cantilever beam attached to the lid and carries 25%

HOLTEC INTERNATIONAL COPYRIGHTED MATERIAL

of the lid weight. The bending moment and shear force at the root of the cantilever (where it is attached to the lid) is computed and the maximum stress is compared with the minimum of the yield strength/6 or the ultimate strength/10. As required, increasing the lid weight by 15% includes inertia effects. Using the calculated bending moment and shear force at the root of the lug, the structural evaluation of the weld attaching the lug to the lid is performed and compared with the requirements of Regulatory Guide 3.61. The results from these two calculations demonstrate that the required safety factors are substantially greater than 1.0 (exceeding the requirements of ANSI N14.6 and Reg. Guide 3.61, respectively). The details of the calculations are presented in the calculation package supporting this submittal [3.I.27]. Lifting slings that attach to the lugs shall be sized to meet the safety factors set forth in ANSI B30.3.

To evaluate the global state of stress in the lid body, a finite element model of the lid, which includes contact interfaces between steel and concrete, is constructed to evaluate the state of stress under lifting conditions. Figure 3.I.1 shows the constructed ANSYS finite element model. The lifted scenario is simulated by fixing the four lifting locations at the lift lug sling attachment location, and applying an appropriate weight density to match the lifted weight. The results are evaluated for satisfaction of normal condition (ASME Level A) limits at the appropriate locations.

The table below summarizes key results obtained from the lifting analyses for the HI-STORM 100U VVM Closure Lid for a bounding set of input design loads.

HI-STORM 100U VVM Lid Lifting Analyses (Load Case 05 in Table 2.I.5)			
Item	Calculated Value	Allowable	Safety Factor
Bending of Lift Lugs (kip)(ANSI N14.6)	4.000	5.275	1.32 (see Note 1)
Shear in Lift Lugs (kip)(ANSI N14.6)	1.609	3.165	1.97 (see Note 1)
Load in Welds Near Lifting Lugs (kip) (Reg. Guide 3.61)	5.657	6.33	1.12 (see Note 2)
Primary Stress in Lid (ksi)(ASME Level A Limit)	< 10	26.25	> 2.63
Note 1: Computed safety factors represent the margin over that required by ANSI N14.6-1993 (0.1 x ultimate load). Note 2: Computed safety factor is based on 60% of yield strength for base metal and represents margin over limit set by Reg. Guide 3.61.			

It is concluded that all structural integrity requirements are met during a lift of the HI-STORM 100U VVM Closure Lid. All factors of safety, using applicable criteria from the ASME Code Section III, Subsection NF for Class 3 plate and shell supports, from USNRC Regulatory Guide 3.61, and from ANSI N14.6, are greater than 1.0.

3.I.4.4 <u>Heat</u>

i. Summary of Pressures and Temperatures

Tables 2.I.1 and 2.I.2 present applicable design inputs for the HI-STORM 100U VVM. No new inputs are required for the HI-TRAC and the MPC.

ii. Differential Thermal Expansion

All clearances between the MPC and the HI-STORM 100U VVM are equal to or larger than the corresponding clearances in the aboveground HI-STORM 100 systems (see Section 4.4). Therefore, no interferences between the MPC and the VVM will occur due to thermal expansion of the loaded MPC. The Divider Shell is insulated on one surface and is exposed to heated air on the other shell surface. Therefore an analysis to demonstrate that free axial thermal expansion of the Divider Shell will not close the initial gap between the top end of the Divider Shell and the base of the Closure Lid is provided. The Divider Shell is considered as a heated member, subject to an average temperature increase over its entire length. The actual axial absolute temperature profile can be integrated over the length of the Divider Shell to define the average absolute temperature. Once the average absolute temperature is known, the free thermal growth is computed and compared with the provided gap between the Divider Shell and the Closure Lid.

The average temperature rise above ambient is bounded by DT (ambient is 80°F per Table 2.I.1, and average metal temperature over the length of the Divider Shell is from Table 4.I.3, footnote):

DT = (300°F – 80°F) = 220°F

From Table 3.I.3 (a), a bounding coefficient of thermal expansion, appropriate to DT, is:

$\alpha = 6.27 \times 10^{-6}$ in/in-°F

The nominal length of the divider shell is:

L = 221.5625"

Therefore, the free thermal expansion, based on the nominal length is α x L x DT, and is computed and compared against the nominal gap provided (as shown in the licensing drawing).

Key Result from Free Thermal Growth Analysis of Divider Shell

Item	Bounding Value	Allowable Value*	Safety Factor
Thermal Growth (inch)	< 0.4	0.5	>1.25 (against contact)
*This is the nominal gap provided between the top end of the Divider Shell and the Closure Lid Surface (see Dwg. 4501, sheet 4 in Subsection 1.I.5).			

iii. Stress Calculations – VVM Components

a. HI-STORM 100U VVM Stresses Under Transporter Loading and Substrate Overburden (Load Case 07 in Table 2.I.5)

During HI-STORM 100U system loading, a HI-TRAC transfer cask with a fully loaded MPC is placed over a HI-STORM 100U VVM using a specially designed transporter and a lifting device meeting "single-failure proof" requirements, as applicable. The transfer cask is connected to the CEC using an ancillary mating device (see Figure 3.I.4). Although a handling accident is not credible, the CEC must possess the capacity to support any transporter loads imposed at and below the substrate surface during the short time when the transporter is positioned over a VVM cavity and carrying the weight of the loaded HI-TRAC (i.e., before the HI-TRAC is placed on the mating device). This loading condition leads to a maximum sub-surface lateral pressure on the CEC shell which may potentially cause its ovalization. This configuration also includes the loaded transporter traveling over a previously loaded VVM on its way to an empty CEC.

Table 3.I.1 gives the essential data on the representative transporter including its loaded weight and its track length and width (i.e., size of the load patch (Figure 3.I.5)). The average normal pressure, at the transporter track and TSP interface is computed by dividing the weight of the loaded transporter by the total area of the two load patches.

To determine the stress and displacement field in the CEC due to the combined action of the loaded transporter and the soil overburden, a 3-D ANSYS model of a VVM (see Figure 3.I.2) is prepared. The finite element model has the following attributes:

- The soil is modeled as an elastic continuum with properties specified in Tables 2.I.2 and 3.I.5. The VVM Interface Pad (VIP), which is separated from the Top Surface Pad (TSP) by a construction joint, is unaffected by the deflection of the TSP under the transporter weight. The VIP essentially is a dead weight on the soil column below and is appropriately incorporated in the model. To appropriately model the VIP within the confines of a linearly elastic construct, it is represented by a material with a very low Young's Modulus, but the correct weight density. This modeling assumption provides the appropriate weight on the substrate from the VIP but provides no additional strength to the TSP or to the CEC.

- The minimum CEC pitch from the licensing drawing is used.

- The TSP, shown in the licensing drawings, is represented by its appropriate elastic properties (Table 3.I.4).

- The soil mass surrounding the ISFSI is assumed to be constrained from expansion across the planes of symmetry (so as to maximize the Poisson compression load on the CEC). The bottom of the soil continuum extends to the SFP.

- The CEC shell is assumed to have its nominal un-corroded thickness; the stress and strain results are subsequently adjusted to reflect the postulated corrosion allowance (see Table 2.I.1).

HOLTEC INTERNATIONAL COPYRIGHTED MATERIAL

- To linearize the problem, the soil is assumed to be bonded to all interfacing surfaces.

The results of the stress analysis are pictorially shown in Figure 3.I.11 where stress intensity in the CEC is plotted. As can be seen from this figure, the maximum primary stress intensity value is 1,390 psi based on the nominal shell thickness of 1 in. Accounting for the corrosion allowance in the CEC shell, the maximum stress intensity (essentially bending in nature) is appropriately adjusted to 1,816 psi ((1 in/0.875 in)^2 x 1390 psi). When compared with the Level A stress limit from ASME code Section III, Subsection NF (per Table 2.I.5), the maximum computed stress intensity provides a factor of safety:

$$SF = \frac{allowable}{actual} = \frac{26.25}{1.82} = 14.4$$

Because the stresses in the CEC shell remain elastic, no reduction in the diametral opening of the CEC due to plastic deformation is indicated. Therefore, the retrievability of the MPC is assured.

b. HI-STORM 100U Lid Integrity Evaluation for Normal plus Explosion Loads, CEC Container Shell Evaluation Under Bounding Vertical Load (Load Case 02 in Table 2.I.5), and Design Basis Fire (Load Case 06 in Table 2.I.5)

The VVM Closure Lid rests on the CEC and resists vertical loads, arising from dead weight, and from induced loadings from explosions, from seismic accelerations, and from tornado missile impact. In this subsection, the analysis considers only the normal loading condition plus the steady pressure bounding the explosion pressure (see Table 2.I.1). The finite element model shown in Figure 3.I.1 is used to obtain this solution; the Closure Lid vertical support is now all around and is provided by the CEC Container Shell Flange (instead of by the lift lugs). The stresses from the solution are compared, per the criteria in Table 2.I.5, with allowable stress values for plate and shell structures as provided in ASME Section III Code, Subsection NF. The allowable stress intensity is per Table 3.I.3 (c) for Level D conditions at a bounding temperature of 350°F.

The vertical load on the Container Shell ring flange, which can be computed from equilibrium, does not bound the vertical load under normal conditions when the Closure Lid is removed and replaced by a loaded HI-TRAC plus a Mating Device. The bounding vertical load during the transfer operation is an input for the evaluation of the Container Shell for this load case using Strength of Materials methodology. Key results from the analysis of the Closure Lid under the normal loading condition plus the steady pressure, and the follow-on analysis of the corroded Container Shell under the bounding vertical load (during the MPC transfer operation) are summarized in the following table:

HOLTEC INTERNATIONAL COPYRIGHTED MATERIAL

Stress Analysis of the Closure Lid and CEC Container Shell Under Bounding Vertical Load During Normal Operations (Load Case 02 in Table 2.I.5)			
Item	Bounding Value from calculations	Allowable Limit	Safety Factor
Maximum Primary Principal Stress Anywhere in Lid (ksi)	< 12.0	59.65(Level D Stress Intensity Limit) 26.25 (Level A Stress Limit)	> 4.97* > 2.19*
CEC Container Ring Flange Weld (kips)	< 300	3,018	> 10.06
Compression Stress in CEC Container Shell Under Bounding Vertical Load (ksi)	< 1.425**	17.5	> 12.28
* The results from the analysis are presented in terms of principal stresses for simplicity. Safety factors are determined by comparison with the Level D stress intensity limits (Table 3.I.3(c)), or with Level A stress limits (Table 3.I.3 (b)). Regardless of the measure used, the safety factors are large. ** The bounding compressive stress is based on a fully corroded shell thickness and also conservatively includes the full weight of the CEC in addition to the bounding load at the top.			

From the above results, it is concluded that there is minimum structural demand on the HI-STORM 100U Closure Lid and CEC Container Shell during normal operation (even if the explosion pressure is conservatively considered as a normal condition).

With respect to the fire event (Load Case 06 in Table 2.I.5), where the Closure Lid steel temperature rises to the limit set in Table 2.I.5, it is noted from Tables 3.I.3 (a) and (b) that the Level A stress limit is reduced to 0.68 of the room temperature value, the yield strength is reduced to 0.66 of its room temperature value, and the ultimate strength is reduced to 0.92 of its room temperature value. From the stress values obtained in the lid (even with the explosion 10 psi surface pressure load included), it is evident that a total collapse of the lid due to reduction of the ultimate strength is not credible.

Seismic loading on the VVM is considered in Subsection 3.I.4.7 (Load Case 04 in Table 2.I.5). Subsection 3.I.4.8 considers tornado missile impact (Load Case 03 in Table 2.I.5).

iv. <u>Stress Calculations – ISFSI Structures</u>

The 100U ISFSI consists of plate-type reinforced concrete structures whose minimum section strength properties are defined by Table 2.I.2 and the licensing drawings. The ISFSI is supported by the subgrade underneath the SFP, which may include pilings, if required, to meet the effective stress wave velocity in Table 2.I.2. The loadings on the ISFSI are:

a. Dead load of the VVM and the concomitant effect of settlement over the Design Life of the system. (D in Table 2.I.11). The method to incorporate the effect of long-term settlement of the subgrade underneath the SFP (may also be referred to as the undergrade), described in Subsection 2.I.2, is used. This method essentially consists of using the deflection properties of the different layers to define equivalent elastic properties of the subgrade underneath the SFP. In the finite element analysis of the SFP, the degraded elastic properties of the subgrade underneath the SFP are utilized to account for the effect of long-term settlement. The long-term settlement of the subgrade underneath the TSP and VIP is also considered in a similar manner.

   The Dead load on the SFP from the weight of the loaded VVM's nearly equals the weight of the earth removed. Therefore, the long-term settlement of the SFP is expected to be quite small. Likewise, the dead load on the TSP and the VIP is relatively small (from self-weight of the pads).
   The retaining wall under excavated condition (see Subsection 2.I.2) supports the soil overburden pressure (classified herein as Dead load).

b. Live load from the loaded transporter acts directly on the TSP (see Figure 3.I.4 and 3.I.5). This load also adds to the overall load on the SFP (L in Table 2.I.11). The load from the transporter is the sole live load applicable to the ISFSI structures. For structural qualification, the loaded transporter (live load) is assumed to be situated over the centrally located cavity.

c. Seismic load is computed using the methodology presented in Subsection 3.I.4.7. This load, denoted as E in Table 2.I.11, is the aggregate of the peak dynamic load exerted on the ISFSI less the dead weight. For conservatism, the load E is applied as a static load in the stress analysis of ISFSI structures even though it is impulsive in nature.

Paragraph 3.I.4.7.3 contains details on the stress analysis of the ISFSI structures to demonstrate ACI code compliance.

3.I.4.5 Cold

Due to its subterranean configuration, the structural components of the VVM are relatively protected from extremes in the ambient temperature in comparison to the HI-STORM 100 or 100S overpacks. Therefore, no new analyses are identified for the HI-STORM 100U system.

3.I.4.6 Flood

The buried configuration of the HI-STORM 100U system renders it immune from sliding under the action of a design basis flood. No new analyses are needed for an actual extreme environmental event.

Although the condition does not necessarily arise due to a flood, a limiting uplift scenario where the VVM CEC is in place and the surrounding substrate produces a buoyant force by unspecified means

HOLTEC INTERNATIONAL COPYRIGHTED MATERIAL

is considered. For this condition (Load Case 01 in Table 2.I.5), the limiting uplift condition determines the minimum weight that needs to be in place to prevent uplift during construction. This could be in the form of a temporary cover. The upward directed buoyant force exerted on the CEC cavity is computed assuming a weight density of water and compared with the dead weight of the CEC. Under the postulated condition, the net uplift load (Buoyant Force – Weight of CEC) can be calculated. The required temporary weight that is needed to produce a net downward force is calculated in [3.I.27] and specified in Table 2.I.5.

For the case of a loaded VVM with the Closure Lid in place, or for an empty CEC with the Closure Lid in-place, the buoyant force is less than the vertical download, so there is no uplift.

Should the full buoyant force develop from any means, a lateral pressure load is imposed on the CEC bottom plate. Conservatively assuming an empty VVM, the full buoyant force provides a pressure causing bending of the CEC Bottom Plate, which is partially restrained against rotation by the CEC shells (note that in a loaded VVM, the MPC also helps to support the Bottom Plate of the CEC as its weight causes the central shim to act as a support for the Bottom Plate of the CEC). The stress intensity resulting from CEC Bottom Plate bending is compared to the Level D allowable stress intensity. Using the solutions for maximum stress in a clamped and simply supported plate, and averaging the results from the two solutions to approximately account for the rotational restraint provided by the CEC Container Shell, gives the following bounding safety factor for stress in the bottom plate under the postulated buoyancy loading:

Allowable Stress = 66,875 psi (Table 3.I.3(c) @ 125°F per Table 2.I.5). Safety factor is calculated to be greater than 4.0.

3.I.4.7 Seismic Event - HI-STORM 100U (Load Case 04 in Table 2.I.5)

The HI-STORM 100U system, plus its contents, may be subject to the Design Basis Earthquake (DBE) defined by the response spectra in Figure 2.I.4. As mentioned in supplement 2.I and further explained in this subsection, the DBE has been defined for the 100U ISFSI to insure that the operative spectra (Figure 2.I.4) essentially envelope the corresponding site DBE spectra at virtually all US sites. Because the VVM is buried in the substrate, tip-over of the VVM is not credible. The entire VVM can move laterally with the surrounding and supporting substrate.

Under the action of lateral seismic loads, the CEC Container Shell globally acts as a beam-like structure supported on a foundation driven by the site seismic accelerations. During a seismic event, the lateral loading on the CEC consists of:

i) Inertia force from CEC self-weight
ii) Inertia forces from the Closure Lid self-weight
iii) Inertia forces from the self weight of the VIP
iv) Interface forces from the rattling of the MPC within its confines of the CECand the rattling of the contents inside the MPC
v) Interface forces from the subgrade and from the SFP

HOLTEC INTERNATIONAL COPYRIGHTED MATERIAL

The CEC Container Shell develops longitudinal stresses as it bends like a beam to resist the input seismic loads. In addition, the CEC Container Shell tends to ovalize under the loads. Both effects are captured in the seismic analysis.

The Design Basis Seismic Model (DBSM) used to perform the safety analysis of the 100U ISFSI under the Design Basis Earthquake (DBE) defined by Figure 2.I.4 is described in the following.

3.I.4.7.1 Design Basis Seismic Model

Parametric studies were performed to support the initial certification of the HI-STORM 100U VVM. These studies defined the Design Basis Seismic Model. In particular, a non-linear dynamic model on LS-DYNA was found to produce much greater response and internal stresses than a linear analysis on SASSI. Further, a 5x5 VVM array model was standardized for dynamic analysis purposes. Accordingly, LS-DYNA is used for all required dynamic analysis of the VVM array. The DBSM consists of three discrete models, namely:

1. A VVM Array Model used to characterize the interaction of the ISFSI with the surrounding soil continuum. This is performed using a 5x5 VVM array (see Figure 3.I.3-B).

2. A VVM Array Model for the optional 100U design where retaining walls are in place (see Figure 3.I.3-C). The lateral subgrade beyond the retaining wall is assumed to be removed all the way down to the bottom of the SFP, which conservatively represents an excavation configuration.

3. A single VVM model with a detailed simulation of the internal parts of the VVM to obtain an accurate characterization of the stress/displacement field (see Figure 3.I.3-D).

The seismic analysis consists of three discrete steps, namely:

A. Soil-structure model development.
B. Use of the VVM Array Model to determine the bounding dynamic loads applied to the ISFSI Structures.
C. Use of the Single VVM Model to compute stresses in the VVM Components.

A. Soil–Structure Model Development

i. Based on the lower bound shear wave velocity profile of US nuclear power plants (Figure 2.I.6), a two-step earthquake response analysis using the computer code SHAKE2000 and LS-DYNA is performed to establish a bounding seismic loading condition for the 100U underground fuel storage system. The Design Basis Earthquake for the HI-STORM 100U system thus obtained is defined by the seismic response spectra at both the ground surface and the ISFSI foundation surface elevations as shown in Figure 2.I.4. The input seismic acceleration time history used in the first step (SHAKE) analysis is derived from the

Regulatory Guide 1.60 seismic response spectrum and designated as the rock outcrop motion. The input acceleration time history is scaled to yield ground surface ZPAs (at the top of grade elevation) specified in Table 2.I.2. The 1-D SHAKE analysis model consists of 21 native soil layers of the 100U ISFSI site with a total thickness of 101 ft; the top of the 6^{th} soil layer is aligned with the bottom of the SFP. The total soil depth of the SSI Model is about five times the height of the underground ISFSI (Due to the limitation of the linear code, a further increase of the soil depth in the SHAKE model leads to questionable seismic response results in the case of a strong seismic motion and weak soil properties). The averaged strain compatible shear wave velocity is 450 ft/s for the soil layers above the SFP and is 485 ft/s for the layers below the SFP, which has been set as the lower-bound soil design data in Table 2.I.2 for a candidate 100U ISFSI site. The finite element soil model in the second step (LS-DYNA seismic response analysis) uses the average strain-compatible wave velocities obtained from the SHAKE analysis to represent the soil layers above and below the SFP elevation. The acceleration time history at the soil column bottom surface, also obtained from the SHAKE analysis in the first step, is used as the input seismic motion for the LS-DYNA seismic response analysis. The response spectrum plots shown in Figure 2.I.4 are the results of the LS-DYNA seismic response analysis.

Figure 3.I.3-A shows the LS-DYNA soil model for the seismic response analysis. Note that the lateral dimension of the ISFSI soil model is significantly greater than that of the ISFSI. The periphery nodes of the soil model space at the same elevation are constrained to move together to simulate the seismic response of the semi-infinite space of soil. According to the numerical study on various lateral boundary conditions of the finite element soil model [2.I.10], this lateral boundary condition, also known as a "slave boundary condition", is appropriate to predict the soil response in a seismic event. The same soil model and input seismic motion used in the LS-DYNA seismic response analysis will be used for the LS-DYNA soil-structure interaction analysis for the 100U ISFSI loaded with VVMs. The boundaries of the soil model are sufficiently away from the ISFSI pads to ensure that structural response of the ISFSI will not be significantly affected.

ii. The spectra in Figure 2.I.4 define the seismic input against which the spectra at a candidate ISFSI site should be compared to determine whether the generic analysis in this FSAR is bounding or additional site specific analysis set down per sub-section 2.I.6 are required.

iii. Consistent with the sketch in Figure 2.I.5, the 100U soil-structure LS-DYNA model consists of loaded VVMs, concrete pads, and soil spaces with properties as defined in Tables 2.I.2 and 3.I.4. The ISFSI model is developed based on a 5×5 VVM configuration, which has previously been approved under LAR 1014-6 and is considered to be appropriate for capturing the effect of the ISFSI size on the structural analysis results. Depending on the purpose of the analysis, the 100U soil-structure model may include 5x5 fully loaded VVMs or just one loaded VVM. Similarly, a loaded Vertical Cask Transporter (VCT) may be considered in the model to obtain the bounding load applied to the TSP and to demonstrate the seismic stability of the loaded VCT. For the optional ISFSI design including a retaining wall, the soil-structure model is developed based on the governing configuration where the subgrade outside the retaining wall is excavated all the way to the depth of the SFP elevation. Therefore, a total of three 100U soil-structure LS-DYNA models (see Figures 3.I.3-B to 3.I.3-D) are developed to perform the design basis earthquake analysis.

iv. The corrosion of the CEC is considered by using a reduced thickness (i.e., 1/8" thinner than the nominal thickness) in the soil-structure LS-DYNA models.

v. Proper element size and time step controls in the dynamic model are implemented following the guidance in references [3.I.28] and [3.I.29].

B. VVM Array Model

The object of the VVM Array model is to obtain conservative values of the loads on the ISFSI structures under the Design Basis Earthquake (Figure 2.I.4). The VVM Array model has the following essential attributes:

i. The MPC is represented by a solid rigid cylinder of mass equal to its total mass. This means that all internal masses will move in unison and the inertia forces of the MPC are maximized, which will conservatively result in greater impact loads applied to MPC guides and the CEC base plate.
ii. The Divider Shell and the CEC shell are modeled as elastic shells but the Closure Lid and the Lid Ring are simulated as rigid bodies. Note that the combination of elastic shells and rigid lid ring used in the finite element model has little effect on the load path between the Divider Shell and the CEC flange during the seismic event.
iii. The ISFSI pads (i.e., TSP, SFP, etc.) are simulated as a flexible plate-type structure, as is the retaining wall, if used. The retaining wall is added to the finite element model in the optional ISFSI design case (see Table 3.I.6).
iv. The SFP is fully loaded with a 5×5 VVM array.
v. A loaded VCT is assumed to be located at the center of the fully populated ISFSI except for the case with retaining walls. The VCT, along with the carried transfer cask, is modeled as a freestanding rigid body.
vi. The elastic material model is used for all ISFSI concrete structures except for the TSP, which is characterized by an inelastic concrete model to account for energy dissipation in the concrete due to the impact loading from the loaded VCT. For the case where cracking of the concrete needs to be considered, the Young's Modulus of the SFP is reduced to 50% of its nominal value per the guidance in Section 3.4 of [3.I.29].

C. Single VVM Model

The Single VVM model is used to perform the safety evaluation of the VVM components and the stored MPC under the Design Basis Earthquake. The applicable acceptance criteria are provided in Table 2.I.6. To conservatively evaluate the structural integrity of the VVM components, the Young's Modulus for the SFP is assumed to be equal to 50% of its nominal value. This is prompted

HOLTEC INTERNATIONAL COPYRIGHTED MATERIAL

by the results of VVM Array Model runs (see Table 3.I.7), which indicate that the VVM Components experience amplified responses if the reduced modulus is used for the SFP.

The Single VVM model complies with the provisions set forth in the following:

i. The SFP is loaded with only one VVM at the edge of the SFP. A loaded VCT, modeled as a freestanding rigid body, is conservatively assumed to be located above the center of the loaded VVM.
ii. The Cavity Enclosure Container (CEC) is discretized by an appropriate finite element grid to simulate its Container Shell and Bottom Plate, the Divider Shell, and the MPC guides in an explicit manner. The true stress-strain relationship of the material is used to obtain the realistic deformation of these structural members.
iii. The MPC shell, baseplate, and top lid are modeled using sufficient element discretization so that the peak primary stresses of the MPC components under the seismic loading condition can be captured for structural evaluation.
iv. The fuel basket is modeled with thin shell finite elements arrayed to simulate inter-cell connectivity in an explicit manner.
v. Nominal small gaps between the fuel basket and the MPC are explicitly modeled, as is the nominal gap between the MPC and the CEC at the upper and lower MPC guide locations.
vi. Each fuel assembly is represented by an equivalent homogeneous, isotropic prismatic beam of an equivalent elastic modulus whose fundamental lateral natural frequency accords with that of the actual fuel assembly. A bounding fuel assembly weight is used and the fuel basket is assumed to be fully populated with fuel assemblies.
vii. The seismic responses of MPC structural components are simulated using the elastic material model so that the stress results can be directly compared with the corresponding ASME NB stress limits.

3.I.4.7.2 Qualification of VVM Components

The CEC Components and parts of the MPC subject to significant loadings during the DBE event are:

a. CEC shell and Divider Shell (subject to ovalization)
b. MPC shell (bending of the shell as a beam, resulting in axial membrane stress in the shell)
c. MPC top and bottom guides
d. Lateral loading on the fuel basket panels.
e. Localized strain in the MPC shell (due to impact of the MPC with the MPC guides attached to the Divider Shell)

The safety analysis of each component under the DBE event is summarized below:

a. CEC shell and Divider Shell: Maximum radial deformation of the two shells is tracked for the single VVM simulation scenario in Table 3.I.6. The ratio of the original ovalization to the actual ovalization gives the safety factor:

$$Safety\ Factor = \frac{Permissible\ radial\ displacement}{Maximum\ computed\ radial\ displacement\ from\ Figure\ 3.I.23}$$

$$= \frac{2.5''}{0.1325''} = 18.86$$

b. Primary stress in the MPC shell: The maximum stress intensity in the MPC shell is computed under the single VVM simulation scenario. The allowable stress intensity for this case corresponds to the Level D condition. The safety factor is computed as:

$$Safety\ Factor = \frac{Level\ D\ allowable\ Stress\ Intensity\ from\ Table\ 3.I.3(d)}{Maximum\ computed\ primary\ Stress\ Intensity\ from\ Figure\ 3.I.24}$$

$$= \frac{42{,}000\,psi}{12{,}860\,psi} = 3.26$$

c. Top and Bottom MPC Guides: The maximum lateral load bearing capacity of the top and bottom plate guides is computed in Supplement 4 of Reference [3.I.27]. The maximum dynamic impact loads from the single VVM model can be extracted from the impact load time history results shown in Figure 3.I.25. The safety factor is calculated as:

$$Safety\ Factor = \frac{MPC\ Guides\ Lateral\ Load\ Bearing\ Capacity}{Maximum\ MPC\ to\ MPC\ Guides\ Contact\ Force}$$

$$= \frac{4.41 \times 10^5\,lb}{108{,}826\,lb} = 4.05$$

For the tubular MPC top guide design, the MPC impact analysis documented in Supplement 11 of Reference [3.I.27] demonstrates that the tube guide would not experience any global plastic deformation under the Design Basis Earthquake condition. This means that there is no risk of progressive flattening of the guide tubes from repetitive impacts during the seismic event.

d. Loading on the Fuel Basket panel: The fuel basket panels are qualified to withstand 45 g's of lateral acceleration (during the non-mechanistic tip-over event). The maximum fuel g-load predicted by the LS-DYNA simulation is 2.5 g's as shown in Figure 3.I.26. The factor of safety, therefore, will be equal to the ratio of the two. Hence,

HOLTEC INTERNATIONAL COPYRIGHTED MATERIAL

$$Safety\ Factor = \frac{45}{2.5} = 18$$

e. Maximum Local Strain in the Confinement Boundary in the Impact Region:

The small clearance between the MPC and the MPC guides can lead to a high localized strain in the region of the shell where the impact from rattling of the canister under a seismic event occurs. The extent of local strain from impact is minimized by locating the MPC guide in the vertical direction such that the mid-height of the impact footprint is aligned with the bottom surface of the closure lid. Thus the location of impact is removed from the lid-to-shell weld junction. It is necessary to insure that the maximum value of the local (true) strain in the shell (confinement boundary) region of impact is well below the failure strain. For this purpose, the recommendation in [3.I.31] is used. The methodology for computing the local strain is presented in the following and applied to the seismic problem analyzed in this subsection.

A finite element model of the MPC suitable for implementation in LS-DYNA is prepared with special emphasis on the top region of the canister where a very fine grid is employed. All elements have elasto-plastic and large strain capability. The solid elements in the lid and the lid-to-shell weld are of type 2 (fully integrated) and those in the shell are type 16 (fully integrated). The integration across the shell wall employs the maximum number of points available in LS-DYNA (10 points). A mesh sensitivity study has been performed using a finer grid size for the MPC shell to verify that the results are converged.

The MPC contents, namely the fuel basket and the SNF, are modeled exactly as set forth in the DBSM in the foregoing (articles (iii.), (iv.), and (v.) in Subsection 3.I.4.7.1 C Single VVM Model). To define a conservative scenario of MPC/MPC guide impact, the velocity time history of the top of the MPC is surveyed from the dynamic analysis of the VVM using the DBSM. The maximum velocity thus obtained is assumed to exist as the initial condition in the LS-DYNA simulation. This assumption is most conservative because it assumes that the cyclic motion transmitted by the earthquake does not detract from the canister's momentum before impact occurs (observations show that the canister slows down by the earthquake's cyclic energy input, thus significantly lessening the severity of the impact). In addition, the MPC guide is fixed at its base, which conservatively ignores the deformation of the divider shell and therefore maximizes the impact. The finite element model is shown in Figure 3.I.12. To implement the above model, the search for the maximum velocity in the dynamic solution yielded less than 24.7 in/sec as shown in Figure 3.I.27. Applying an initial velocity of 26.0 in/sec as the initial condition to the above model provided the strain field shown in Figure 3.I.13 for the tubular guide design. The impact between the MPC and the MPC top guides results in an MPC shell maximum plastic (true) strain of less than 1.52×10^{-2} in/in for the tubular guide design and 3.1×10^{-2} in/in for the optional plate guide design (see Calculation 11 of

[3.I.27]), respectively, which are only a small fraction of the acceptable value (0.1) per [3.I.31]. Therefore the integrity of the confinement boundary is assured.

3.I.4.7.3 Strength Qualification of the ISFSI Structure

Under the Design Basis Earthquake (Figure 2.I.4), the loads exerted on the Support Foundation Pad and the Top Surface Pad (as illustrated in Figure 3.I.4) are obtained from the LS-DYNA SSI simulations listed in Table 3.I.6. Table 3.I.7 lists the peak ISFSI interface loads obtained from various LS-DYNA runs listed in Table 3.I.6. In order to incorporate an additional margin of safety in the ISFSI structural analysis, the structural evaluation of ISFSI components uses input loads (see Table 3.I.8) that bound the peak ISFSI interface loads from the LS-DYNA SSI simulations in Table 3.I.7. The use of the bounding loads is in keeping with a similarly bounding value of settlement specified for the strength analysis of the SFP and the TSP (see Table 2.I.2).

The SFP and TSP shall meet the minimum structural requirements set down in Table 2.I.2 and the licensing drawings. The SFP and TSP are required to satisfy ACI-318 (2005) strength limits under all applicable load combinations (Table 2.I.11).

Likewise, the retaining wall, if used, shall meet the minimum concrete and rebar requirements provided in Table 2.I.2 and the licensing drawings. The site specific design may utilize a thicker and more heavily reinforced wall, if necessary, at user's option.

Table 3.I.8 provides the loading data used in the strength analysis of the ISFSI structures. The following discrete analyses are required:

(i) Compute the long-term settlement of the undergrade supporting the SFP assuming all VVM locations are loaded for the entire Design Life: Determine the "effective" elastic modulus of the subgrade under the SFP to simulate the effect of differential settlement in the structural analyses model. As discussed in Section 2.I.4, the long-term settlement of the undergrade from the loaded VVMs and the dead weight of the SFP is very small because the combined equivalent density of the loaded VVM's and the SFP is nearly equal to the density of the excavated subgrade.

(ii) Compute the long-term settlement of the subgrade under the TSP/VIP relative to the SFP from subgrade weight in addition to the dead weight of the TSP and VIP. Determine the "effective" elastic modulus of the subgrade between the TSP/VIP and the SFP to simulate the effect of long term differential settlement in the structural analyses model. As discussed in Section 2.I.4, the long-term settlement of the well conditioned subgrade under the TSP is appreciably small because of the small long-term loadings acting on the TSP.

(iii) Prepare a finite element model of the pads in ANSYS and determine the stress field under the factored Dead and Live loads with the settlement based "degraded" elastic moduli for the soil regions directly beneath the TSP and SFP (Spaces A and C in Figure 2.I.5). For the lateral subgrade adjacent to the HI-STORM 100U ISFSI (Spaces B and D in Figure 2.I.5), the dynamic (strain compatible) elastic moduli from Table 3.I.4 are conservatively used as input to maximize the flexural moments due to differential settlement.

(iv) Compute the stress field in the pads under factored seismic loads using dynamic elastic modulus corresponding to the minimum shear wave velocity of the subgrade specified in Table 2.I.2.

(v) Use the bounding loads listed in Table 3.I.8 to compute the stress fields in the pads (SFP and TSP) from the DBE.

(vi) Combine the factored loads and determine the total stress resultants. Compare with the respective section strengths to establish the factors of safety for the SFP and TSP.

(vii) Compute the bearing stress (or load) on the subgrade under the TSP using the combined factored loads from the transporter and the TSP/VIP and compare with the corresponding allowable limit to establish the safety factor for the subgrade under the TSP.

A comprehensive summary of the analyses and the associated margins of safety are discussed below:

The structural evaluation of the HI-STORM 100U ISFSI is performed using the commercial computer code ANSYS [3.I.33]. The constituents of the ISFSI namely the Support Foundation Pad (SFP), the subgrade under the SFP (the undergrade), the Top Surface Pad (TSP) and the subgrade lateral to the CEC under the TSP are all modeled using linear elastic SOLID45 elements. The VVM interface pad (VIP), which carries no load except for its self-weight, is conservatively omitted in the model. The lateral subgrade adjacent to the HI-STORM 100U ISFSI (Spaces B and D in Figure 2.I.5) is also included in the model, and it extends laterally for a distance that exceeds the overall depth of the model. The element mesh is intentionally kept fine in the areas of load application on the SFP and the TSP. For convenience of load application, the footprint of the CEC base on the SFP is carefully articulated in the finite element model. The substrate under the SFP is terminated at approximately 101 ft below the TSP, which is consistent with the Design Basis Seismic Model discussed in Subsection 3.I.4.7.1. The "base" model (Simulation Model I) considers that all the storage locations in ISFSI are populated and experience identical peak vertical seismic loading from Table 3.I.8, which bounds the peak result obtained from the LS-DYNA SSI solution as discussed previously. Because of the symmetric geometry and loading, a quarter symmetric finite element model is sufficient to represent the fully loaded ISFSI. Figure 3.I.14-A shows the finite element model of HI-STORM 100U ISFSI. The "degraded" elastic moduli of the subgrade under the SFP and the subgrade between the TSP and SFP is appropriately computed to account for the long-term differential settlement effects as described in Subsection 2.I.4. The long-term settlement and the "effective" subgrade elastic moduli are derived using the governing soil characteristics following guidelines from [2.I.6]. Table 3.I.5 lists the bounding subgrade characteristics and the concomitant elastic moduli effective under dynamic loading. To address different loading patterns on the ISFSI and for completeness, additional partially loaded ISFSI configurations are considered in the evaluations. The partial configurations include a single row loaded ISFSI (the middle row of VVM locations is loaded) and a single VVM loaded ISFSI (a single VVM location centered near the periphery of the ISFSI is loaded). Figures 3.I.20 through 3.I.21 illustrate the partial loading configurations for the ISFSI. These are hereinafter referred to as Simulation Models II and III, respectively. For Simulation Models I through III, the optional retaining walls are not included in the finite element model.

The effects of the retaining wall are evaluated in a fourth simulation model (Simulation Model IV), which is shown in Figure 3.I.14-B. In this model, the lateral subgrade surrounding the retaining walls is completely removed to bound any future excavation activities associated with the construction of a new underground ISFSI, and for consistency with the LS-DYNA SSI simulation model (see Figure 3.I.3-C). For Simulation Model IV, the middle row of VVM locations is loaded similar to Simulation Model II (see Figure 3.I.22).

To simulate the material continuity at the extreme boundary surfaces of the model, translations are constrained at the lateral face of the subgrade. The extreme bottom surface of the model is fixed representing the bedrock (or competent soil) elevation.

The following individual load steps are considered in the analysis:

1. Bounding load transmitted by the VVM, as determined from the LS-DYNA SSI analysis and summarized in Table 3.I.8, is applied as an effective pressure on the footprints of the CEC base at all VVM locations.
2. The load from the transporter is applied as a normal pressure (see Figures 3.I.15, 3.I.20 and 3.I.21) over the transporter load patch on the TSP. For Simulation Model IV, the transporter load is not applied to the TSP since no VVM loading/unloading operations are expected to occur during excavation activities associated with the construction on a new underground ISFSI.
3. The dead weight from VIP is applied as normal pressures on the substrate elements directly beneath the VIP.
4. In-plane tensile loads on the SFP and TSP from the retaining wall are applied as lateral pressures on the SFP and TSP boundaries for Simulation Model IV.
5. To simulate the self weight of the modeled portion of the ISFSI, a 1g gravity load is applied. The densities of the various constituents are appropriately input in the model to accurately reflect the individual component weights.

It must be noted that the structural analysis of the ISFSI conservatively considers the peak dynamic loads from the LS-DYNA SSI analysis. However, it shall be permitted to use equivalent static loads obtained by removing high frequency components that would not contribute to the structural response using appropriate filters.

Since the peak loads from the LS-DYNA SSI analyses are substantially larger in comparison to the dead and live loads, the load combination LC-3 from Table 2.I.11 governs for the ISFSI structural evaluation. However, the analyses are carried out for load combinations LC-2 and LC-3, and the corresponding results substantiate that the load combination LC-3 is governing.

Figures 3.I.16 through 3.I.19 depict the maximum in-plane stresses in the ISFSI concrete structures (viz. SFP and TSP) for the governing load combination LC-3 for all the ISFSI configurations analyzed. The in-plane axial and bending stress on the SFP and the TSP elements are post-processed to compute the equivalent moments. The induced moments are compared to the respective moment capacities to determine the corresponding factor of safety. Table 3.I.10 summarizes the results for the SFP and the TSP respectively for all ISFSI configurations analyzed.

HOLTEC INTERNATIONAL COPYRIGHTED MATERIAL

The minimum flexure safety factor is produced by Simulation Model III, and it is associated with the TSP. In the Simulation Models I, II and III , the peak load from the LS-DYNA SSI analysis acting on one transporter track (bearing on the TSP) is conservatively applied as a static load on both transporter tracks simultaneously, thereby significantly overestimating the load on the TSP. As mentioned previously, the peak dynamic loads obtained from the LS-DYNA SSI analyses from a DBE event are of impulsive nature. Use of the peak loads for static structural evaluations of the ISFSI is evidently conservative. Furthermore, no credit is taken for the Dynamic Increase Factor of 25% for flexure and 10% for shear permitted by [3.I.32] in the strength qualification of reinforced concrete.

The Table 3.I.11 summarizes the punching shear safety factor for the SFP and TSP. The minimum punching shear safety factor is associated with the TSP under the transporter seismic load, and it is well above 1.0.

The peak transporter load on the TSP from the LS-DYNA SSI analyses plus the load from the TSP are used to compute the maximum bearing stress in the substrate surface under the TSP. According to ACI-360 [2.I.8], the bearing stress can be calculated by uniformly distributing the load over the entire bearing area of the pad. For conservatism, the bearing stress calculation for the 100U sub-grade is performed using a bearing area significantly less than that of the smallest TSP (i.e., the TSP of one-VVM ISFSI). The maximum bearing stress in the sub-grade (Table 3.I.12) is smaller than the presumptive bearing stress limit, resulting in minimum safety factor above 2.0 imposed by the ACI code [2.I.8].

The evaluation of the CEC shell under the loads from the transporter load in addition to the subgrade overburden is presented in Subsection 3.I.4.4.

Finally, the structural integrity of the retaining wall is evaluated for the Design Basis Earthquake loading condition; the structural demand to the wall under normal operational conditions is small and therefore not structurally governing. Since the retaining wall is connected with the TSP and SFP through a shear key at the top and dowels at the bottom (see licensing drawing in Section 1.I.5), it can be treated as a simply supported plate (along its top and bottom edges) in the structural analysis. Therefore, the wall essentially experiences bending stress in the DBE event due to lateral soil pressure. The maximum bending moment of the retaining wall, which can be determined based on Figure 3.5-1 of Reference [3.I.28] or based on the retaining wall stress results obtained from the LS-DYNA SSI analysis for Case 3 in Table 3.I.6 (both approaches yield approximately the same result), is shown in Table 3.I.10 to be well below the bending capacity of the wall. The shear connections at the top and bottom of the retaining wall have also been evaluated for the loads induced during a Design Basis Earthquake. The results of the strength evaluation are provided in Table 3.I.13.

3.I.4.8 Tornado Missile Evaluation

3.I.4.8.1 HI-STORM 100U Lid Integrity Evaluation for Tornado Missile Strike (Load Case

03 in Table 2.I.5)

Design basis tornado missiles are specified in Table 2.2.5. The Closure Lid is the only above ground component of the VVM; therefore, missile impact analyses focus on this component. Large and intermediate tornado missiles are assumed to strike the center top surface of the lid at the design basis speed (see Table 2.2.5). For both missile analyses, a finite element model of the Closure Lid is employed (using dimensions from licensing drawings and applicable material properties), and includes contact between concrete and steel (see Figure 3.I.1). LS-DYNA is used to perform dynamic simulations of the impacts to demonstrate that neither missile completely penetrates the composite structure. The ANSYS model shown in Figure 3.I.1 is simplified to develop an input file for the LS-DYNA simulation. Elastic-Plastic Material 24 is used for the steel and Material 72 is used for the concrete. For a conservative result, engineering stress relations for the lid steel work are used with an assumed ultimate strain of 21% (per ASME Code, Sec. II, Part A). As LS-DYNA expects that true stress-strain data is input, the use of true stress-strain data, to obtain a more realistic result, is permitted (if appropriate justification is provided for the true stress-strain relation). The solution obtained using engineering stress strain data is clearly conservative in that material failure is set at the engineering ultimate strain limit rather than reflecting the true strain at failure, which will be considerably larger. A strain rate effect is incorporated by increasing the yield and ultimate strengths by a maximum of 50% (depending on the rate) as suggested by data for SA-36 steel [3.I.19]. This is the same strain rate increase used in the evaluations to assess the performance of the aboveground HI-STORM when impacted by a jet fighter aircraft [3.I.16]. A time history normal pressure loading is applied over the metal annular region around the outlet opening to simulate the large missile, and the global deformation damage to the lid is assessed. The formula from "Topical Report – Design of Structures for Missile Impact", BC-TOP-9A, Rev. 2, 9/74 [3.I.17] is used to establish appropriate pressure-time data. For the speed and mass associated with the large missile, the impact force-time curve has the form

F(t) = 0.625 sec/ft x 184.8 ft/sec x 4000 lb x sin (20t) = 462,000 lb x sin (20t) for t< 0.0785 sec.
= 0 for t >= 0.0785 sec.

This representation of the large missile impact load is appropriate as recent full-scale impact testing of a modern passenger vehicle demonstrates. Figure 3.I.6 shows the force-time history from the full-scale test of a full-size Ford passenger vehicle [3.I.18]. The test was performed at an impact speed of 35 mph and the vehicle had approximately the same weight as the design basis large deformable missile. Since the force is directly proportional to the pre-impact momentum, an estimate of the peak force at 126 mph for the vehicle is obtained by a simple ratio of the impact velocities and missile mass. Estimating the peak value from the plot produces a resulting peak force of 496,000 lb, which is the same order of magnitude as the peak value predicted from the Bechtel Topical Report, although the shape and duration of the curve is different. The results from the analysis using the load-time function from the Bechtel formula show no significant lid damage from the large missile strike on the lid because of the concrete backing. Inspection of the result concludes that the deformed shape after the event does not preclude lid removal, the lid remains in-place, and the MPC has not been impacted. The maximum lid vertical deflection during the strike is less than 0.1 inch and there are a few local regions of permanent effective plastic strain. The details of this calculation are found in [3.I.27]. The large missile impact is not the bounding strike because of the large area of impact and significant energy loss that occurs when the vehicle is crushed upon impact; the rigid, intermediate missile imparts more local and global damage to the Closure Lid.

The impact of the intermediate missile is conservatively simulated as a rigid 8" diameter cylindrical steel bar weighing 275 lb (per Table 2.2.5), traveling at 126 mph and striking the Closure Lid at the most vulnerable location, which is through the top vent opening. The strike can be at either the center of the inner shield dome or slightly off-center so as to miss the central steel connecting bar. In order to strike the MPC top lid, the intermediate missile must penetrate the steel weldment and encased concrete (see licensing drawings in Section 1.I.5). Figures 3.I.7 and 3.I.8 show the intermediate impact scenarios considered. Figures 3.I.9 and 3.I.10 show the lid state at the time of maximum bottom plate vertical displacement. For both cases, no dislodgement of the lid is indicated and plastic strains occur only in the immediate vicinity of the strike. A summary of results that bound the computed results for the two intermediate missile strikes is presented in Table 3.I.9.

Next, consider that the intermediate or large missile is traveling horizontally and strikes the side of the Closure Lid. A large missile strike at this location with a horizontal orientation is most likely not credible because of the low profile of the lid. The large missile would rotate as it broke up, resulting only in a glancing blow to the lid. However, an evaluation of the Closure Lid flange ring in either missile side strike is needed to ensure that the Closure Lid will not be driven sideways under the impact and separate from the CEC. A key structural element is the weld connecting the Closure Lid restraint ring to the Closure Lid. The capacity of the welds in the load path that resist the lateral impact load is:

Closure Lid Weld Capacity = 8,381,000 lb.

This capacity is computed assuming a limiting weld stress of 60% of the ultimate tensile strength of the base material. In any of the evaluated missile strikes from above, the peak impact load (filtered at 350 Hz (see similar filtering in the HI-STAR 100 transport license)) does not exceed 1,200,000 lb. Interface loads from top impacts are expected to bound impact loads from side impacts because of the geometry involved; therefore, the safety factor on the CEC Container Shell flange ring, acting to hold the lid in-place, is:

SF (flange ring) = Closure Lid Weld Capacity/ Filtered Peak Impact Load > 6.9

Finally, a small missile entering the outlet duct will not damage the MPC because there is no direct line-of-sight to the MPC, and even if it arrives at the MPC, it will have undergone multiple impacts with the duct walls, and can only impact the thick MPC lid. Therefore, MPC damage from the small missile is not credible.

An assessment of all simulation results concludes that the postulated missile strikes will not preclude MPC retrievability, will not cause loss of confinement, and will not affect criticality. In no scenario, does the lid become dislodged.

HOLTEC INTERNATIONAL COPYRIGHTED MATERIAL

3.I.4.8.2 Tornado Missile Protection during Construction

The number of VVMs in a HI-STORM 100U ISFSI may vary depending on a user's need. While there is a minimum spacing (pitch) requirement (see licensing drawing in Subsection 1.I.5), there is no limitation on the maximum spacing. Furthermore, a module array may have a non-rectangular external contour such as shown in the licensing drawing with a trapezoidal contour. Finally, an ISFSI may be constructed in multiple campaigns to allow the user to align the VVM cavity construction schedule with the plant's fuel storage needs. Any ISFSI constructed in one campaign shall have the following mandatory perimeter protection features:

i. The Radiation Protection Space (RPS) shall extend to an appropriate distance beyond the outer surface of the CEC shell (see licensing drawing in Subsection 1.I.5). Calculations have been performed (see [3.I.27]) that confirm that a 10' distance beyond the outer surface of the CEC shell is sufficient to prevent the 8" diameter rigid cylindrical missile (defined in Table 2.I.1 and is the most penetrating of the missile types considered in this FSAR) from contacting the CEC shell should this missile strike the exposed cut from the adjacent construction. The penetration analysis conservatively assumed a subgrade with minimum resistance to missile penetration and the formulation described in [3.I.30].

ii. Unless a retaining wall (see licensing drawing) has been built to confine and retain the subgrade at the boundary of the RPS (or beyond) in the particular direction of excavation, an Excavation Exclusion Zone (EEZ) shall be defined within which any excavation activity during an operating ISFSI is prohibited (see Subsection 2.I.2). The retaining wall is the EEZ boundary if the retaining wall is located at or beyond the RPS.

3.I.4.9 HI-STORM 100U VVM Service Life

The VVM is engineered for 40 years of design life, while satisfying the conservative design requirements defined in Supplement 2.I. For information supporting the 40 year design life addressing chemical and galvanic reactions as well as other potentially degrading factors see Subsection 3.I.4.1. Requirements for periodic inspection and maintenance of the HI-STORM 100U VVM throughout the 40-year design life are defined in Supplement 9.I. The VVM is designed, fabricated, and inspected under the comprehensive Quality Assurance Program discussed in Chapter 13.

3.I.5 FUEL RODS

No new analysis of fuel rods is required for storage of an MPC in a HI-STORM 100U VVM.

3.I.6 SUPPLEMENTAL DATA

3.I.6.1 Additional Codes and Standards Referenced in HI-STORM 100 System Design and Fabrication

No additional Codes and Standards are added for the HI-STORM 100U system.

3.I.6.2 Computer Programs

ANSYS 5.7, 7.0, 9.0, 11.0, and LSDYNA (previously known as DYNA3D) [3.I.2] are used for the finite element analyses prepared by Holtec and summarized in this supplement.

ANSYS

ANSYS is a public domain code, well benchmarked code, which utilizes the finite element method for structural analyses. It can simulate both linear and non-linear material and geometric behavior. It includes contact algorithms to simulate surfaces making and breaking contact, and can be used for both static and dynamic simulations. ANSYS has been independently QA validated at Holtec International. In this FSAR submittal, ANSYS is used within [3.I.27] and the element size used in the application follows the recommendation of the code developers.

LS-DYNA

LS-DYNA is a nonlinear, explicit, three-dimensional finite element code for solid and structural mechanics. It was originally developed at Lawrence Livermore Laboratories and is ideally suited for study of short-time duration, highly nonlinear impact problems in solid mechanics. LS-DYNA is commercially available and has been independently validated at Holtec following Holtec's QA procedures for commercial computer codes. This code has been used to analyze the Non-Mechanistic Storage tip-over for the HI-STORM 100 Part 72 general license. In this supplement, the code is used to establish the performance of the HI-STORM 100U under a design basis seismic event, and to evaluate the response to a design basis missile.

LS-DYNA is currently supported and distributed by Livermore Software. Each update is independently subject to QA validation at Holtec.

3.I.6.3 Appendices Included in Supplement 3.I

None.

3.I.6.4 Calculation Packages

A calculation package [3.I.27] containing the structural calculations supporting Supplement 3.I has been prepared and archived according to Holtec International's Quality Assurance Program (see Chapter 13), and submitted with this application. A second calculation report [3.I.14], documenting the SASSI analyses, has been prepared by a Holtec subcontractor under the subcontractor's QA program.

3.I.7 COMPLIANCE WITH NUREG-1536

The material in this supplement for the HI-STORM 100U system provides the same information as

HOLTEC INTERNATIONAL COPYRIGHTED MATERIAL

previously provided for the aboveground HI-STORM 100 systems. Therefore, to the extent applicable, the information provided is in compliance with NUREG-1536.

3.I.8 REFERENCES

The references in Section 3.8 apply to the VVM to the extent that they are appropriate for use with an underground system. The additional references below are specific to Supplement 3.I.

[3.I.1] SHAKE2000, A Computer Program for the 1-D Analysis of Geotechnical Earthquake Engineering Problems, G.A. Ordonez, Dec. 2000.

[3.I.2] LS-DYNA, Version 971, Livermore Software, 2006.

[3.I.3] USNRC Interim Staff Guidance (ISG-15), "Materials Evaluation", Revision 0, January 2001.

[3.I.4] ANSI/AWWA C105/A21.5-99, "American National Standard (ANSI) for Polyethylene Encasement for Ductile-Iron Pipe Systems".

[3.I.5] M. B. Bruce and M. V. Davis, "Radiation Effects on Organic Materials in Nuclear Plants", Final Report, 1981. (Prepared by Georgia Institute of Technology for EPRI)

[3.I.6] ANSI D 4082-02, "American National Standard (ANSI) Standard Test Method for Effects of Gamma Radiation on Coatings for Use in Light Water Nuclear Power Plants".

[3.I.7] USNRC Regulatory Guide (RG-1.54), "Service Level I, II and III Protective Coatings Applied to Nuclear Power Plants, Revision 1, July, 2000.

[3.I.8] ANSI D 3843-00, "American National Standard (ANSI) Standard Practice for Quality Assurance for Protective Coatings Applied to Nuclear Facilities".

[3.I.9] ANSI C 210-03, "American National Standard (ANSI) Standard Practice for Liquid-Epoxy Coating Systems for the Interior and Exterior of Steel Water Pipelines".

[3.I.10] Keeler & Long Inc. Product Data Sheet for Kolor-Proxy™ Primer KL3200 Series, Product Code KL3200.

[3.I.11] Samuel A. Bradford, "Practical Handbook of Corrosion Control in Soils", ASM International and CASTI Publishing Inc., 2004.

[3.I.12] L. M. Poukhonto, "Durability of Concrete Structures and Constructions – Silos,

HOLTEC INTERNATIONAL COPYRIGHTED MATERIAL

Bunkers, Reservoirs, Water Towers, Retaining Walls", A. A. Balkema Publishers, 2003.

[3.I.13] 49CFR Part 195 Subpart H "Corrosion Control", Title 49 of the Code of Federal Regulations, Oct, 1 2004 Edition, Office of the Federal Register, Washington, D.C.

[3.I.14] HI-2084023, SSI Analysis of HI-STORM 100U Using SASSI, Rev. 0 (a Subcontractor report prepared for Holtec by International Civil Engineering Consultants, Rev. 2, April 2008) (Holtec Proprietary) .

[3.I.15] S. Stojko, Application of DYNA3D to Non-Liner Soil Structure Interaction (SSI) Analysis of Retaining Wall Structures, International LS-DYNA3D Conference, March 1993.

[3.I.16] ASLB Hearings, Private Fuel Storage, LLC, Docket # 72-22-ISFSI, ASLBP 97-732-02-ISFSI, February 2005.

[3.1.17] Topical Report – Design of Structures for Missile Impact", BC-TOP-9A, Rev. 2, Bechtel Corporation, 9/74

[3.I.18] SAE Technical Paper 2000-01-0627, Development and Validation of High Fidelity Vehicle Crash Simulation Models, S.W. Kirkpatrick, Applied Research Associates, Inc.

[3.I.19] H. Boyer, Atlas of Stress Strain Curves, ASM International, 1987, p.189.

[3.I.20] Thermal Ceramics Inc., Product Data Sheet for Blanket Products (Kaowool® Blanket).

[3.I.21] NACE Standard RP0285-2002 "Corrosion Control of Underground Storage Tank Systems by Cathodic Protection", NACE International.

[3.I.22] API RP1632, "Cathodic Protection of Underground Petroleum Storage Tanks and Piping Systems", American Petroleum Institute.

[3.I.23] NACE RP0169-96, "Control of External Corrosion on Underground or Submerged Piping Systems", NACE International.

[3.I.24] 49CFR Part 192 Subpart I "Requirements for Corrosion Control, Title 49 of the Code of Federal Regulations, Oct, 1 2004 Edition, Office of the Federal Register, Washington, D.C.

[3.I.25] ACI 544.3R-93 (or latest), Guide for Specifying, Proportioning, Mixing, Placing, and

Finishing Steel Fiber Reinforced Concrete.

[3.I.26] ASTM C1116-03 (or latest) Standard Specification for Fiber-Reinforced Concrete and Shotcrete

[3.I.27] HI-2053389, Calculation Package Supporting Structural Evaluation of HI-STORM 100U, Revision 9, September 2010, (Holtec Proprietary)

[3.I.28] ASCE 4-98, Seismic Analysis of Safety-Related Nuclear Structures and Commentary, American Society of Civil Engineers, 2000.

[3.I.29] ASCE/SEI 43-05, Seismic Design Criteria for Structures, Systems, and Components in Nuclear Facilities, American Society of Civil Engineers, 2005.

[3.I.30] Sandia National Laboratory Contractor Report SAND97-2426, Penetration Equations, C.Y. Young, Applied Research Associates, Inc., Albuquerque NM 87110.

[3.I.31] Doug Ammerman and Gordon Bjorkman, "Strain-Based Acceptance Criteria for Section III of the ASME Boiler and Pressure Vessel Code", Proceedings of the 15th International Symposium on the Packaging and Transportation of Radioactive Materials, PATRAM 2007, October 21-26, 2007, Miami, Florida, USA.

[3.I.32] ACI-349 (2001), Code Requirements for Nuclear Safety Related Concrete Structures (ACI 349-01) and Commentary (ACI 349R-01), Appendix C, American Concrete Institute, 2001.

[3.I.33] ANSYS 11.0, ANSYS Inc., 2007 and ANSYS 13.0, Ansys Inc. Copyright 2010 SAS IP, Inc.

HOLTEC INTERNATIONAL COPYRIGHTED MATERIAL

TABLE 3.I.1

HI-STORM 100U BOUNDING WEIGHT DATA

Item	Bounding Weight (lb)
MPCs	
• Without SNF	See Table 3.2.1
• Fully loaded with SNF and Fuel Spacers	90,000
HI-STORM 100U VVM	
• Closure Lid (with shielding concrete)	24,000
• CEC (empty without Closure Lid)	33,000
• Maximum Loaded Weight (with bounding MPC)	147,000
Loaded Transporter (Typical)	
• Carrying a loaded HI-TRAC	400,000
• Empty	160,000
• Length & width of each load patch (2 load patches per transporter)	197.1875 inch by 29.5 inch
• Computed average normal pressure on two load patches	34.4 psi
Loaded HI-TRAC and Mating Device	275,000
Note 1: CEC and Closure Lid include an overage up to 5%. Note 2: Transporter weight is based on representative units used in the industry.	

HOLTEC INTERNATIONAL COPYRIGHTED MATERIAL

TABLE 3.I.2

CENTER OF GRAVITY DATA FOR THE HI-STORM 100U SYSTEM

Component	**Height of CG Above Datum (in)**
MPC	See Table 3.2.3
HI-STORM 100U VVM CEC (empty without Closure Lid)	108.7
HI-STORM 100U VVM Closure Lid	20.26
Note: Datum for CEC is at the top surface of the foundation; datum for Closure Lid is at bottom surface of baseplate of lid.	

TABLE 3.I.3 (a)*
RELEVANT MATERIAL PROPERTIES FOR THE HI-STORM 100U
Yield, Ultimate, Linear Thermal Expansion, Young's Modulus

Temp. (Deg. F)	SA516 and SA515, Grade 70			
	S_y	S_u	α	E
-40	38.0	70.0	---	29.95
100	38.0	70.0	5.53 (5.73)	29.34
150	36.3	70.0	5.71 (5.91)	29.1
200	34.6	70.0	5.89 (6.09)	28.8
250	34.15	70.0	6.09 (6.27)	28.6
300	33.7	70.0	6.26 (6.43)	28.3
350	33.15	70.0	6.43 (6.59)	28.0
400	32.6	70.0	6.61 (6.74)	27.7
450	31.65	70.0	6.77 (6.89)	27.5
500	30.7	70.0	6.91 (7.06)	27.3
550	29.4	70.0	7.06 (7.18)	27.0
600	28.1	70.0	7.17 (7.28)	26.7
650	27.6	70.0	7.30 (7.40)	26.1
700	27.4	70.0	7.41 (7.51)	25.5
750	26.5	69.3	7.50 (7.61)	24.85
800	25.3	64.3	7.59 (7.71)	24.2
* Footnotes in corresponding table in Section 3.3 apply to the values in parentheses.				

TABLE 3.I.3 (b)
DESIGN AND LEVEL A: ALLOWABLE STRESS FROM ASME NF

Material : **SA516 Grade 70, SA515 Grade 70**
Service Conditions: **Design and Level A Stress**
Item: **Stress**

Temp. (Deg. F)	Classification and Value (ksi)		
	S	Membrane Stress	Membrane plus Bending Stress
-20 to 650	17.5	17.5	26.3
700	16.6	16.6	24.9
750	14.8	14.8	22.2
800	12.0	12.0	18.0

TABLE 3.I.3 (c)
LEVEL D: STRESS INTENSITY

Code: **ASME NF**
Material: **SA516, Grade 70**
Service Conditions: **Level D**
Item: **Stress Intensity**

Temp. (Deg. F)	Classification and Value (ksi)		
	S_m	P_m	$P_m + P_b$
-20 to 100	23.3	45.6	68.4
200	23.1	41.5	62.3
300	22.5	40.4	60.6
400	21.7	39.1	58.7
500	20.5	36.8	55.3
600	18.7	33.7	50.6
650	18.4	33.1	49.7
700	18.3	32.9	49.3

HOLTEC INTERNATIONAL COPYRIGHTED MATERIAL

TABLE 3.I.3 (d)

Code: ASME NB
Material: Alloy X
Service Conditions: Level D
Item: Stress Intensity

Temp. (Deg. F)	Classification and Value (ksi)		
	P_m	P_L	$P_L + P_b$
-20 to 100	48.0	72.0	72.0
200	48.0	72.0	72.0
300	46.2	69.3	69.3
400	44.9	67.4	67.4
500	42.0	63.0	63.0
600	39.4	59.1	59.1
650	38.4	57.6	57.6
700	37.4	56.1	56.1
750	36.5	54.8	54.8
800	35.8	53.7	53.7

HOLTEC INTERNATIONAL COPYRIGHTED MATERIAL

TABLE 3.I.4
REFERENCE AND DERIVED PROPERTIES OF ISFSI REINFORCED CONCRETE, SUBGRADE, AND UNDERGRADE

Property	Value
Concrete Compressive Strength (psi)	4,500
Concrete Rupture Strength (psi)	335.4
Allowable Bearing Stress (psi)	4,972.5*
Mean Coefficient of Thermal Expansion (in/in-deg. F)	5.5E-06
Modulus of Elasticity (psi)	57,000 x (Concrete Compressive strength (in psi))$^{1/2}$
Subgrade Yield Stress (psi)	25[¥]
Subgrade Strain Compatible Modulus of Elasticity (ksi) (see Figure 2.I.5)	Space A: 18.8 Space B: 14.0 Spaces C and D: 17.7

* Per ACI-318 (2005), Sec. 10.17.1 and Sec. 9.3.2.4. Since the ISFSI concrete is always confined, the allowable value is doubled.

¥ Only applied to Space A.

TABLE 3.I.5
SOIL PROPERTIES, COMPUTED SETTLEMENT, AND CORRESPONDING ELASTIC MODULII FOR THE SUBGRADE

Item		Value
1.	Characteristics for Subgrade Below SFP: Water Content 'w_n' Soil Parameter 'a' Soil Parameter 'b' Poisson's Ratio	 14% 0.18 0.13 0.45
2.	Derived Properties for the Subgrade Below SFP (Note 1): Computed Long-Term Settlement (in) (Note 2) Computed Elastic Modulus (psi)	 0.189 5,377
3.	Values used in the Structural Analyses Model for Subgrade Below SFP: Limiting Long-Term Settlement (in) Corresponding Elastic Modulus (psi)	 From Table 2.I.2 5,081
4.	Soil Characteristics for Subgrade Above SFP: Water Content 'w_n' Soil Parameter 'a' Soil Parameter 'b' Poisson's Ratio	 14% 0.09 0.13 0.45
5.	Derived Properties for the Subgrade Above SFP (Note 3): Computed Long-Term Settlement (in) (Note 2) Computed Elastic Modulus (psi)	 0.39 5,073
6.	Values used in the Structural Analyses Model for Subgrade Above SFP: Long-Term Settlement (in) Corresponding Elastic Modulus (psi)	 From Table 2.I.2 4,946

Note 1: The substrate characteristics are obtained using the density data from Table 2-3 and Table 5-1 of reference [2.I.7]. The soil compaction index 'Cc' is a direct function of soil parameters w_n, a, and b per [2.I.7]. The long-term settlement and the elastic modulus are derived using the relationships in [2.I.6].

Note 2: See Table 2.I.2 for the values of settlement (greater than those computed here for conservatism) used as the Design Basis data for qualification of the ISFSI structures.

Note 3: The Design Basis settlement has been set at a higher value than that computed for the TSP and SFP to allow for the variation in the soil parameters at a host site.

TABLE 3.I.6
MENU OF LS-DYNA RUNS (SSI ANALYSES)

No.	Case	Comment
1.	VVM array model (5x5 array) with 100% concrete modulus for the SFP	To obtain interface load for the ISFSI structures
2.	VVM array model (5x5 array) with 50% concrete modulus for the SFP	To obtain interface load for the ISFSI structures
3.	VVM array model (5x5 array) for the optional ISFSI design with retaining walls	To obtain interface load for the ISFSI structures
4.	Design Basis Single VVM seismic model	To qualify VVM components.

TABLE 3.I.7

ISFSI INTERFACE LOADS OBTAINED FROM LS-DYNA SSI SIMULATIONS

Interface Load	Case 1	Case 2	Case 3	Case 4
CEC to SFP Impact Load, lb	6.499×10^5	6.267×10^5	6.590×10^5	6.433×10^5
Transporter to TSP Contact Load per Track, lb	1.078×10^6	1.109×10^6	N/A	1.148×10^6
Soil Compressive Load on the Retaining Wall, lb	N/A	N/A	3.290×10^6	N/A
In-Plane Tensile Load on TSP from Retaining Wall, lb	N/A	N/A	9.672×10^5	N/A
In-Plane Tensile Load on SFP from Retaining Wall, lb	N/A	N/A	2.287×10^6	N/A

HOLTEC INTERNATIONAL COPYRIGHTED MATERIAL

TABLE 3.I.8

LOADS APPLIED IN THE ISFSI STRUCTURAL EVALUTION†

Load on ISFSI	Simulation Models I, II and III	Simulation Model IV
Load on SFP at each VVM location ‡, lbf	660,000	660,000
Total Load on TSP due to Transporter ‡, lbf	$5.6 \times 400000 = 2.24 \times 10^6$	N/A
In-Plane Tensile Load on TSP Extreme Face, lbf	N/A	9.68×10^5
In-Plane Tensile Load on SFP Extreme Face, lbf	N/A	2.29×10^6

Notes:

† For conservatism, the loads used for ISFSI structural evaluation bound the peak loads obtained from SSI simulations (see Table 3.I.7).

‡ The listed load is a sum of dead and seismic components. These loads are appropriately divided as dead and seismic in ANSYS prior to applying the appropriate load factors and combinations per Table 2.I.11.

TABLE 3.I.9*

RESULTS FROM TORNADO MISSILE ANALYSIS (LOAD CASE 03 OF TABLE 2.I.5)			
Item	**Bounding Value, inch**	**Allowable Value, inch**	**Safety Factor**
Maximum Vertical Displacement of lid (inch) (inclined impact)	< 3	12**	> 4
Perforation of Inner Shield Dome Steel	Yes (see Fig. 3.I.7)	N/A	N/A
Maximum Peak Impact Force (kips)	< 1,000	1,849	>1

* Details of the calculations can be found in [3.I.27]
** This is the minimum distance between the Closure Lid bottom plate and the top lid of the MPC.

TABLE 3.I.10
MOMENT RESULTS AND CORRESPONDING MINIMUM SAFETY FACTORS FOR THE ISFSI STRUCTURES

Support Foundation Pad (SFP)‡			
ISFSI Load Configuration	Maximum Moment Induced (lbf-in/in)	Moment Capacity (lbf-in/in)	Minimum Safety Factor
Fully Loaded (Model I)	192,000	263,270	1.371
Middle Row Loaded (Model II)	230,920	272,710	1.602
Single VVM Loaded (Model III)	168,140	269,140	1.601
Middle Row Loaded w/ Retaining Walls (Model IV)	170,170	180,580	1.061
Top Surface Pad (TSP)‡			
Fully Loaded (Model I)	318,070	347,750	1.093
Middle Row Loaded (Model II)	293,240	312,850	1.067
Single VVM Loaded (Model III)	277,670	290,860	1.048
Middle Row Loaded w/ Retaining Walls (Model IV)	82,161	228,790	2.785

TABLE 3.I.10 (continued)
MOMENT RESULTS AND CORRESPONDING MINIMUM SAFETY FACTORS FOR THE ISFSI STRUCTURES

Retaining Wall †			
ISFSI Load Configuration	Maximum Moment Induced (lbf-in/in)	Moment Capacity (lbf-in/in)	Minimum Safety Factor
Fully Loaded (Case 3 of Table 3.I.6)	80,000	175,000	2.19

‡ The moment capacities for the SFP and TSP are calculated using axial-force-moment interaction diagram corresponding to the axial force and moment induced in the limiting element. Moreover, the flexural safety factors for the SFP and TSP calculated above are based on the maximum moment induced in a single element, which is very conservative. Averaging over the width of the loaded section would result in much higher safety factors.

† The moment capacity for the Retaining Wall is based on the pure bending.

HOLTEC INTERNATIONAL COPYRIGHTED MATERIAL

TABLE 3.I.11
PUNCHING SHEAR SAFETY FACTORS FOR ISFSI STRUCTURES

ISFSI Structure	Punching Safety Factor
SFP†	2.1
TSP	1.32
† Note that the punching shear calculation for the SFP is conservatively based on a bounding load of 950 kips.	

TABLE 3.I.12
PRESUMPTIVE SOIL BEARING

Computed Bearing Stress (psi)	Allowable Bearing Stress (psi)	Safety Factor	Minimum Safety Factor Required per [2.I.8]
42.8	90	2.1	2.0

TABLE 3.I.13
RESULTS OF STRENGTH EVALUATION FOR RETAINING WALL SHEAR CONNECTIONS

Component	Minimum Safety Factor
Top Shear Key	9.41
Bottom Dowels	1.56

HOLTEC INTERNATIONAL COPYRIGHTED MATERIAL

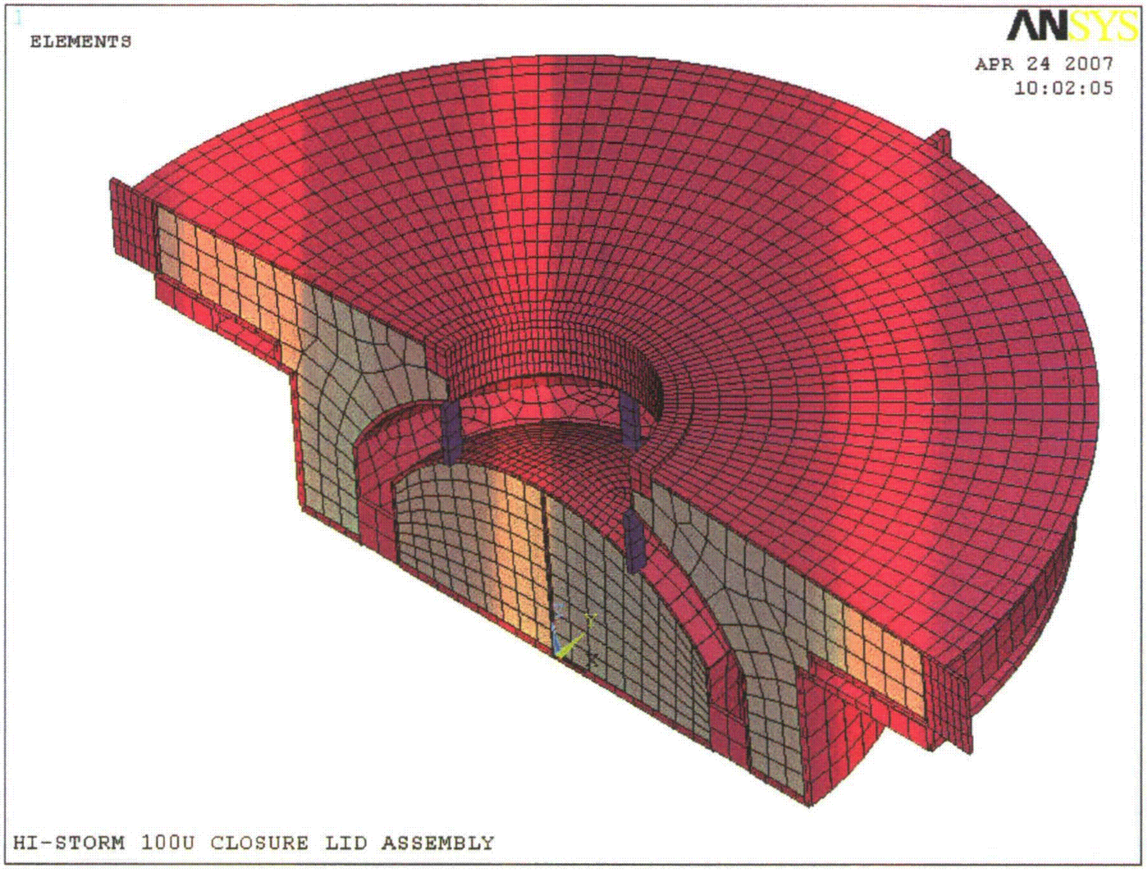

Figure 3.I.1; 3-D ANSYS/LSDYNA Finite Element Model of Closure Lid (Current Configuration)

HOLTEC INTERNATIONAL COPYRIGHTED MATERIAL

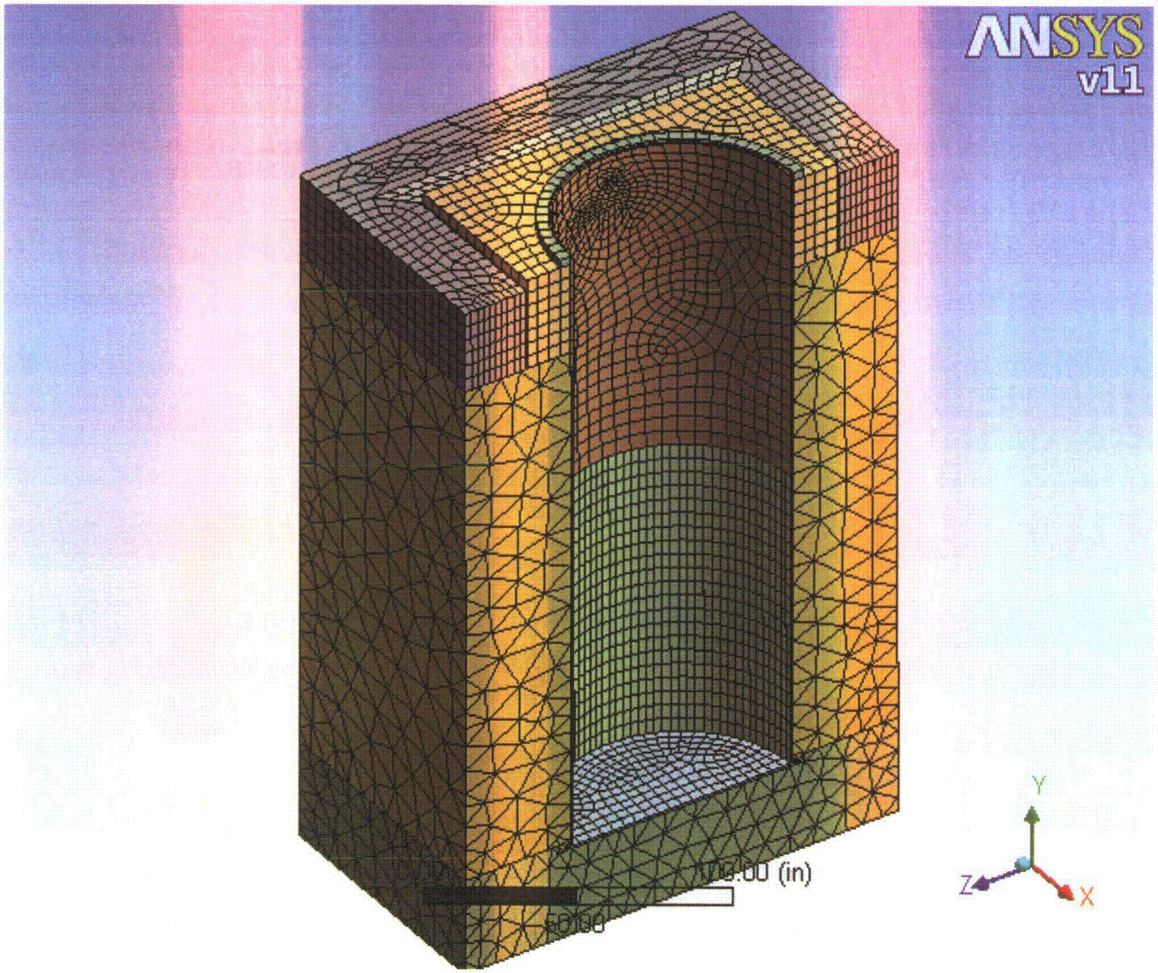

Figure 3.I.2; 3-D ANSYS Finite Element One-Half Model of Substrate Surrounding VVM, CEC Container Shell, TSP, and VIP

HOLTEC INTERNATIONAL COPYRIGHTED MATERIAL

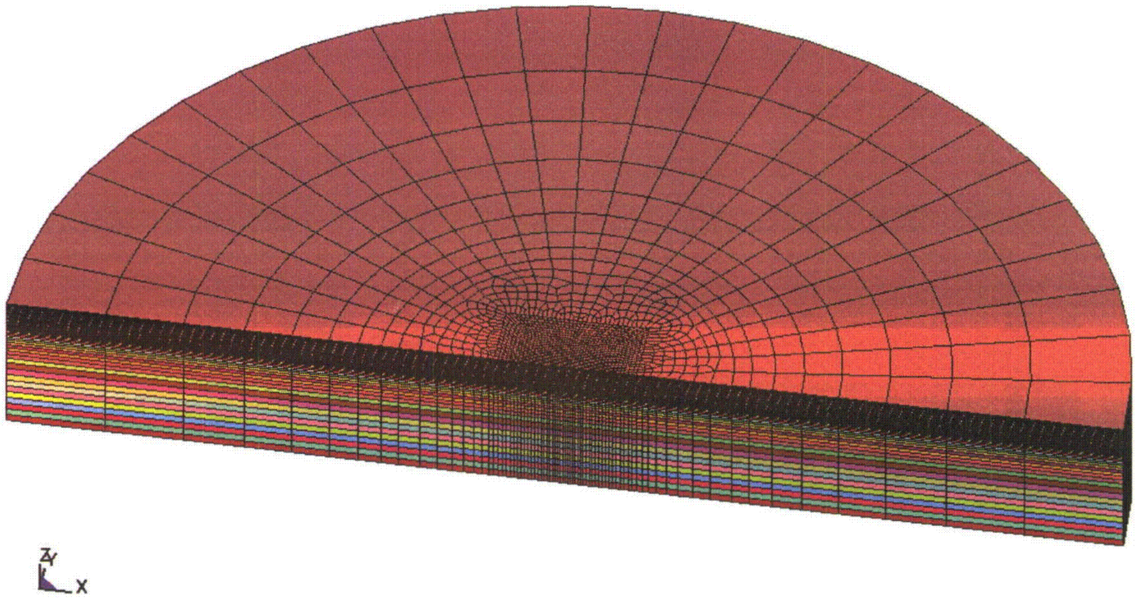

Figure 3.I.3-A; 3-D LSDYNA Soil Model for Design Basis Seismic Response Analysis

HOLTEC INTERNATIONAL COPYRIGHTED MATERIAL

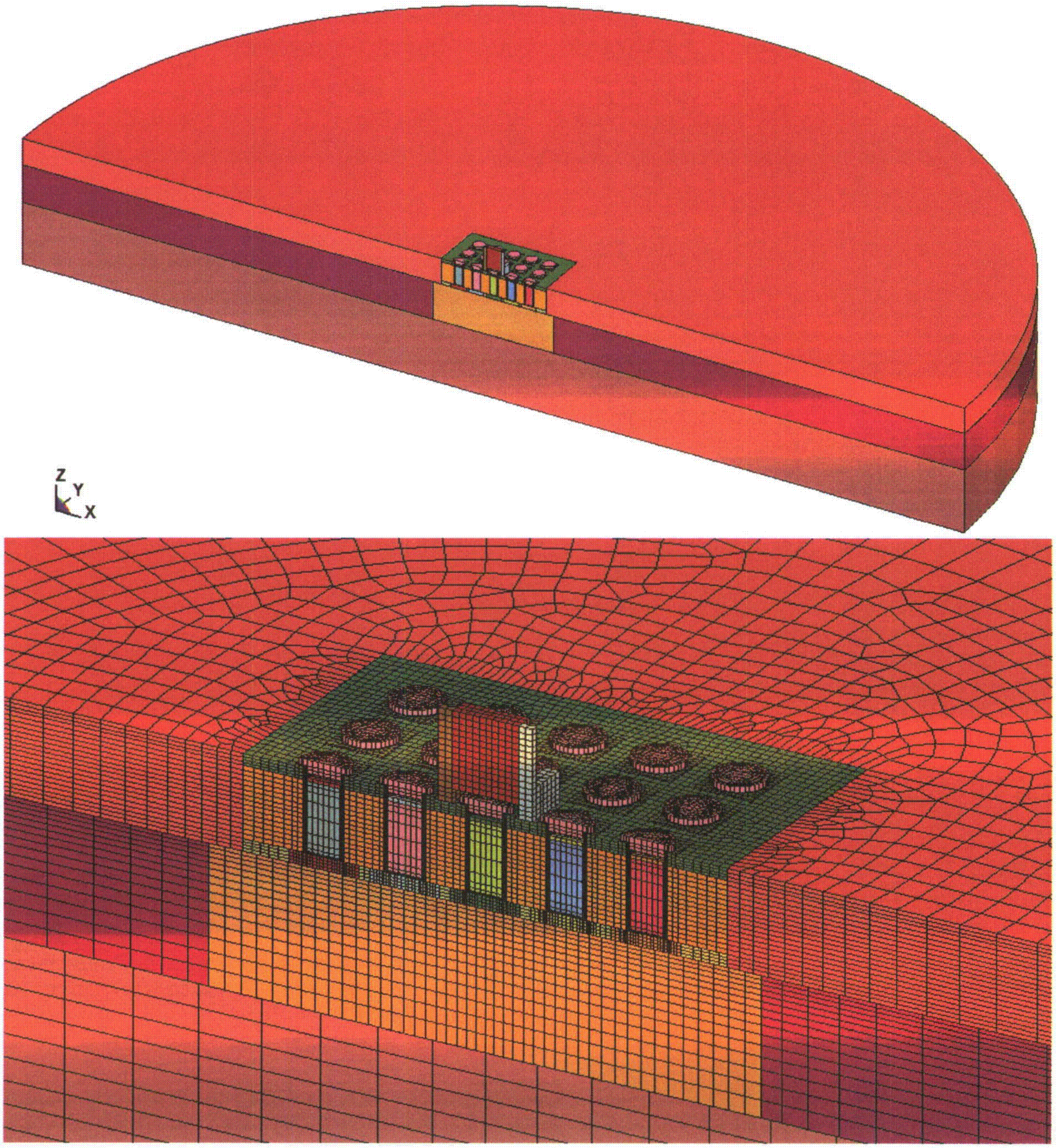

Figure 3.I.3-B; 3-D LSDYNA Model for Non-Linear SSI Analysis of 5x5 loaded VVMs on the Support Foundation

HOLTEC INTERNATIONAL COPYRIGHTED MATERIAL

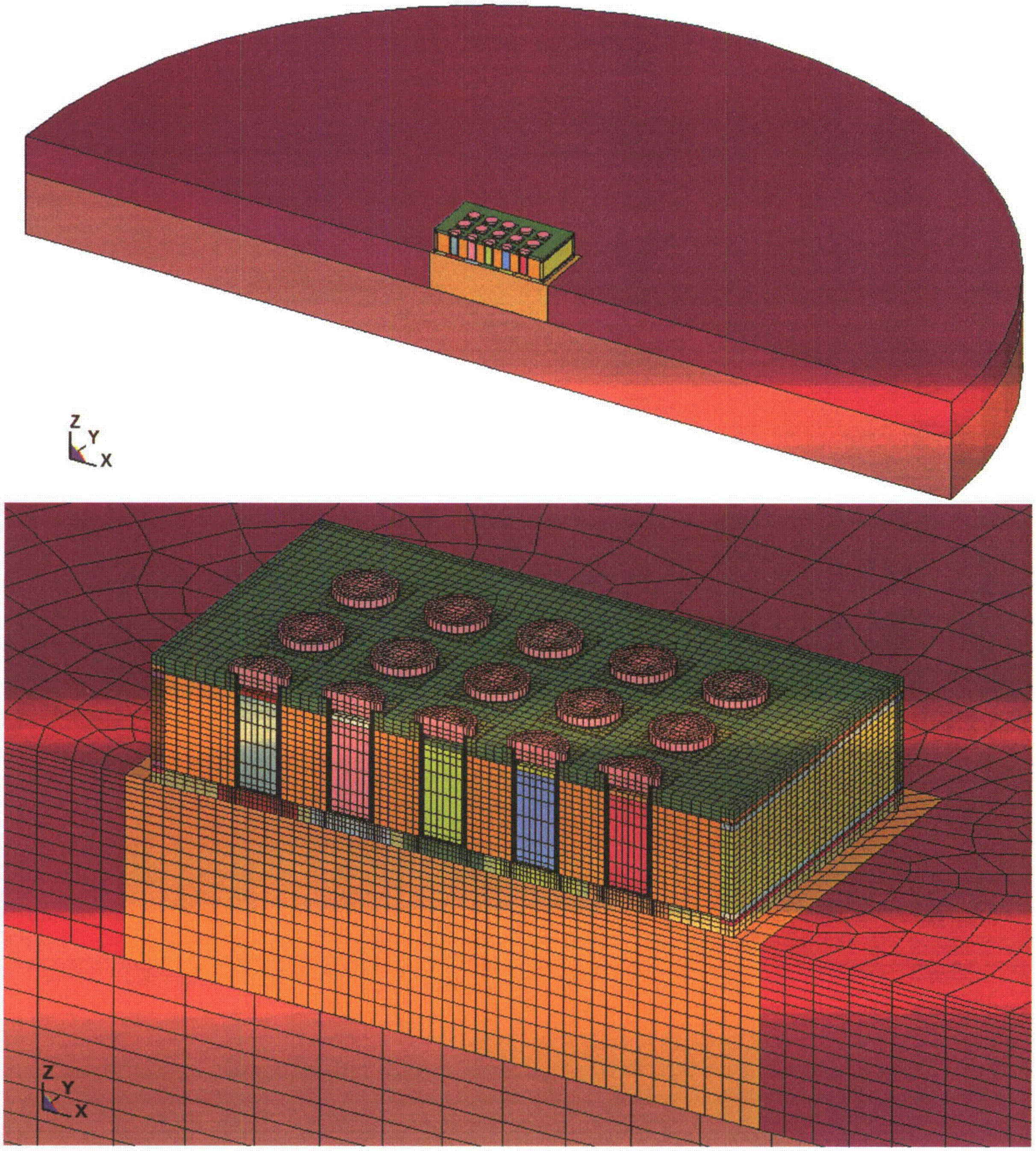

Figure 3.I.3-C; 3-D LSDYNA Model for Non-Linear SSI Analysis of 5x5 loaded VVMs on the Support Foundation with Retaining Walls

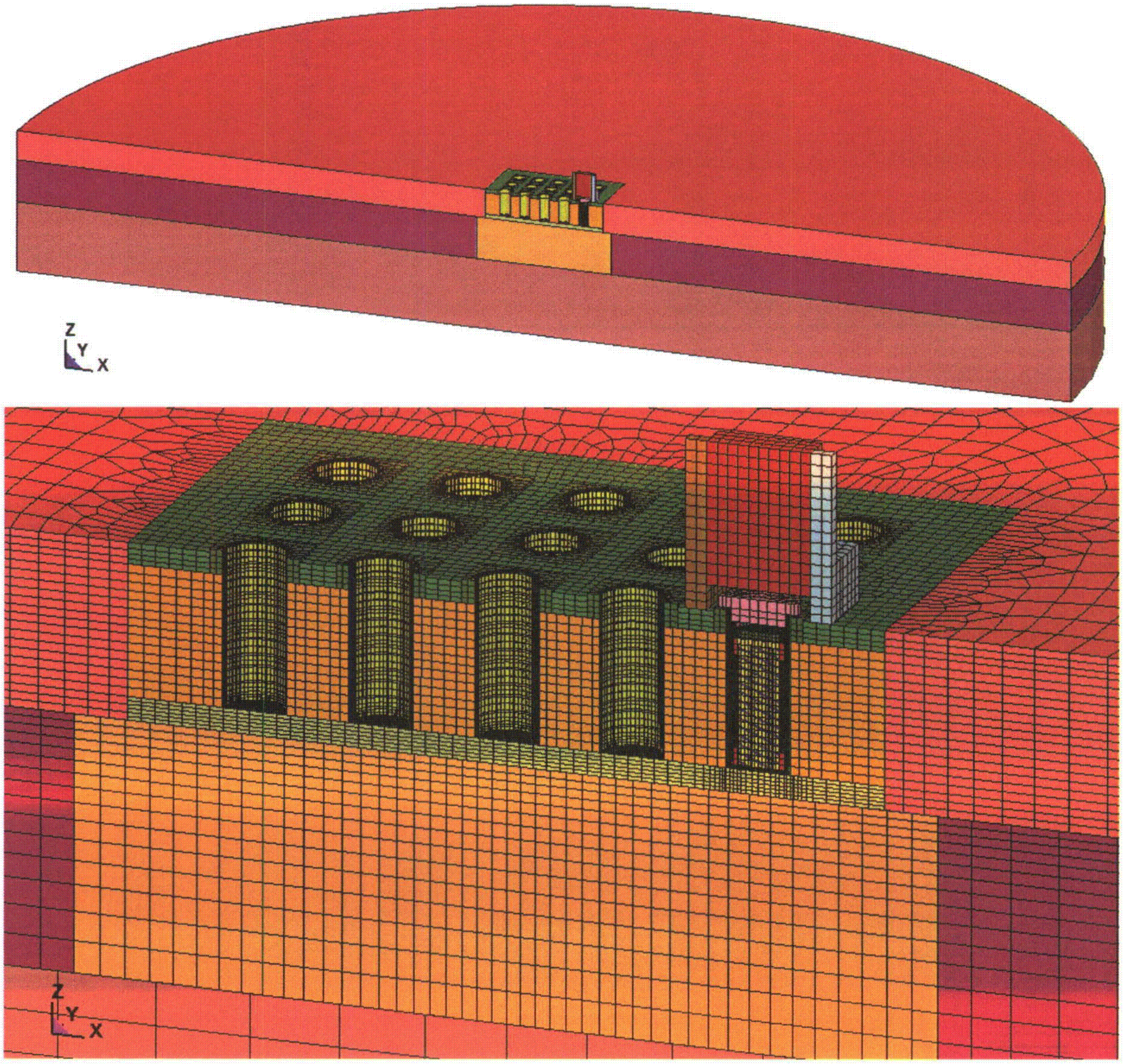

Figure 3.I.3-D; 3-D LSDYNA Model for Non-Linear SSI Analysis of a single VVM on Support Foundation

HOLTEC INTERNATIONAL COPYRIGHTED MATERIAL

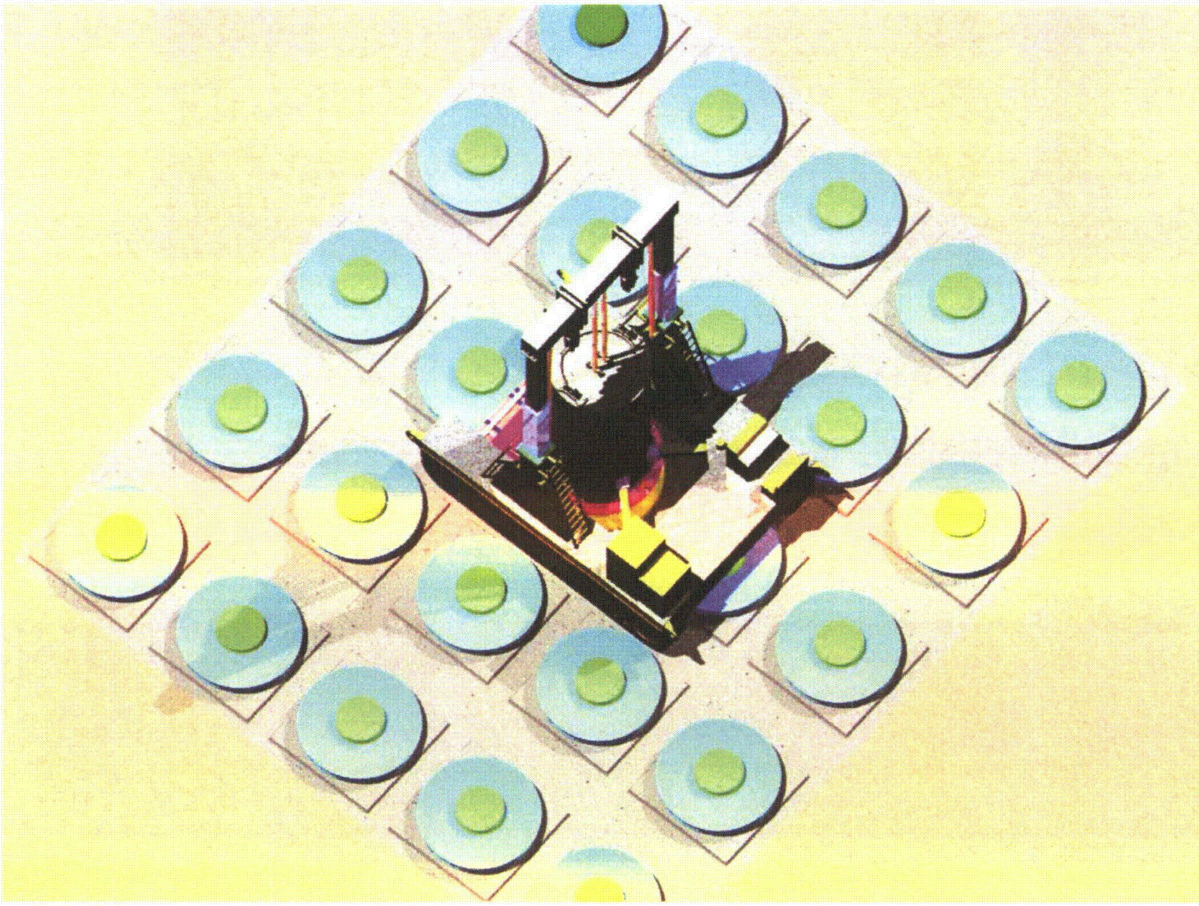

Figure 3.I.4; Cask Transporter on the ISFSI Positioned to Transfer MPC in the Central Cavity in the 5x5 VVM Array (illustrative analysis case)

HOLTEC INTERNATIONAL COPYRIGHTED MATERIAL

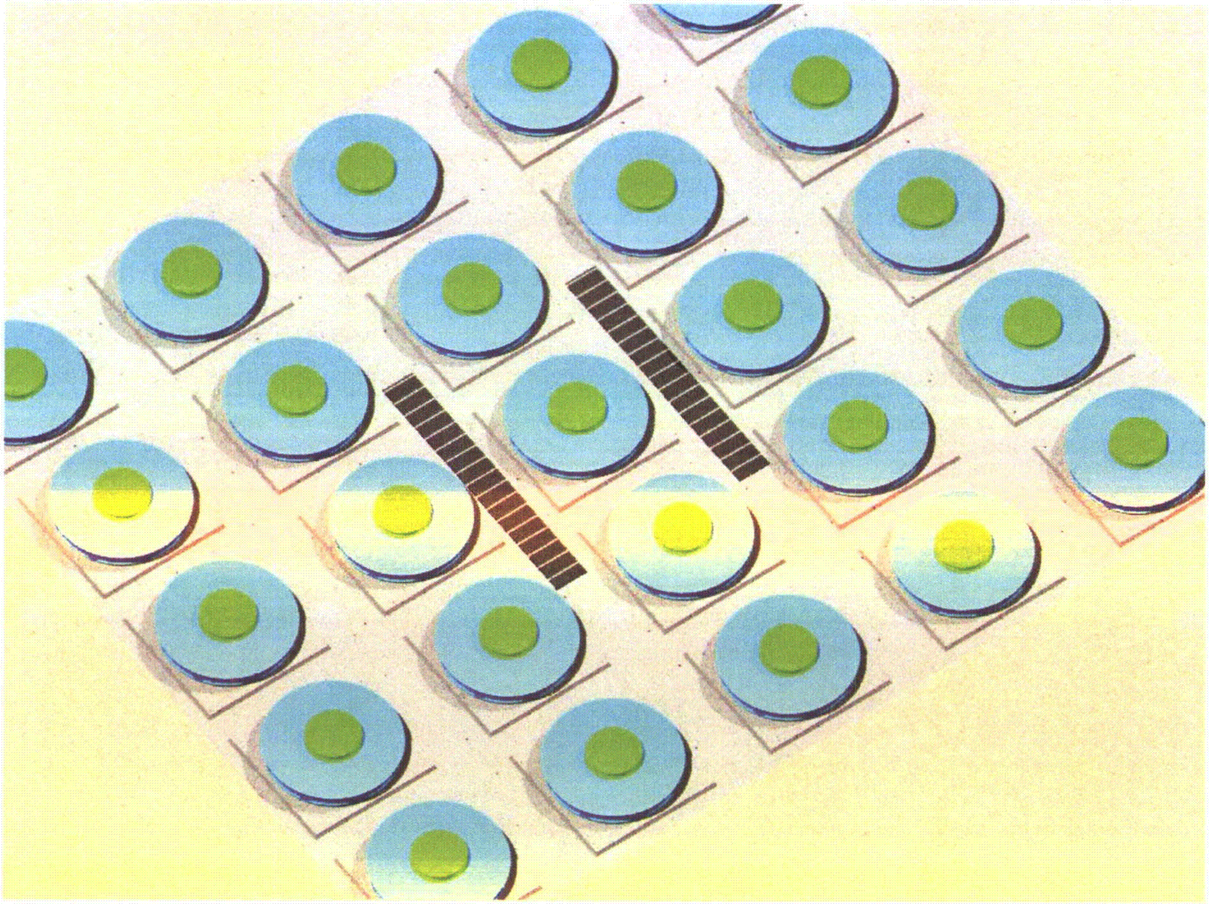

Figure 3.I.5; Load patch from the loaded Transporter in Figure 3.I.19
(Illustrative analysis case)

HOLTEC INTERNATIONAL COPYRIGHTED MATERIAL

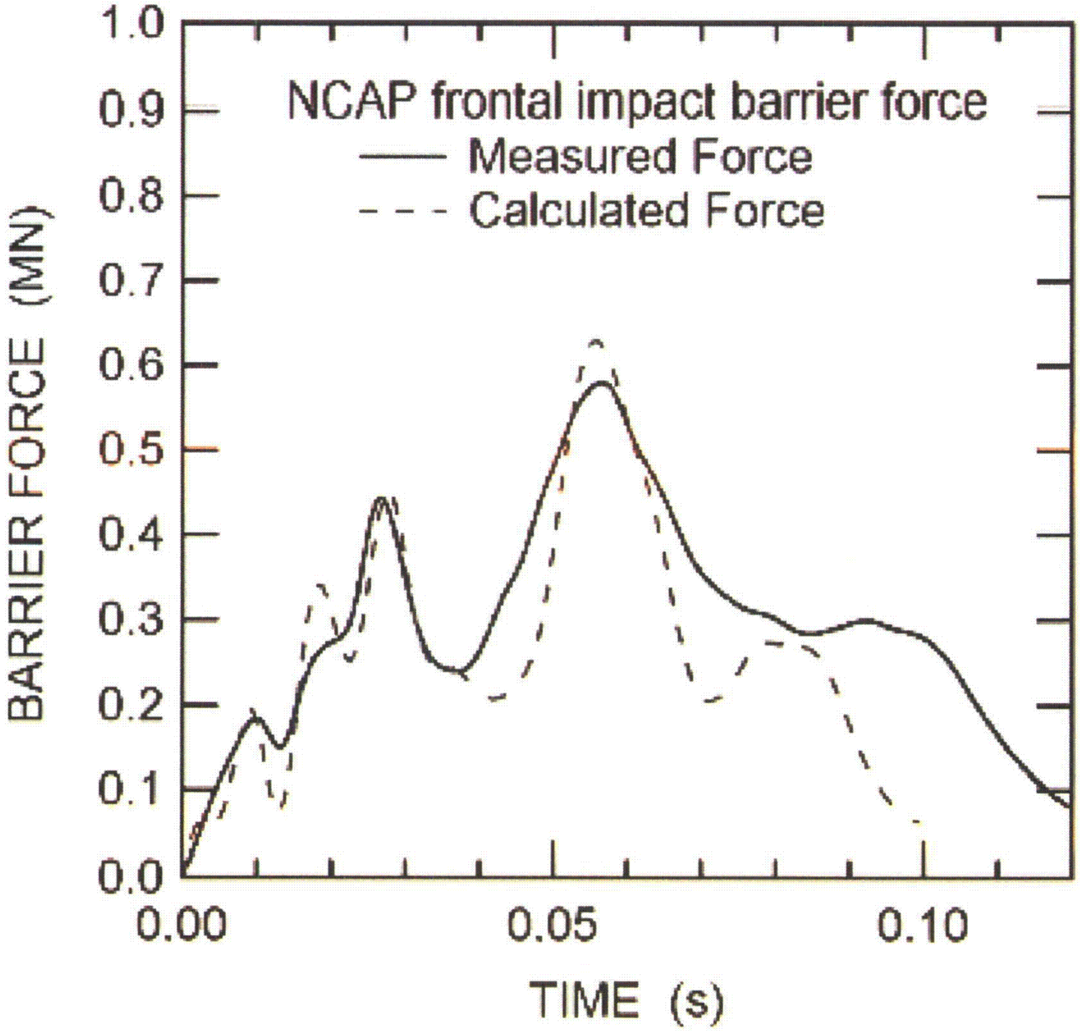

Figure 3.I.6; Test Results from 35mph Impact of a Ford (1705 Kg) Against a Rigid Wall

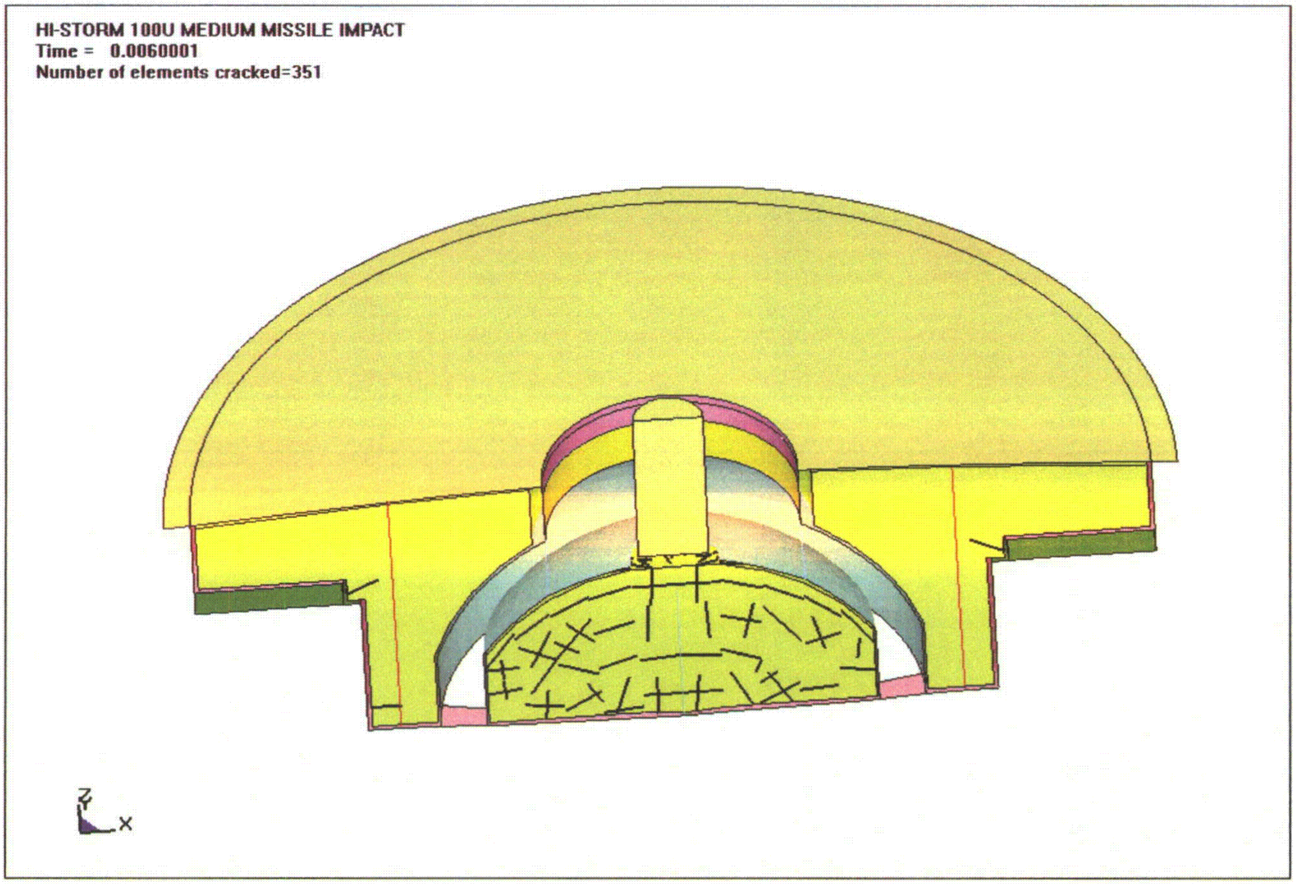

Figure 3.I.7; LSDYNA Model Section for Central Intermediate Missile Strike (subsequent to impact)

HOLTEC INTERNATIONAL COPYRIGHTED MATERIAL

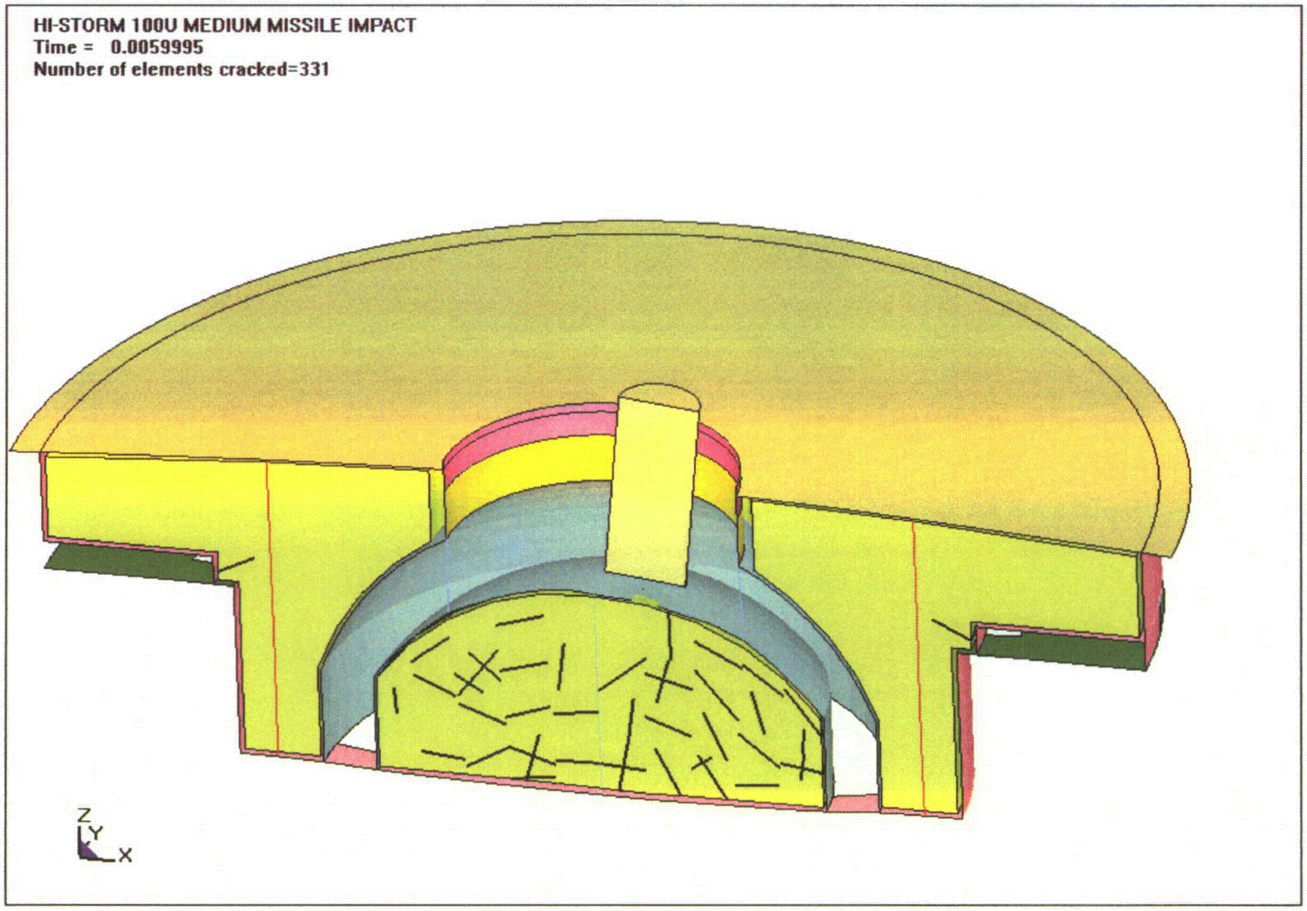

Figure 3.I.8; LSDYNA Model Section for Inclined Intermediate Missile Strike (subsequent to impact)

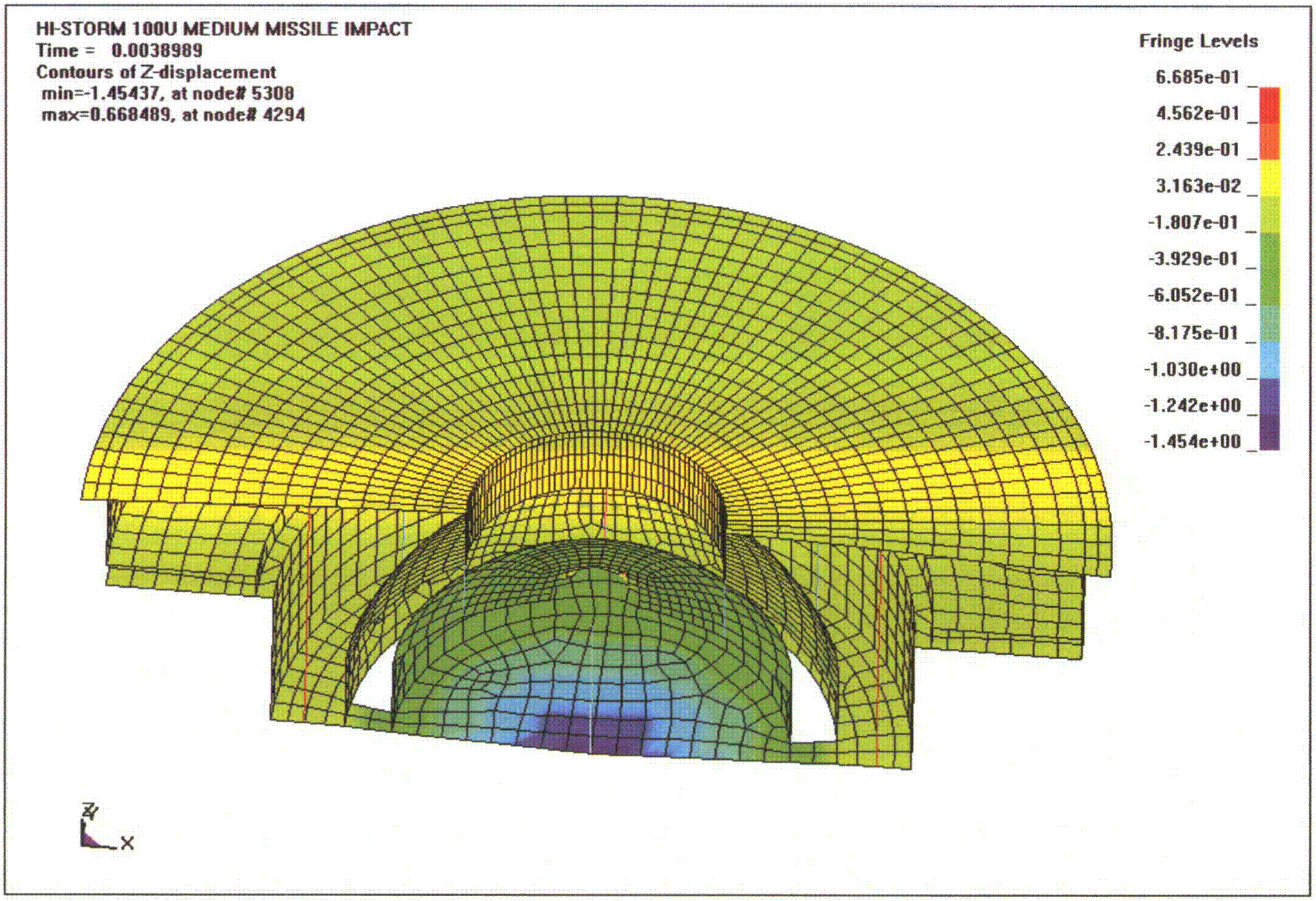

Figure 3.I.9; Deformation Profile at Time of Maximum Deformation – Central Strike

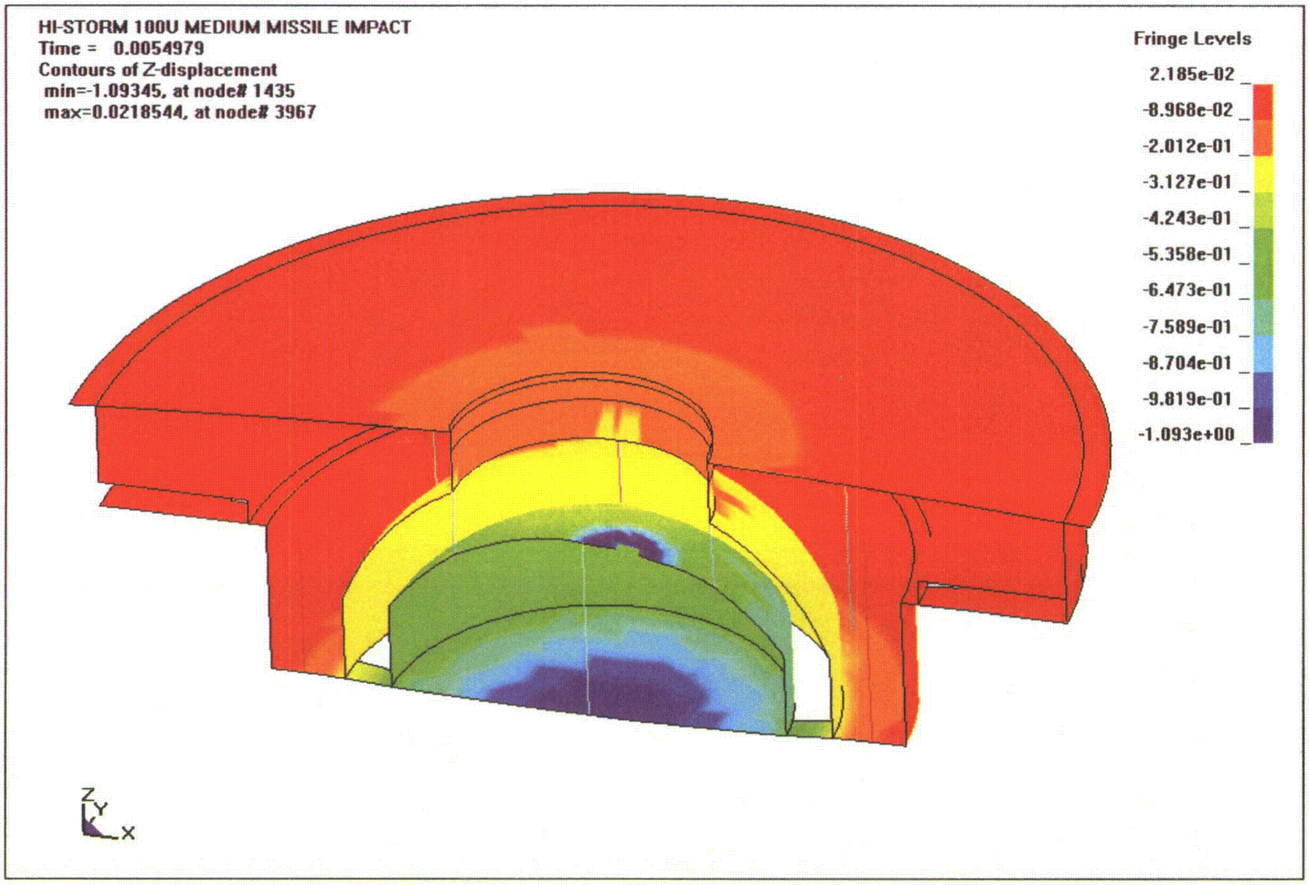

Figure 3.I.10; Deformation Profile at Time of Maximum Deformation – Inclined Strike

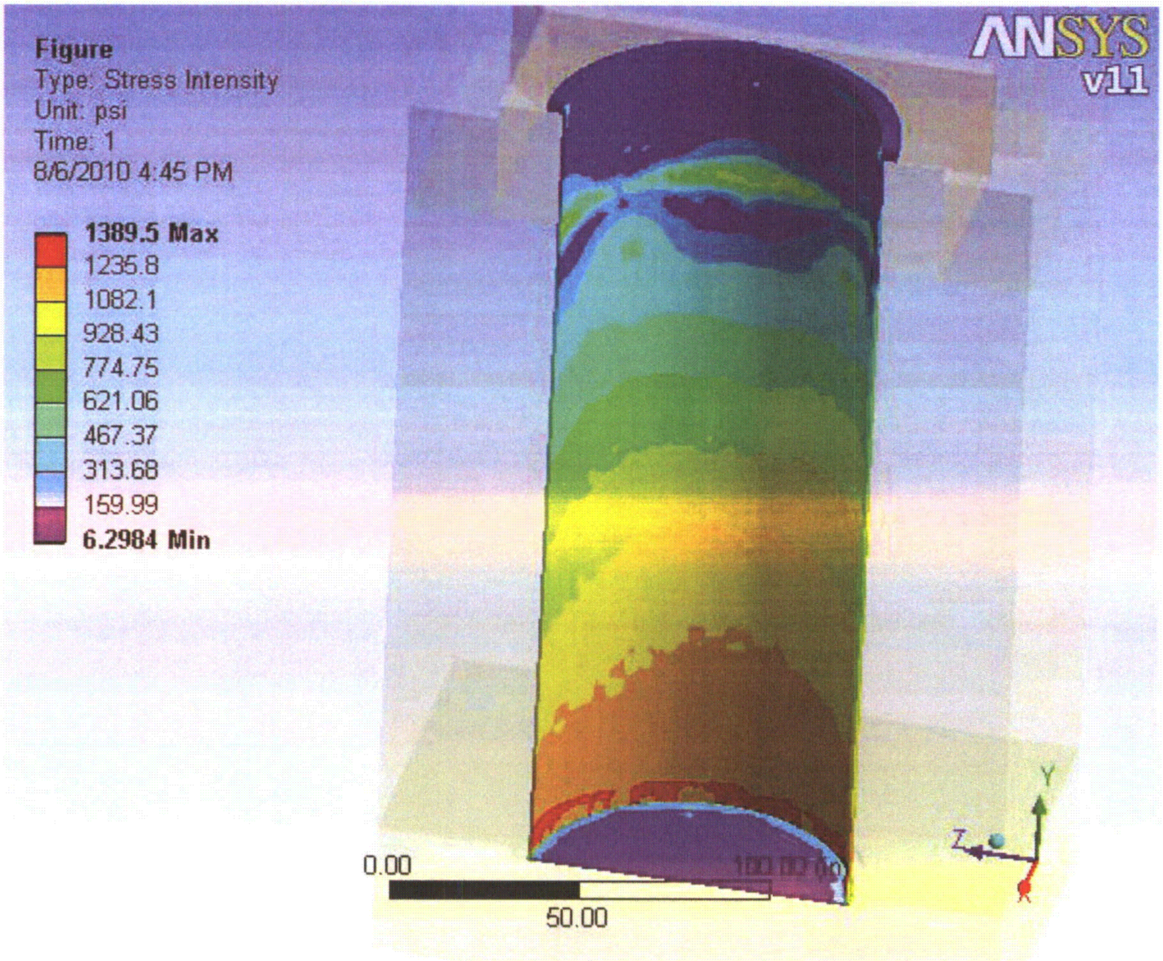

Figure 3.I.11; Stress Distribution in CEC Shell from Transporter and Substrate (Load Case 07)

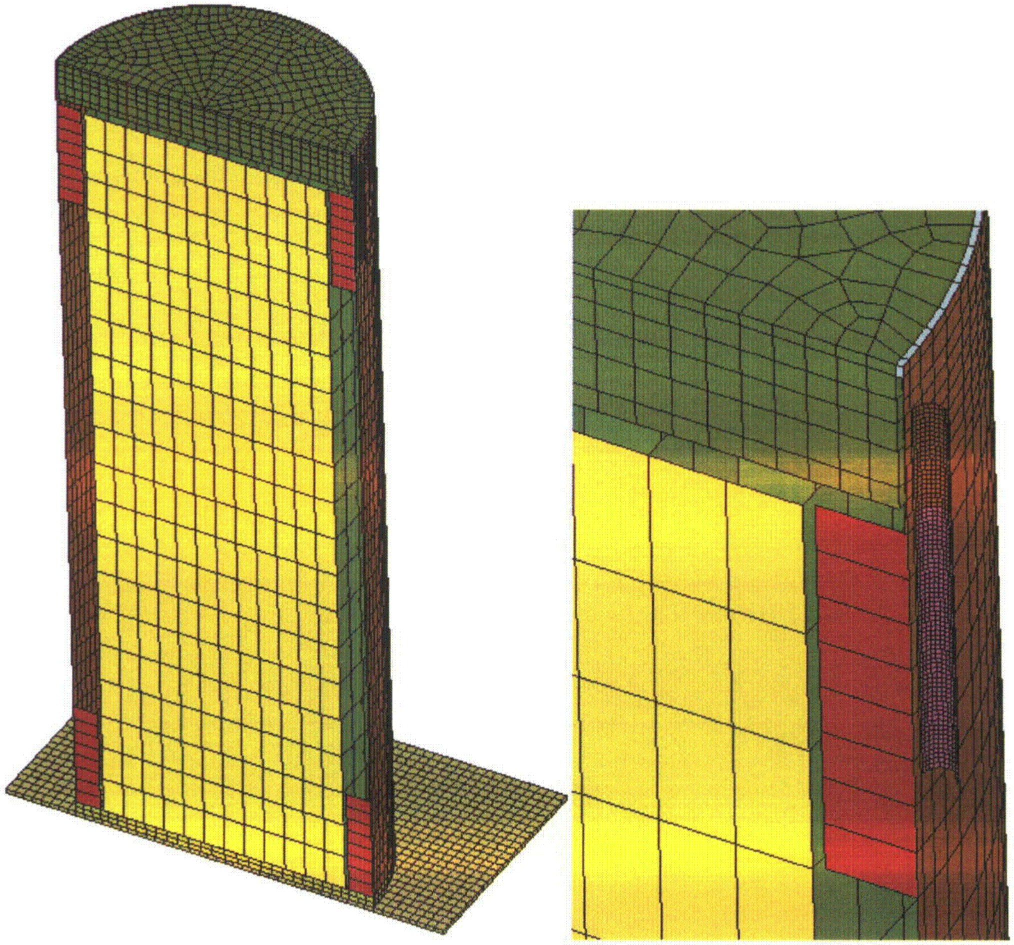

Figure 3.I.12; MPC Guide/MPC Impact LS-DYNA Model

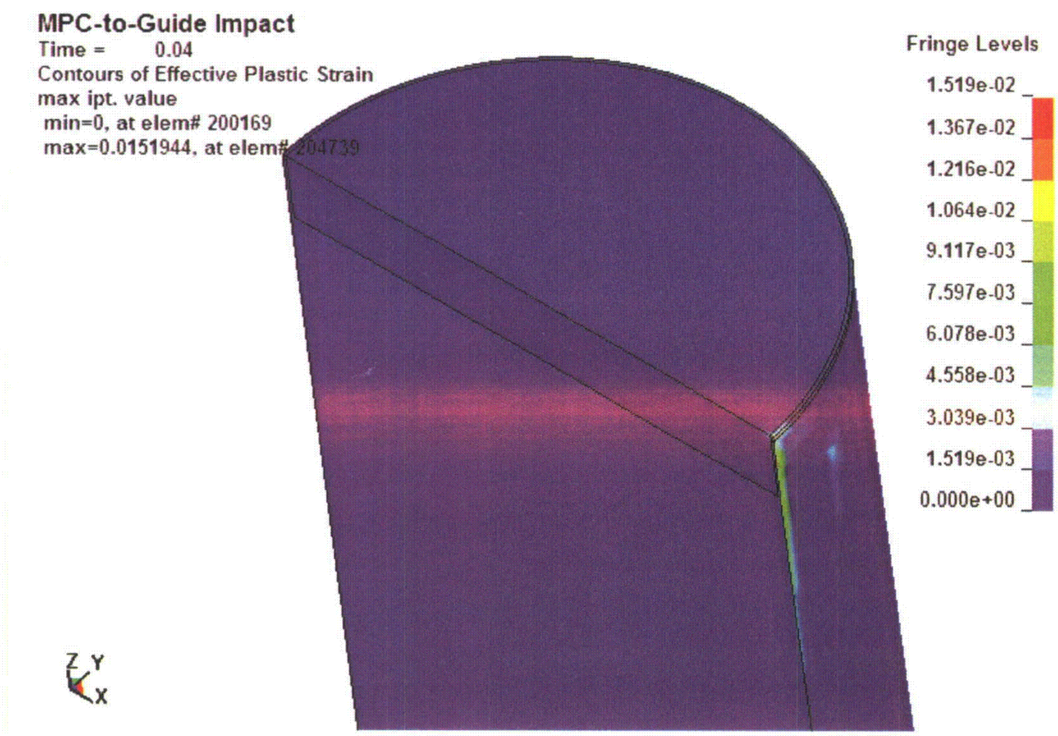

Figure 3.I.13; Maximum Plastic Strain of the MPC Enclosure Vessel in the Impact Region

Figure 3.I.14-A; Finite Element Model of the ISFSI Reinforced Concrete Structures for Simulation Models I through III

Figure 3.I.14-B; Finite Element Model of the ISFSI Reinforced Concrete Structures for Simulation Model IV

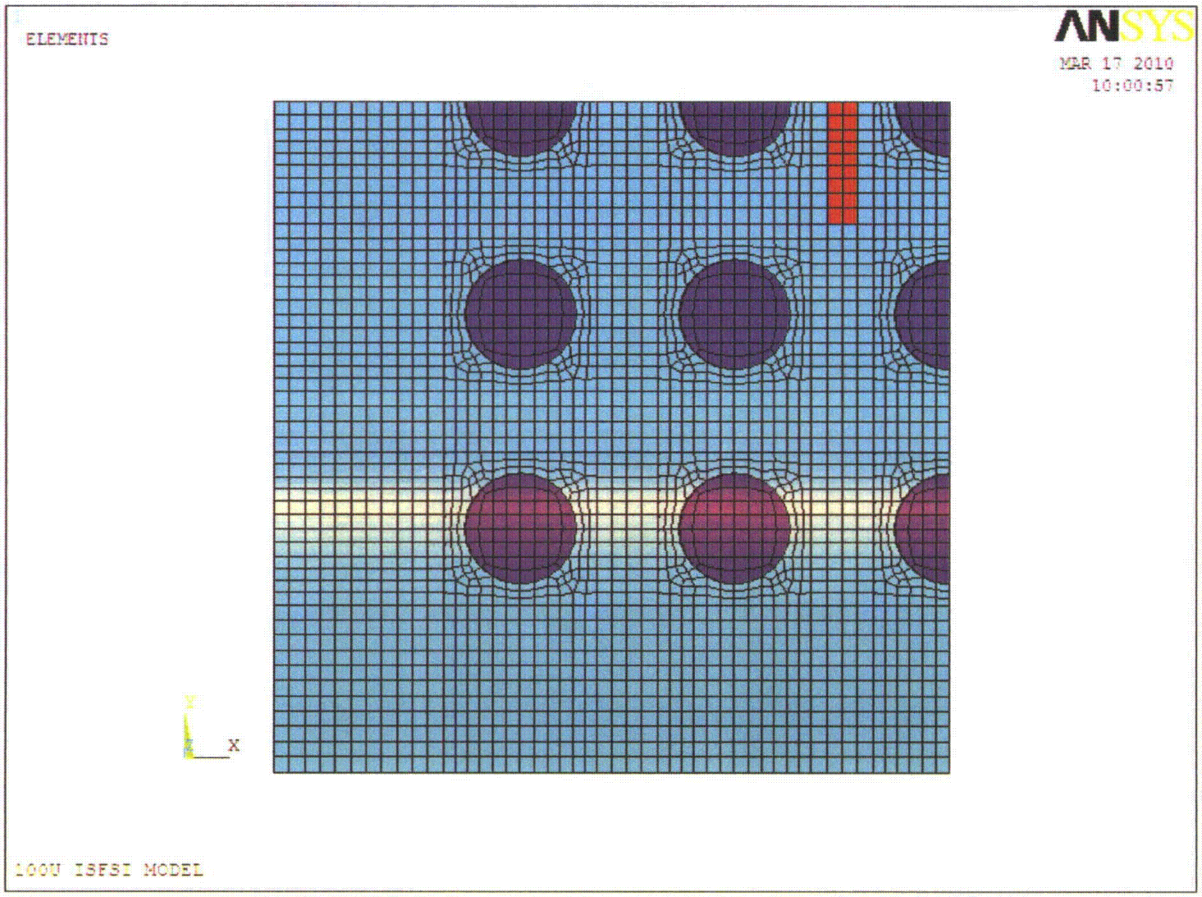

Note: The blue footprint shows the loaded VVM locations on the SFP and the red footprint represents the loaded TSP area with the cask transporter.

Figure 3.I.15; ANSYS Finite Element Model of ISFSI Showing the Fully Loaded Configuration (Simulation Model I)

Figure 3.I.16; Normal Stress in the ISFSI in the Direction of the Transporter Path for Simulation Model I – Load Combination LC-3 from Table 2.I.11

Figure 3.I.17; Normal Stress in the ISFSI in the Direction of the Transporter Path for Simulation Model II – Load Combination LC-3 from Table 2.I.11

HOLTEC INTERNATIONAL COPYRIGHTED MATERIAL

Figure 3.I.18; Normal Stress in the ISFSI in the Direction of the Transporter Path for Simulation Model III – Load Combination LC-3 from Table 2.I.11

HOLTEC INTERNATIONAL COPYRIGHTED MATERIAL

Figure 3.I.19; Normal Stress in the ISFSI in the Direction for Simulation Model IV – Load Combination LC-3 from Table 2.I.11

HOLTEC INTERNATIONAL COPYRIGHTED MATERIAL

Note: The blue footprints show the loaded VVM locations on the SFP and the red footprint represents the loaded TSP area with the transporter.

Figure 3.I.20; ANSYS Finite Element of ISFSI Showing the Showing the Center Row Loading (Simulation Model II)

Note: The blue footprints show the loaded VVM locations on the SFP and the red footprint represents the loaded TSP area with the transporter.

Figure 3.I.21; ANSYS Finite Element of ISFSI Showing the Single VVM Loaded (Simulation Model III)

Note: The blue footprints show the loaded VVM locations on the SFP and there is no transporter load.

Figure 3.I.22; ANSYS Finite Element of ISFSI with Retaining Wall Optional Design (Simulation Model IV)

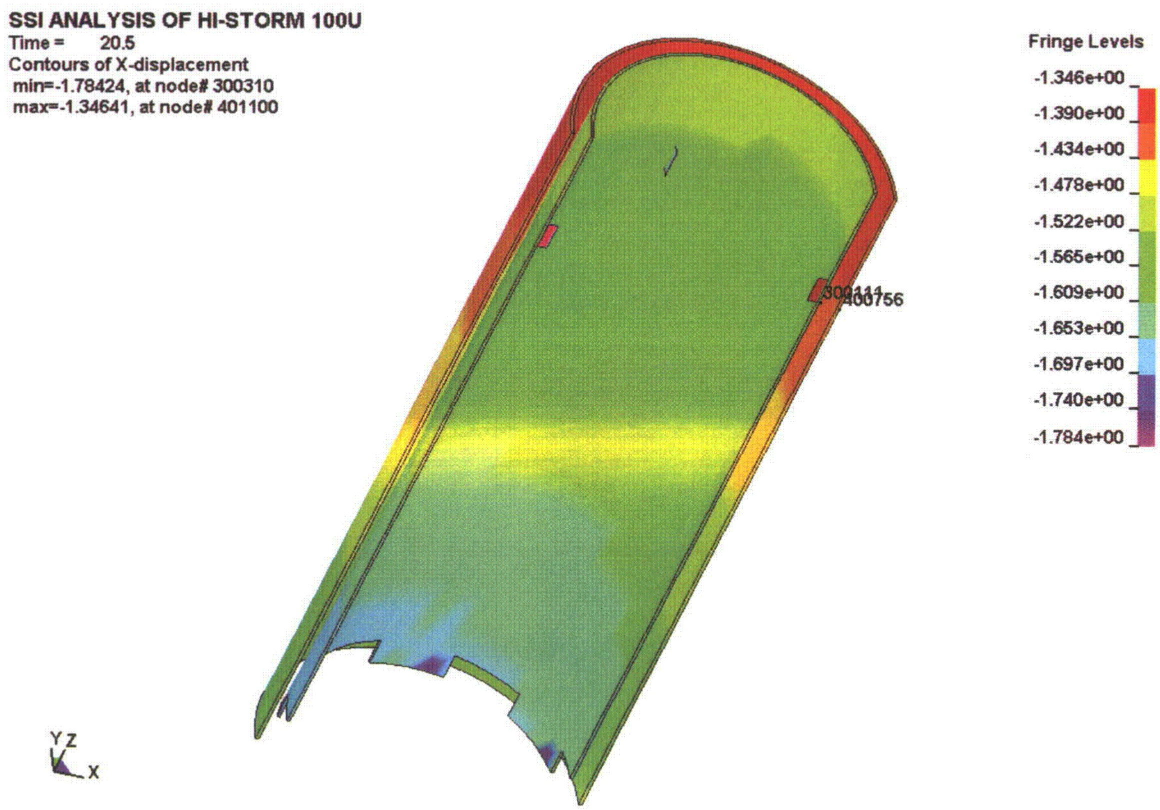

Figure 3.I.23-A; Divider and CEC Shell Displacement Distribution at the End of the Earthquake

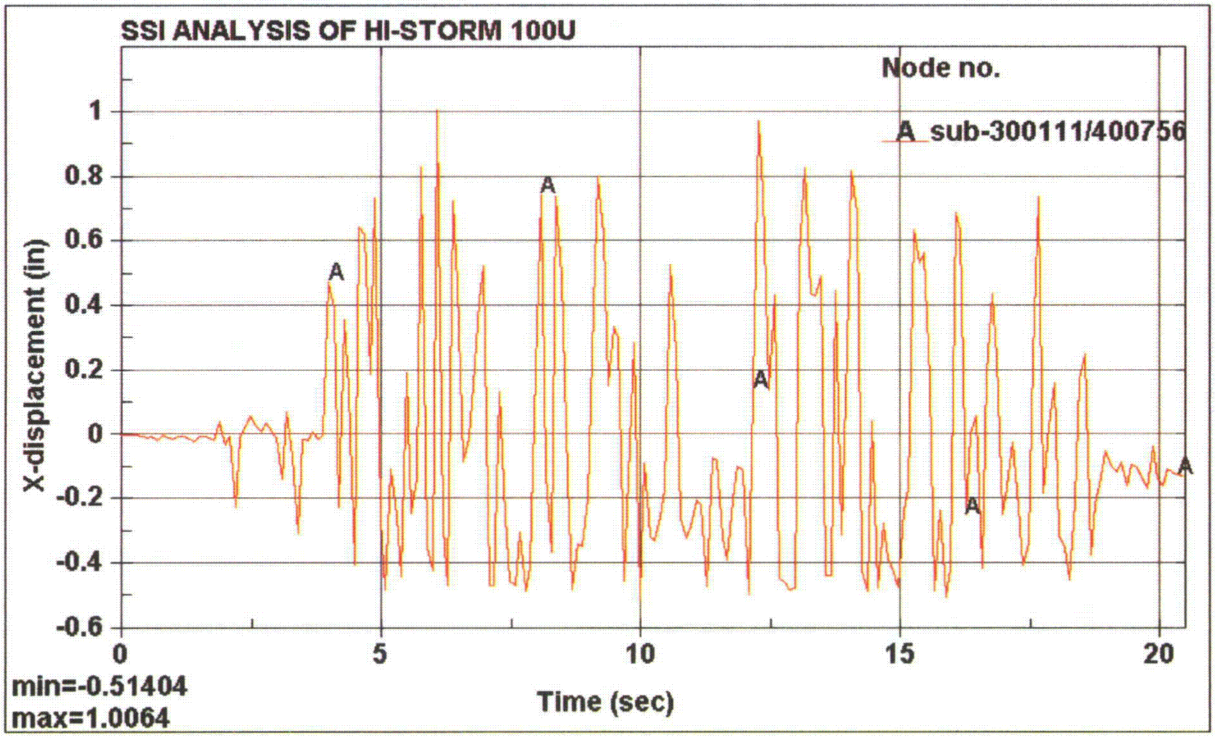

Figure 3.I.23-B; Changes of the Radial Gap between CEC Shell and Divider Shell Measured at the Top Guide Elevation
(Radial gap change at the end of earthquake = 0.1325 inches)

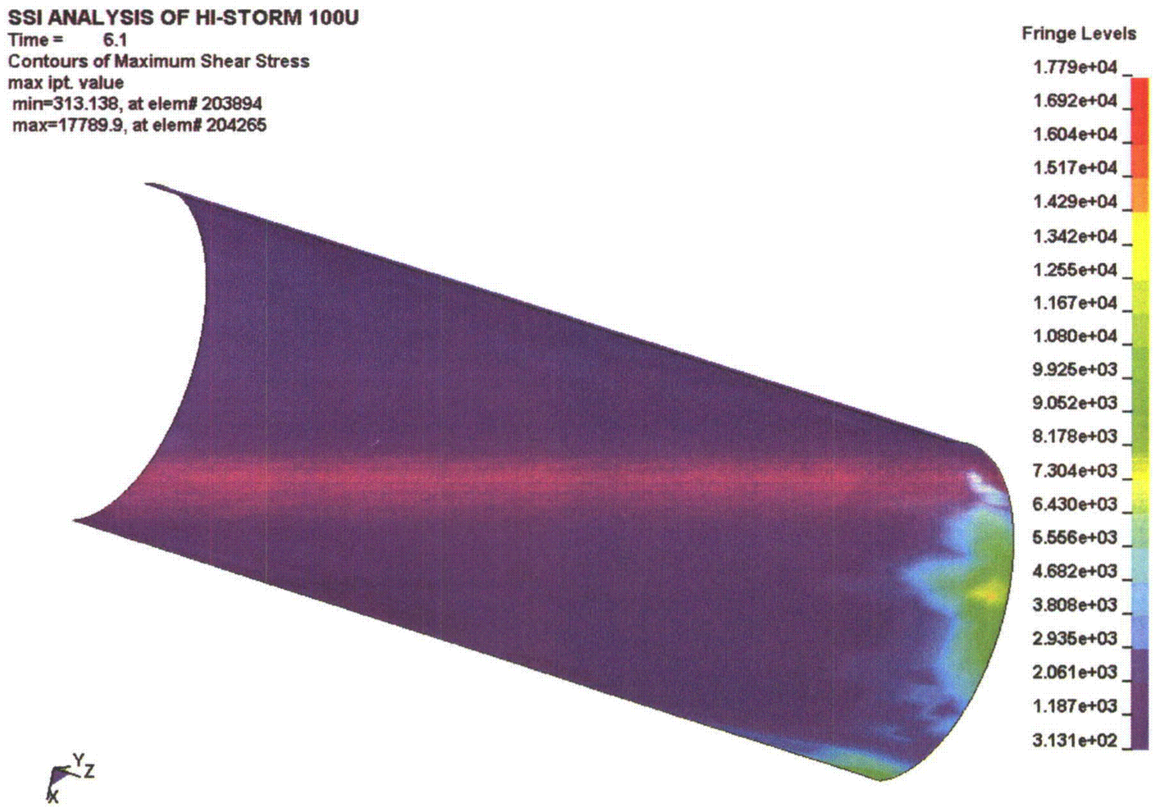

Figure 3.I.24; Maximum Shear Stress of the MPC Shell
(Maximum Primary Stress Intensity = 2×6,430 psi = 12,860 psi)

HOLTEC INTERNATIONAL COPYRIGHTED MATERIAL

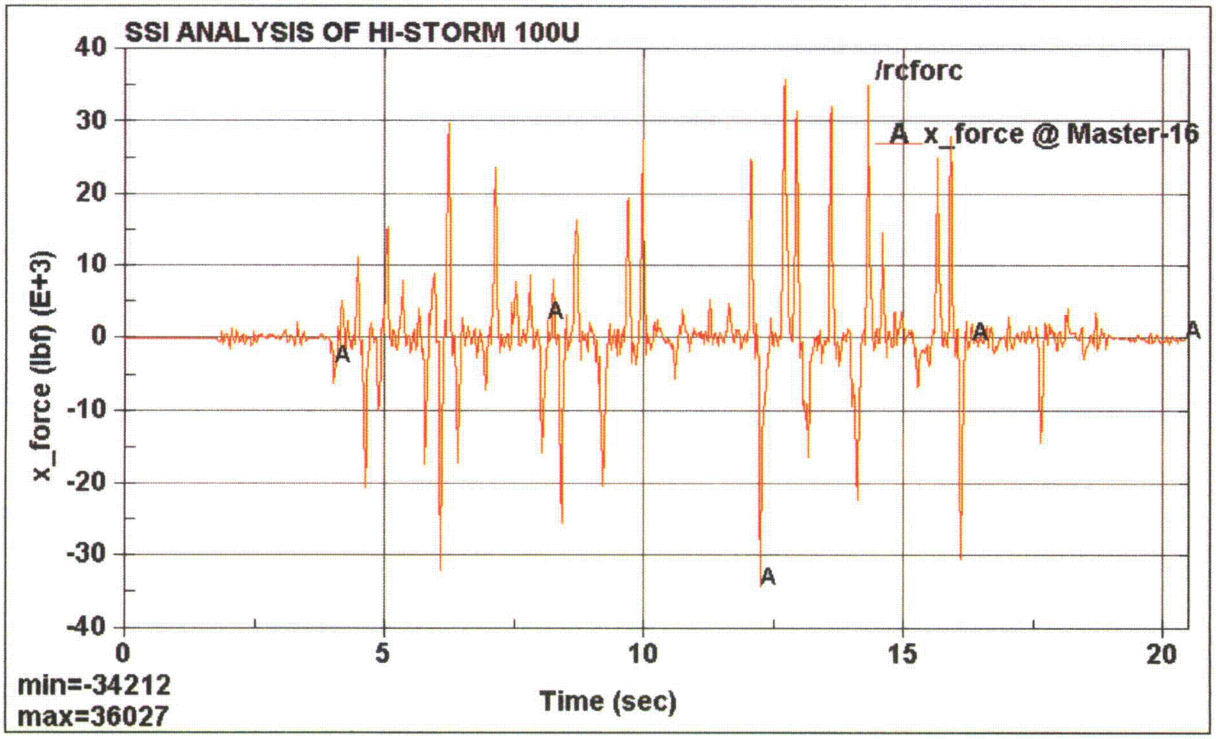

Figure 3.I.25-A; Impact Force between the MPC and MPC Top Guides
(Maximum Impact Force = 2×36,027 lb = 72,054 lb to account for half-symmetric model)

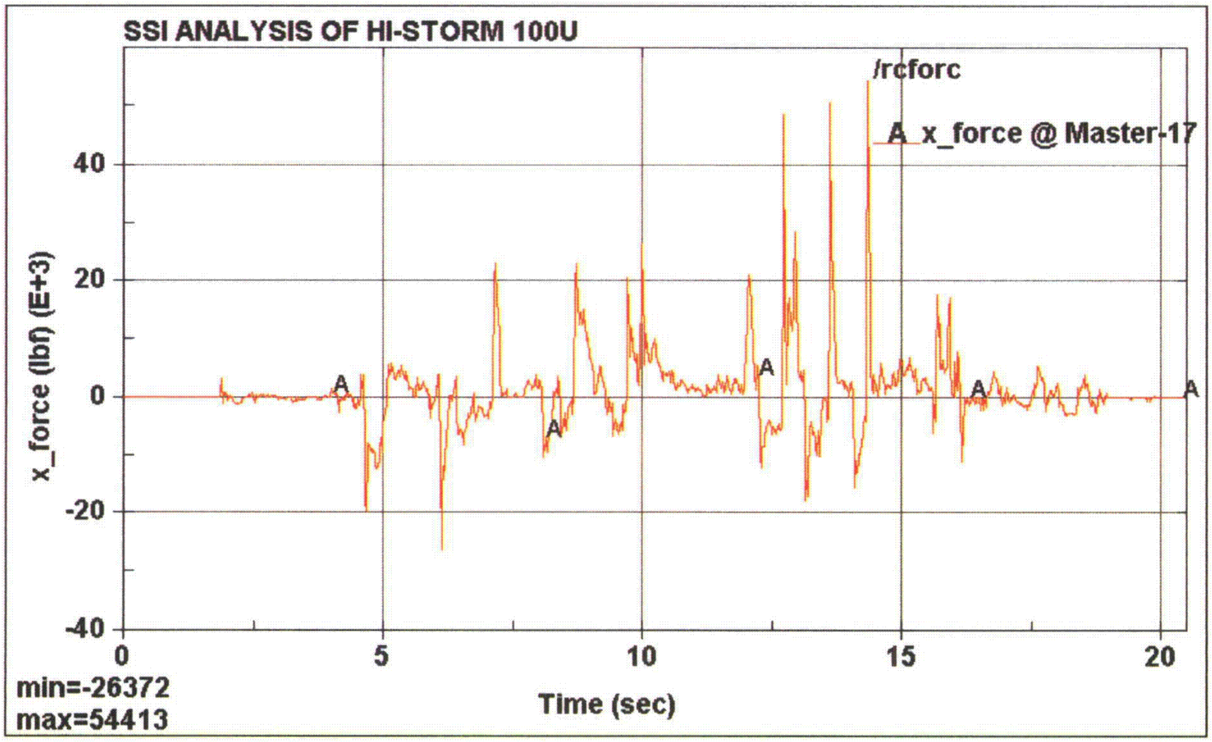

Figure 3.I.25-B; Impact Force between the MPC and MPC Bottom Guides
(Maximum Impact Force = 2×54,413 lb = 108,826 lb to account for half-symmetric model)

HOLTEC INTERNATIONAL COPYRIGHTED MATERIAL

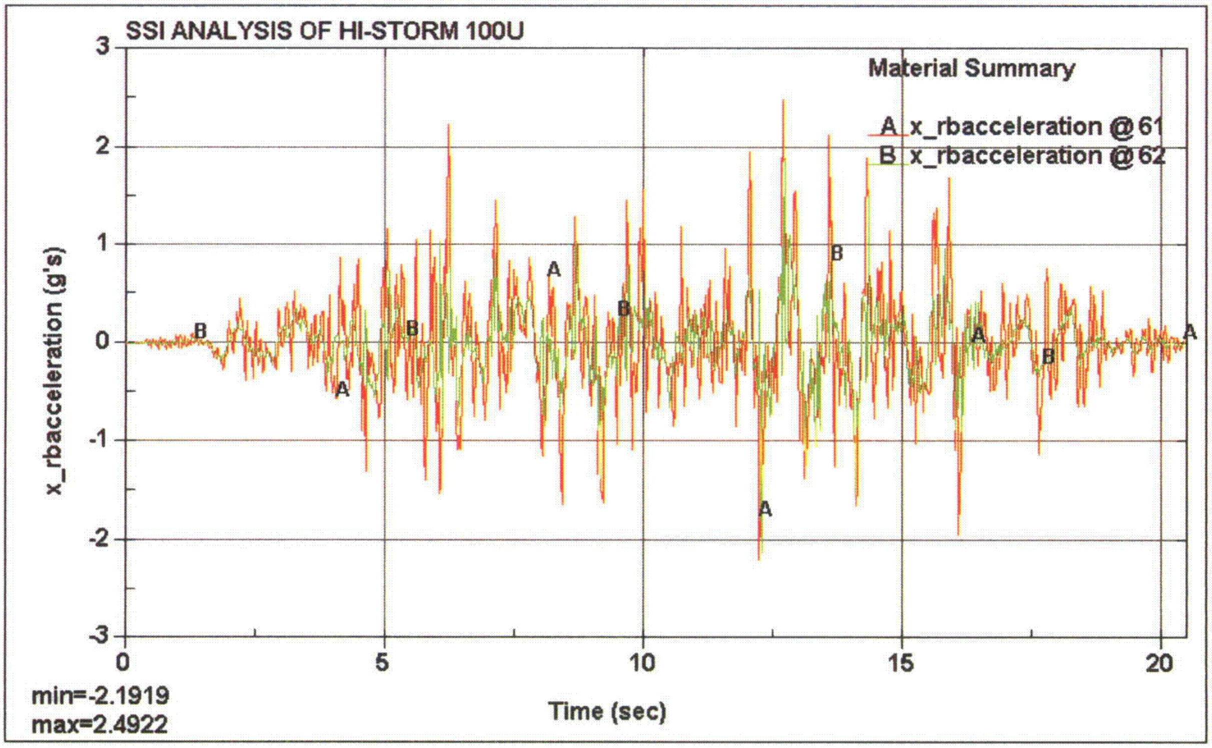

Figure 3.I.26; MPC Lid and Baseplate Lateral Acceleration Time Histories
(A - MPC Lid; B - MPC Baseplate)

HOLTEC INTERNATIONAL COPYRIGHTED MATERIAL

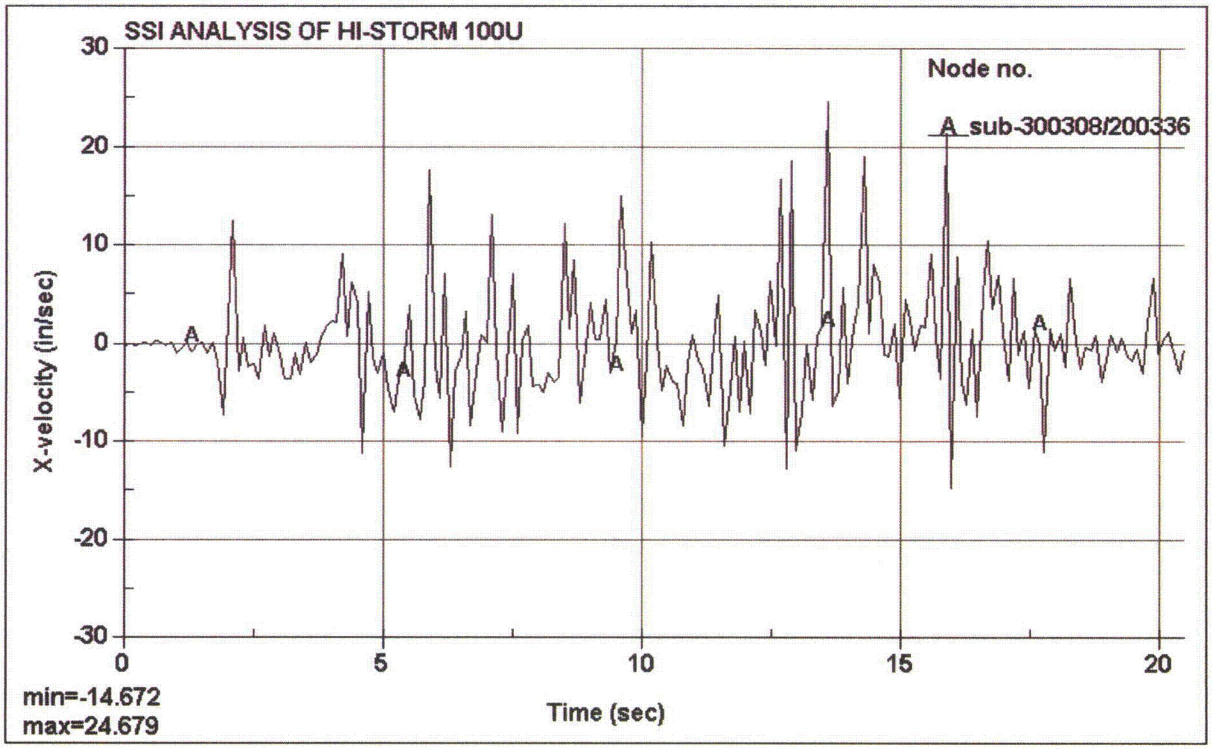

Figure 3.I.27; MPC Lid to MPC Top Guide Approaching Velocity Time History

HOLTEC INTERNATIONAL COPYRIGHTED MATERIAL

AFFIDAVIT PURSUANT TO 10 CFR 2.390

I, Tammy S. Morin, being duly sworn, depose and state as follows:

(1) I have reviewed the information described in paragraph (2) which is sought to be withheld, and am authorized to apply for its withholding.

(2) The information sought to be withheld are Attachments 4 through 7 and enclosed DVD to Holtec Letter 5014725, which contain Holtec Proprietary information.

(3) In making this application for withholding of proprietary information of which it is the owner, Holtec International relies upon the exemption from disclosure set forth in the Freedom of Information Act ("FOIA"), 5 USC Sec. 552(b)(4) and the Trade Secrets Act, 18 USC Sec. 1905, and NRC regulations 10CFR Part 9.17(a)(4), 2.390(a)(4), and 2.390(b)(1) for "trade secrets and commercial or financial information obtained from a person and privileged or confidential" (Exemption 4). The material for which exemption from disclosure is here sought is all "confidential commercial information", and some portions also qualify under the narrower definition of "trade secret", within the meanings assigned to those terms for purposes of FOIA Exemption 4 in, respectively, Critical Mass Energy Project v. Nuclear Regulatory Commission, 975F2d871 (DC Cir. 1992), and Public Citizen Health Research Group v. FDA, 704F2d1280 (DC Cir. 1983).

AFFIDAVIT PURSUANT TO 10 CFR 2.390

(4) Some examples of categories of information which fit into the definition of proprietary information are:

a. Information that discloses a process, method, or apparatus, including supporting data and analyses, where prevention of its use by Holtec's competitors without license from Holtec International constitutes a competitive economic advantage over other companies;

b. Information which, if used by a competitor, would reduce his expenditure of resources or improve his competitive position in the design, manufacture, shipment, installation, assurance of quality, or licensing of a similar product.

c. Information which reveals cost or price information, production, capacities, budget levels, or commercial strategies of Holtec International, its customers, or its suppliers;

d. Information which reveals aspects of past, present, or future Holtec International customer-funded development plans and programs of potential commercial value to Holtec International;

e. Information which discloses patentable subject matter for which it may be desirable to obtain patent protection.

The information sought to be withheld is considered to be proprietary for the reasons set forth in paragraphs 4.a and 4.b above.

(5) The information sought to be withheld is being submitted to the NRC in confidence. The information (including that compiled from many sources) is of a sort customarily held in confidence by Holtec International, and is in fact so held. The information sought to be withheld has, to the best of my knowledge and belief, consistently been held in confidence by Holtec International. No public disclosure has been made, and it is not available in public sources. All

disclosures to third parties, including any required transmittals to the NRC, have been made, or must be made, pursuant to regulatory provisions or proprietary agreements which provide for maintenance of the information in confidence. Its initial designation as proprietary information, and the subsequent steps taken to prevent its unauthorized disclosure, are as set forth in paragraphs (6) and (7) following.

(6) Initial approval of proprietary treatment of a document is made by the manager of the originating component, the person most likely to be acquainted with the value and sensitivity of the information in relation to industry knowledge. Access to such documents within Holtec International is limited on a "need to know" basis.

(7) The procedure for approval of external release of such a document typically requires review by the staff manager, project manager, principal scientist or other equivalent authority, by the manager of the cognizant marketing function (or his designee), and by the Legal Operation, for technical content, competitive effect, and determination of the accuracy of the proprietary designation. Disclosures outside Holtec International are limited to regulatory bodies, customers, and potential customers, and their agents, suppliers, and licensees, and others with a legitimate need for the information, and then only in accordance with appropriate regulatory provisions or proprietary agreements.

(8) The information classified as proprietary was developed and compiled by Holtec International at a significant cost to Holtec International. This information is classified as proprietary because it contains detailed descriptions of analytical approaches and methodologies not available elsewhere. This information would provide other parties, including competitors, with information from Holtec International's technical database and the results of evaluations performed by Holtec International. A substantial effort has been expended by Holtec International to develop this information. Release of this information would improve a competitor's position because it would enable Holtec's competitor to copy our technology and offer it for sale in competition with our company, causing us financial injury.

AFFIDAVIT PURSUANT TO 10 CFR 2.390

(9) Public disclosure of the information sought to be withheld is likely to cause substantial harm to Holtec International's competitive position and foreclose or reduce the availability of profit-making opportunities. The information is part of Holtec International's comprehensive spent fuel storage technology base, and its commercial value extends beyond the original development cost. The value of the technology base goes beyond the extensive physical database and analytical methodology, and includes development of the expertise to determine and apply the appropriate evaluation process.

The research, development, engineering, and analytical costs comprise a substantial investment of time and money by Holtec International.

The precise value of the expertise to devise an evaluation process and apply the correct analytical methodology is difficult to quantify, but it clearly is substantial.

Holtec International's competitive advantage will be lost if its competitors are able to use the results of the Holtec International experience to normalize or verify their own process or if they are able to claim an equivalent understanding by demonstrating that they can arrive at the same or similar conclusions.

The value of this information to Holtec International would be lost if the information were disclosed to the public. Making such information available to competitors without their having been required to undertake a similar expenditure of resources would unfairly provide competitors with a windfall, and deprive Holtec International of the opportunity to exercise its competitive advantage to seek an adequate return on its large investment in developing these very valuable analytical tools.

AFFIDAVIT PURSUANT TO 10 CFR 2.390

STATE OF NEW JERSEY)
) ss:
COUNTY OF BURLINGTON)

Ms. Tammy S. Morin, being duly sworn, deposes and says:

That she has read the foregoing affidavit and the matters stated therein are true and correct to the best of her knowledge, information, and belief.

Executed at Marlton, New Jersey, this 29th day of July, 2011.

Tammy S. Morin
Holtec International

Subscribed and sworn before me this 29th day of July, 2011.

Maria C Massi

MARIA C. MASSI
NOTARY PUBLIC OF NEW JERSEY
My Commission Expires April 25, 2015